

Copyright
by
Murat Torlak
1999

**ESTIMATION AND CAPACITY OF CHANNELS IN
SMART ANTENNA WIRELESS COMMUNICATION
SYSTEMS**

by

MURAT TORLAK, B.S., M.S.

DISSERTATION

Presented to the Faculty of the Graduate School of
The University of Texas at Austin
in Partial Fulfillment
of the Requirements
for the Degree of

DOCTOR OF PHILOSOPHY

THE UNIVERSITY OF TEXAS AT AUSTIN

August 1999

**ESTIMATION AND CAPACITY OF CHANNELS IN
SMART ANTENNA WIRELESS COMMUNICATION
SYSTEMS**

APPROVED BY
DISSERTATION COMMITTEE:

Supervisor: _____

Supervisor: _____

To my wife, my son, and parents with love

Acknowledgements

I would like to express my deepest appreciation and gratitude to Prof. Guanghan Xu, my thesis advisor, for his guidance, encouragement, and enthusiasm throughout the course of my graduate research. For his judgment and trust that made my admission to UT Austin possible and introduced me such a interesting field. I have been fortunate in being able to benefit from his experiences. I will always remember numerous nights working with him until morning and the day that we missed the flight to a conference after such a night. I also learned from him how to be confident about my own research.

I also wish to express my appreciation to Prof. Brian L. Evans for his contribution as a co-advisor. Especially his expertise in Mathematica and his offering coffee in 2:00 AM have helped me find the near-optimum solution for downlink weight vector design problem. I would also like to acknowledge him for suggesting ways for fast implementations, for helping me to improve the presentation of material, and for providing computer support. He also deserves sincere appreciation for always taking time to chat whenever I stop by his office. Close interactions with Prof. Xu and Prof. Evans have given me special opportunities for learning many important aspects of the academic life.

I wish to thank Prof. Edward J. Powers and Dr. Wolfhard J. Vogel for their generous support during the course of this research. My sincere appreciation also goes to the other members of the committee, Prof. Mircea M. Driga

and Dr. Srinivas V. Bettadpur, for their helpful comments and understanding. I also thank Prof. Hui Liu at University of Washington for his suggestion to develop on uplink channel estimation algorithm in CDMA systems. Numerous interactions with them, directly or indirectly, have had a considerable impact on this research.

I would like to sincerely thank Alberto Arredondo for his assistance in the proof-reading phase. I also extend my thanks to my colleagues Guner Arslan, Kapil Dandekar, Lars K. Hansen, Adnan Kavak, and Garret Okamoto for their valuable help, enthusiasm, and humor. I also thank Sang-Youb Kim, Ahmed R. Syed, Shiann S. Jeng, Weidong Yang, Liang Dong, and Hang Li of Telecom Lab. and Greg Allen, David Brunke, Niranjan Damera-Venkata, Srikanth Gummadi, Biao Lu, Wade Schwartzkopf, Clint Slatton, and Magesh Valliappan of the Embedded Signal Processing Laboratory.

I am especially indebted to my wife, Zuhail, for her patience and love. She provided all of the emotional support to help me when things seemed difficult. I also thank my parents, Hatice Torlak and Halil Ibrahim Torlak, and my sister, Selda, for their encouragement, and my friends for their support and caring. Finally, I would like to thank my son, Furkan for sharing the computer with me whenever I need it.

MURAT TORLAK

The University of Texas at Austin
August 1999

Preface

This dissertation is based on research in the area of antenna array applications to wireless systems conducted under the supervision of Prof. Guanghai Xu and Prof. Brian L. Evans. Many of the results presented here appear in conference proceedings and in manuscripts published in or submitted to refereed journals.

The minimum distance idea in Chapter 2 is based on results in

- "A capacity measure for space-division-multiple-access channels," *Proc. IEEE Asilomar Conf. on Signals, Systems, and Computers*, vol. 1, pp. 790–794, Nov. 1998, Pacific Grove, CA (with S. Y. Kim and G. Xu).
- "Minimum distance of space-division-multiple-access channels," *Proc. IEEE Vehicular Technology Conference*, vol. 3, pp. 2223–2227, May 1997, Phoenix, AZ (with G. Xu).

The blind channel estimation algorithms and simulations in Chapter 3 and Chapter 4 are based on results in

- "Blind multi-user channel estimation in asynchronous CDMA systems," *IEEE Trans. on Signal Processing*, vol. 45, pp. 137–147, Jan. 1997 (with G. Xu).

- “Blind channel estimation in CDMA systems with aperiodic spreading sequences,” submitted to *IEEE Journal on Selected Areas in Communications*, July 1999 (with B. L. Evans and G. Xu).

The downlink weight vector estimation algorithm and numerical results in Chapter 5 are based on results in

- “Fast Estimation of Weight Vectors to Optimize Multi-Transmitter Broadcast Channel Capacity,” *IEEE Transactions on Signal Processing*, vol. 46, pp. 243-246, Jan. 1998 (with G. Xu, B. L. Evans, and H. Liu).
- “Optimal weight vectors for broadcast channels,” in *Proc. IEEE Asilomar Conf. on Signals, Systems & Computers*, vol. 1, (Pacific Grove, CA), pp. 65-69, Nov. 1996 (with G. Xu, B. L. Evans, and H. Liu).

In the course of this research, we also obtain results on TDMA with smart antenna systems which appeared in

- “A geometric approach to blind source separation for digital wireless applications,” *Signal Processing*, vol. 73, pp. 153-167, Feb. 1999 (with L. K. Hansen and G. Xu).

ESTIMATION AND CAPACITY OF CHANNELS IN SMART ANTENNA WIRELESS COMMUNICATION SYSTEMS

Publication No. _____

Murat Torlak, Ph.D
The University of Texas at Austin, 1999

Supervisors: Guanghai Xu
Brian L. Evans

The proliferation of digital wireless communication services has been stimulating unprecedented demand for scarce radio spectrum. As the number of subscribers grows, spectral crowding and co-channel interference are becoming increasingly important issues. To alleviate such problems and to achieve the ambitious requirements introduced for existing and future wireless systems, attention has recently turned to spatial filtering methods using advanced antenna techniques, a.k.a *smart antennas*. Smart antennas exploit the spatial dimension as a hybrid multiple access technique (space division multiple access-SDMA) for complementing FDMA, TDMA and CDMA to improve the quality and spectral efficiency of communications over wireless channels.

This dissertation develops new signal processing methods and derives upper bounds on capacity for smart antenna wireless communication systems.

In particular, I study channel estimation for uplink and optimum weight vector design to maximize the downlink channel capacity. For uplink, I focus on blind multi-user channel estimation in code division multiple access wireless communication systems. For downlink, I investigate multi-transmitter broadcast systems. A multi-transmitter broadcast channel is a communication channel in which an antenna array system is transmitting to two or more receiving users. In order to optimize performance of the communications system, the *optimal* weight vector must be designed for each message signal that maximizes the overall channel capacity.

Table of Contents

Acknowledgements	v
Preface	vii
Abstract	ix
List of Tables	xiv
List of Figures	xv
Chapter 1. Introduction	1
1.1 Modulation Techniques for Wireless Systems	3
1.2 Smart Antenna Wireless Communication Systems	4
1.2.1 Spatial Signature and Composite Vector FIR Channel	5
1.2.2 Uplink	7
1.2.3 Downlink	7
1.3 Summary of Related Work	8
1.4 Significance and Contributions	12
1.4.1 Fundamental performance measure	12
1.4.2 Downlink weight vector estimation	12
1.4.3 CDMA systems with periodic spreading	13
1.4.4 CDMA systems with aperiodic spreading:	14
1.5 Organization of the Dissertation	14
1.6 Nomenclature	16
1.6.1 Notation	16
1.6.2 Acronyms	17

Chapter 2. A Capacity Measure for Space-Division Multiple-Access Channels	19
2.1 Introduction	19
2.2 Minimum Distance of SDMA Channels	21
2.2.1 Two-User Case	21
2.2.2 Effect of User Positions	22
2.2.3 Effect of the Number of Receivers	24
2.3 P -User SDMA System	24
2.4 Numerical Results	25
2.5 Summary	29
Chapter 3. Fast Estimation of Weight Vectors to Optimize Multi-Transmitter Broadcast Channel Capacity	30
3.1 Introduction	30
3.2 Problem Statement	32
3.3 Decoupling Weight Vectors	33
3.4 Two-User Case	34
3.4.1 Orthogonal Weight Vector Algorithm	36
3.4.2 Optimal Weight Vector Algorithm	37
3.4.3 Near-Optimal Weight Vector Algorithm	38
3.5 Three-User Case	40
3.6 Numerical Examples	41
3.7 Summary	41
Chapter 4. Uplink Channel Estimation: CDMA Systems with Periodic Spreading Sequences	43
4.1 Introduction	43
4.2 Model and Data Formulation	45
4.3 Discrete-Time Representation	46
4.4 Multi-User Channel Estimation	49
4.4.1 Algorithm	50
4.4.2 Identifiability	52
4.4.3 Blind Initial Synchronization	53

4.4.4	Channel order selection	55
4.5	Capacity Increase via Smart Antennas	56
4.6	Algorithm Performance	57
4.7	Computer Simulations	59
4.7.1	Single Antenna	60
4.7.2	Multiple Antennas	63
4.8	Experimental Results	64
4.9	Summary	64
Chapter 5. Uplink Channel Estimation: CDMA Systems with Aperiodic Spreading Sequences		73
5.1	Introduction	74
5.2	Data Model	76
5.3	A Blind Iterative Channel Estimation Approach	78
5.3.1	Step 1: Estimation of Channel Parameters Given Transmitted Symbols	79
5.3.2	Step 2: Estimation of Transmitted Symbols Given Channel Parameters	81
5.4	Blind Estimation Method	82
5.4.1	Complexity Analysis	83
5.4.2	Fast Implementation	85
5.5	Extension to Multirate Systems	88
5.6	Cramér-Rao Bound	89
5.7	Computer Simulations	91
5.8	Summary	94
Chapter 6. Conclusion		97
6.1	Contributions	97
6.2	Future Work	99
Appendix		101
Appendix A. Smart Antenna Testbeds		102
Bibliography		108
Vita		117

List of Tables

3.1	Comparison of implementation complexity	39
4.1	Comparison of RMSEs	65
4.2	Comparison of a 11-user/1-receiver and a 22-user/2-receiver . .	65
4.3	FIR Channel responses of user #11 for $M = 2$ case.	66
4.4	FIR Channel responses of user #22 for $M = 2$ case.	66
5.1	Average number of iterations for the proposed estimation method	93

List of Figures

1.1	Be smart	3
1.2	A base station with antenna array	5
2.1	Illustration of possible minimum distance measures	23
2.2	An SDMA constellation for $P = 2$ BPSK signals	26
2.3	Minimum distance vs. relative angle difference	27
2.4	Minimum distance vs. number of antennas	27
2.5	Error probability vs. the second user DOA.	28
2.6	Minimum distance vs. the second user's DOA	28
3.1	Illustration of search for an optimal weight vector.	36
3.2	Optimum weight vector algorithm	37
3.3	Fast near-optimum weight vector algorithm	39
3.4	Channel capacity using different weight vectors	42
3.5	Maximum channel capacities vs. ϕ	42
4.1	Blind multi-user channel estimation algorithm	51
4.2	An asynchronous-CDMA system	65
4.3	Channel responses and signal constellations	66
4.4	Signal constellations for user #11	67
4.5	Signal constellations for user #9, $P = 14$	67
4.6	BER and RMSE of channel estimates vs. channel length.	68
4.7	BER and RMSE of channel estimates vs. smoothing factor.	68
4.8	RMSE of received constellations vs. SNR for user #1.	69
4.9	Average BER for A-CDMA systems employing different receivers	69
4.10	Comparison of the receiver using proposed method	70
4.11	RMSE and BER of the receiver	70
4.12	Average BER for overloaded A-CDMA systems	71
4.13	2 antennas and 22 users transmitting BPSK signals.	71

4.14	Signal constellations for user #2	72
4.15	Signal constellations for user #25	72
5.1	Channel model for a P -user CDMA System	77
5.2	Proposed blind channel estimation method	84
5.3	Fast implementation of the proposed estimation method	87
5.4	Signal constellations for 1-D RAKE, 2-D RAKE and	92
5.5	Comparison of the mean squared error (MSE) of	94
5.6	Mean-squared error of channel parameter estimates	95
5.7	Root mean-square error of the channel estimates	96
5.8	Root mean-square error of the channel estimates	96
A.1	Overhead view of the 900 MHz Testbed	103
A.2	Front view of the 900 MHz Testbed	103
A.3	Real-time smart antenna testbed base site.	104
A.4	Base site transmit/receive board.	105
A.5	Base site tower with antenna array.	105
A.6	Circular antenna array	106
A.7	A handset and emulator board	106

Chapter 1

Introduction

The proliferation of cellular phones, cordless phones, pagers, and other digital wireless communication devices has demonstrated an unprecedented demand for scarce radio spectrum. For example, from 1990 to 1999, the number of mobile telephone users in the US has grown from 5.1 million to 65 million subscribers. Worldwide, half of a billion mobile network subscribers are predicted by the year 2000.

The first generation of public cellular wireless communication communication networks was introduced in the early 1980s to provide voice telephony services to mobile subscribers over a wide area. These systems used the principles of cellular systems. Frequencies used in one cell cluster could be reused in other cells. Conversations could be handed from cell to cell to maintain constant phone service as the user moves between cells. First-generation systems using analog frequency division multiple access (FDMA) methods were independently invented in various regions of the world. These systems include the Advanced Mobile Phone System (AMPS) in North America, the Nordic Mobile Telephone/Total Access Communication System (NMT/TACS) in Europe, and the Nippon Telephone and Telegraph-800/Japanese Total Access Communication System (NTT-800/JTACS) in Japan.

The second-generation (2G) systems were fielded in the late 1980s to support both voice and low-speed data/facsimile (FAX) services. These systems are based on digital modulation techniques which provided better spectral efficiency. The 2G systems which were successfully deployed worldwide are Global System for Mobile Communications (GSM) and Interim Standard-136 (IS-136) systems based on time division multiple access (TDMA) and IS-95 systems based on code division multiple access (CDMA).

The third-generation (3G) systems, to be introduced in the early 2000s, will offer considerably higher data rates and allow significantly increased flexibility over 2G systems. As the number of subscribers grows, spectral crowding and co-channel interference are becoming increasingly important issues. Co-channel interference may result from frequency reuse whereby multiple cells operate on the same carrier frequency. Furthermore, geographic conditions and physical limitations of the environment introduce fundamental problems such as noise, multipath, and fading for wireless communication channels.

To alleviate such problems and to achieve the ambitious requirements introduced for existing and future wireless systems, attention has recently turned to spatial filtering methods using advanced antenna techniques, a.k.a. smart antennas. A smart antenna array can exploit the spatial dimension as a hybrid multiple access technique (space division multiple access or SDMA) for complementing FDMA, TDMA and CDMA to improve the quality and spectral efficiency of communications over wireless channels. Moreover, it should be capable of simultaneously estimating the channels of several co-channel sources, as well as demodulating the signals themselves. For this to be achieved, fast and efficient co-channel signal capture algorithms must be developed.



Figure 1.1: Be smart.....reprinted with permission of *Wireless Week*, © 1997; All rights reserved.

Wireless communication systems consist of two radio links: *uplink* from the subscriber to the base station, and *downlink* from the base station to the subscriber. In this dissertation, we study the utilization of an antenna array at the base station with advanced signal processing for improving the performance of wireless communication systems. For the uplink, we specifically focus on the use of multiple antennas for CDMA wireless systems. For the downlink, we will consider a more general problem of designing weight vectors for multi-transmitter broadcast channels.

1.1 Modulation Techniques for Wireless Systems

First generation wireless systems employ analog modulation. Frequency modulation (FM) is the most popular analog modulation technique used in wireless systems. FM signals have all their information in the phase or frequency of the carrier. While FM systems have better noise immunity, they require a wider

frequency band in transmitting media in order to obtain the noise immunity.

The second and future-generation systems use digital modulation techniques. Advantages that digital modulation techniques offer include greater noise immunity, robustness to channel impairments, and accommodation of equalization to improve the performance of the overall communication link. In digital wireless communication systems, the modulating signal may be represented as a time sequence of symbols or pulses. Digital modulation also has enabled many different modulation schemes to be introduced such as spread spectrum techniques. These techniques employ a transmission bandwidth that is several orders of magnitude greater than the minimum required signal bandwidth. The advantage of spread spectrum is that many users can share the same bandwidth without significantly interfering with one another.

1.2 Smart Antenna Wireless Communication Systems

Figure 1.2 shows a wireless communication system employing an antenna array which is used to adaptively cancel the interference produced by subscribers using the same frequency band, time slots, or spreading code in nearby cells. More importantly, we can take an even more interesting approach and allow users within a single cell to share the same carrier frequency, time slot, or spreading code and demodulate them by only exploiting their spatial and temporal separation. This is a form of Space Division Multiple Access (SDMA) [1, 2, 3, 4]

Spatial processing with antenna arrays can facilitate a denser use of the available bandwidth and, therefore, an increase in system capacity. This gain in system performance, which is obtained by enabling directional transmission and reception, can provide better coverage at the base station. Consequently,

the number of base stations, as well as the complexity of the Mobile Telephone Switching Office (MTSO), can be reduced. Moreover, signal pre-processing techniques can be used to concentrate the complexity in the centralized base station, so that the user receiver can be simplified.

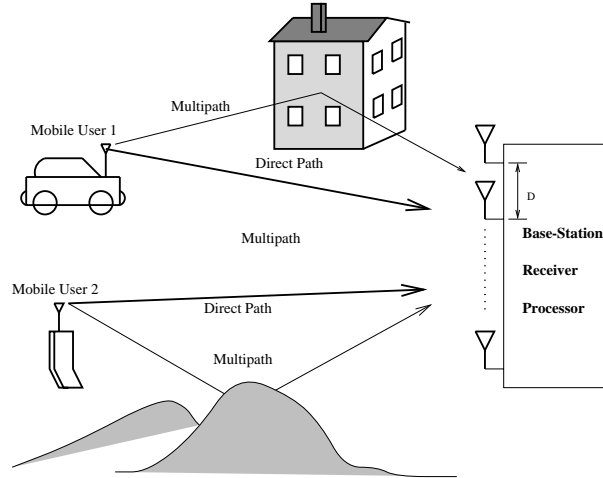


Figure 1.2: A base station with antenna array and two co-channel sources. Uplink (communication from mobile users to basestations) is shown.

1.2.1 Spatial Signature and Composite Vector FIR Channel

To understand the operation of a smart antenna system, we need to first introduce *spatial signatures*. Consider an M -element antenna array at a base station receiving signals from different users at different spatial locations. The array output contains both direct path and multipath signals. Radio propagation environments exhibit multipath effect when the received signal consists of multiple replicas of the transmitted signal, arriving from various directions. The *steering vector* to a transmitting signal $s(t)$ from a direction of arrival θ has the form

$$\mathbf{a}(\theta) = [1, a_2(\theta), \dots, a_M(\theta)]^T, \quad (1.1)$$

where $a_i(\theta)$ is a complex number denoting the amplitude gain and phase shift of the signal at the i^{th} antenna relative to that of the first antenna. For a uniform linear array

$$a_i(\theta) = e^{j\frac{2\pi\Delta\sin\theta}{\lambda}}$$

where Δ is the spacing between adjacent antennas and λ is the wavelength of the carrier.

In a typical wireless scenario, an omni-directional antenna array not only receives signals from a direct path but also from many reflected paths with different DOAs. Therefore, the total signal vector received by the antenna array can be written as

$$\mathbf{x}(t) = \sum_{l=1}^L \alpha_l \mathbf{a}(\theta_l) s(t) = \mathbf{a} s(t), \quad (1.2)$$

where $L - 1$ is the total number of multipath signals, α_l is the phase and amplitude difference between the l^{th} multipath and the direct path, and \mathbf{a} is defined as the *spatial signature* (SS) associated with source $s(t)$. On the other hand, when signals are transmitted from the base station antenna array, it has a vector from $\mathbf{x}^H(t) = [x_1^*(t), \dots, x_M^*(t)]$ due to the multiple transmitters. The transmitter antenna output is given by

$$s(t) = \mathbf{x}^H(t) \mathbf{a}.$$

In some applications, the symbol period of the transmitted signal may be comparable to the multipath spread. Then, a more general data model to accommodate long-delay multipath signals can be described as

$$\mathbf{x}(t) = \sum_{k=1}^L \alpha_k \mathbf{a}(\theta_k) s(t - \tau_k) = \mathbf{h}(t) \otimes s(t) \quad (1.3)$$

where τ_k denotes the delay corresponding to the k^{th} multipath signal. In this model, $\mathbf{h}(t)$ is referred to as a *composite vector* FIR channel.

1.2.2 Uplink

The objective in the uplink signal processor is to estimate the wireless channel parameters based on the data received. Then, using the wireless channel estimates, we can extract the intended user's signal while separating co-channel signals. The exact structure of the signal processor is dependent upon the amount of the information (*i.e.*, the modulation type, the time delay and DOA of each multipath, and the availability of the training signals) available at the base station.

My results for the uplink originated from my research on blind multi-user channel estimation in Asynchronous-CDMA (A-CDMA) systems. In the case of A-CDMA systems transmitting over multipath channels, neither intersymbol interference (ISI), as a result of interchip interference (ICI), nor multiple-access interference (MAI) can be easily eliminated. We develop a blind estimation method that estimates the multi-user channels by exploiting structure in the data and user delays. By utilizing smart antennas, we extend our approach to overloaded systems, where the number of users may exceed the spreading factor. We also develop solutions for blindly estimating multiple co-channel TDMA signals using smart antennas in the presence of multipath fading [5, 6].

1.2.3 Downlink

The downlink distributes signal power so that all signals with the same information can be constructively combined at a certain user's receiver while suppressing undesired interference and noise. In a short-delay multipath scenario, downlink SDMA can be accomplished by transmitting the superposition of weighted signals. With the knowledge of the spatial signatures describing

the downlink channel, transmission schemes may be devised via weight vectors which maximize the power of signal of interest at the user while minimizing co-channel interference and suppressing overall radiated power. Depending on the noise, interference, and downlink spatial signatures, the weight vectors can be designed to satisfy many different criteria [7, 8, 9, 10]. We denote $\{\mathbf{a}_i\}$ as the downlink spatial signatures and $\{\mathbf{w}_i\}$ the downlink weight vectors. Clearly, by transmitting $\mathbf{x}(t) = \sum_{i=1}^P \mathbf{w}_i s_i(t)$ from the base station antenna array, the i^{th} user will receive $\mathbf{a}_i^H \mathbf{x}(t)$. If we use the orthogonality property, *i.e.*

$$\mathbf{a}_i^H \mathbf{w}_j = \delta(i - j),$$

then the output at the i^{th} receiver is

$$\hat{s}_i(t) = \mathbf{a}_i^H \mathbf{x}(t) = \mathbf{a}_i^H \sum_{j=1}^P \mathbf{w}_j s_j(t) = s_i(t).$$

1.3 Summary of Related Work

Antenna array processing techniques were originally developed for target tracking and anti-jamming military communications [11, 12]. After a decade of extensive research (*e.g.* [13]) in this area coupled with rapid advances in microelectronics technology, high resolution antenna array technology can now achieve superior performance with affordable cost. Recently, Smart Antenna Systems [1, 2, 4, 14, 15] have been proposed to overcome some of the major difficulties in current wireless communication systems, *e.g.* multipath fading, intersymbol and co-channel interference, coverage and capacity limitations, handoff, and battery life, by exploiting the spatial diversity. It will not be possible to provide a complete and thorough coverage of the enormous body of work on

array applications to wireless systems. In the next few paragraphs, the major contributions on the subjects related to this dissertation are highlighted.

Since Cover's novel work in single-transmitter broadcast channels [16], researchers have been exploring the use of both multi-transmitter and multi-receiver systems [17, 18]. A multi-transmitter broadcast channel is a communication channel in which an antenna array system is transmitting to two or more receiving users. In order to maximize the performance of the communications system, we must find the *optimal* weight vector for each message signal that maximizes the overall channel capacity. The design of the optimal weight vectors that maximize the overall channel capacity of the broadcast channels, however, is still an open problem. The primary reason is that under certain power constraints, the channel capacity R is a highly nonlinear function of the M -dimensional weight vectors $\{\mathbf{w}_i\}$, where M is the number of transmitters.

One of the topics addressed in this dissertation is channel identification for extracting dispersed communication of direct sequence code division multiple access (CDMA) signals. The channel identification has been a major problem of interest and practical importance for engineers in communications for a long time [19]. Blind channel estimation [20], *i.e.* determining and equalizing the channel response based solely on the channel output without the use of training sequences, was first proposed by Sato [20] in 1975. Two obvious advantages make blind identification attractive. One merit is the bandwidth savings resulting from elimination of training sequences, while the other is the self-start capability before the communications link is established or after it has an unexpected breakdown.

In a CDMA communication environment, the receiver requires the sup-

pression of multipath induced interchip-interference (ICI), which causes intersymbol interference (ISI), and highly structured multiple user interference (MUI). Moreover, the delays should be incorporated in the receivers. Note that a conventional receiver that is matched to the spreading code treats both ISI and MUI as noise. Hence, it is severely interference limited.

Recent research has been devoted to receiver design and signature waveform estimation methods that exploit the structure of the so-called MUI and ICI to achieve better performance and, more importantly, higher capacity. In [21], Tsatsanis and Giannakis have proposed a discrete-time multirate filter bank model (zero-forcing receivers) which completely suppress MUI and ISI (ICI) under some conditions. To design such receivers, however, explicit knowledge of all of the signature waveforms is required.

Recently, adaptive multiuser detection [22, 23, 24] has been proposed to combat fast fading channels. Despite its success in some scenarios, most adaptive reception schemes still require pilot signals to obtain precise signature waveform estimates for all active users. In [25], Honig, Madhow, and Verdú introduced a *blind* adaptive receiver which is potentially of great importance to practical applications in multi-user detection. Although the adaptive receiver eliminates the need for training sequences for every user, the adaptive detection algorithm still requires knowledge of the desired user's signature waveform and associated timing.

In a CDMA wireless system, conventional approaches for estimating the signature waveforms rely on training sequences that are transmitted periodically [11]. Consequently, one must pay the price for using training sequences with a significant reduction of channel efficiency [26]. Alternatively, subspace-

based algorithms [27, 28, 29, 30] have been successfully developed for different CDMA schemes which eliminate the use of training sequences. However, these methods are only applicable when the system is underloaded (the number of users are smaller than the spreading gain) or when a few users are active. For instance, the methods proposed in [27, 28] will fail if the spreading gain (L_c) is less than four times the number of users (P), *i.e.* $L_c \leq 4P$. Although other subspace-based methods in [29, 30] have been proposed to estimate the associated time delay of each user, the method in [29] is only applicable to A-CDMA communication systems operating over an additive white Gaussian noise (AWGN) channel and the extension of this method in [30] can estimate the time delays of a few users, *i.e.* $P \leq L_c/(2L)$ for a free parameter L . Thus, new methods need to be developed to *fully* exploit the rich structure inherent in CDMA systems. In [31], Liu and Xu have developed a blind estimation scheme for synchronous CDMA (S-CDMA) channels. However, this method cannot be directly applied to other forms of CDMA channels.

For asynchronous CDMA systems with periodic spreading sequences, it would be possible to perform blind FIR channel estimation using subspace-based methods and avoid the need for training sequences [21, 27, 32, 31]. Although the periodicity of the spreading codes simplifies the use of multiuser detection techniques [25, 33], one of the practical features of existing and emerging CDMA standards is the use of aperiodic spreading codes.

Aperiodic spreading codes distribute the signal spectrum over the allotted bandwidth uniformly, have inherent interference averaging capabilities, and are beneficial to the soft capacity in IS-95 CDMA systems [34]. RAKE receivers are commonly used to estimate channel parameters and alleviate mul-

tipath fading, but they cannot fully exploit the rich structure of CDMA signals. Aperiodic spreading codes prevent the use of many signal reception and blind channel estimation methods [32, 35] that can fully exploit the structure of CDMA signals.

1.4 Significance and Contributions

This dissertation encompasses a variety of problems and provides a comprehensive study of smart antenna systems – from fundamental channel capacity analysis using information theory, to applicable algorithm development for basic and advanced smart antenna operations, and to experimental studies using a smart antenna testbed. The primary results of the present work are listed below.

1.4.1 Fundamental performance measure

We approach this problem from a fundamental point of view, *i.e.* the minimum distance of the constellation for SDMA channels because the minimum distance determines the bit error rate. Using the minimum distance measure, we can quantify the performance enhancement of the SDMA approach including capacity increase and quality improvement. In particular, we evaluate the minimum distance of SDMA channels in varying scenarios — different number of antennas in the array, co-channel signals and relative user positions.

1.4.2 Downlink weight vector estimation

In a multi-transmitter broadcast system, the weight vector for each message signal can provide an additional degree of freedom for signal enhancement and

interference suppression by taking advantage of the spatial diversity among the users. The design of *optimal* weight vectors that maximize the overall channel capacity is an open problem. Under certain power constraints, the channel capacity R is a nonlinear function of the M -dimensional weight vectors $\{\mathbf{w}_i\}$, where M is the number of transmitters. Hence, finding a closed-form algebraic solution that maximizes R over $\{\mathbf{w}_i\}$ does not seem to be tractable. In this dissertation, we decouple the weight vectors in R to simplify the optimization problem to a search for the maxima of a smooth multidimensional function. Based on this decoupling, we derive and evaluate two algorithms for computing weight vectors for the two-user and three-user cases: orthogonal and optimal. We also propose a near-optimum algorithm for the two-user case. The optimal algorithm requires an iterative search. The orthogonal and near-optimal algorithms are based on closed-form solutions and are easier to implement than the optimal algorithm, especially on a programmable digital signal processor.

1.4.3 CDMA systems with periodic spreading

In CDMA systems transmitting over multipath channels, neither ISI as a result of ICI nor MAI can be easily eliminated. Although it is possible to design multiuser detectors which suppress MAI and ISI, these detectors often require explicit knowledge of at least the desired users' signature waveform. In this dissertation, we study a similar blind estimation scheme that provides estimates of the multi-user channels by exploiting the structure information of the data output and the users' delays. In particular, we show that the subspace of the data matrix contains sufficient information for unique determination of channels, and hence, the signature waveforms. By utilizing smart antennas, we

extend our approach to overloaded systems, in which the number of users may exceed the spreading factor.

1.4.4 CDMA systems with aperiodic spreading:

Blind multiuser channel estimation is complicated in CDMA systems, such as IS-95 and emerging third-generation systems, that use aperiodic spreading sequences. For these CDMA systems, 1-D and 2-D RAKE receivers could perform blind multiuser channel estimation, but they would not be able to exploit the code structure in CDMA signals fully. In this dissertation, we develop a robust blind multiuser channel estimation method for single and multiple antenna CDMA systems with aperiodic spreading sequences. The method jointly estimates the multipath channel parameters and transmitted symbols by using iterative least squares projection to alternate between two new estimation frameworks. One framework computes channel parameters given an estimate of the transmitted symbols, and the other calculates the transmitted symbols given an estimate of the channel parameters. For the method, we provide a fast implementation and an extension to multirate systems. We also derive a Cramér-Rao Bound for CDMA systems with aperiodic spreading sequences.

1.5 Organization of the Dissertation

Chapter 2 analyzes the increase in capacity and performance due to the spatial diversity. Chapter 3 develops fast methods for designing downlink (broadcast) weight vectors to optimize the overall downlink channel capacity for narrow-band systems. I give an optimal solution suitable for a workstation implemen-

tation and near-optimal and orthogonal solutions suitable for a digital signal processor implementation. Chapters 4 and 5 focus on CDMA systems. Chapter 4 presents a blind multiuser channel estimation method for asynchronous CDMA systems. I extend the method to handle an overloaded system. Chapter 5 derives a blind multiuser channel estimation method for CDMA systems with aperiodic spreading sequences. I present a fast implementation of the method and an extension to handle multiple users transmitting at different data rates. Chapter 6 summarizes the dissertation and discusses future areas of research.

1.6 Nomenclature

1.6.1 Notation

$(\cdot)^T$	= transpose of matrix (\cdot)
$(\cdot)^*$	= complex conjugate of matrix (\cdot)
$(\cdot)^H$	= complex conjugate transpose of matrix (\cdot)
\otimes	= convolution
\odot	= Kronecker product
$\Delta(\cdot)$	= first-order perturbation of quantity (\cdot)
$\tilde{(\cdot)}$	= noise-corrupted quantity of (\cdot)
$\hat{(\cdot)}$	= estimation of quantity (\cdot)
$\text{Im}(\cdot)$	= imaginary part of matrix (\cdot)
$\text{Re}(\cdot)$	= real part of matrix (\cdot)
$E(\cdot)$	= expectation of matrix (\cdot)
\mathbf{I}	= identity matrix
\mathbf{A}^\dagger	= pseudo-inverse of a full column rank matrix \mathbf{A}
$\ \mathbf{A}\ _F$	= Frobenius norm of matrix \mathbf{A}
$\det(\mathbf{A})$	= Determinant of square matrix \mathbf{A}
$\text{Tr}(\mathbf{A})$	= Trace of square matrix \mathbf{A}
$\delta(n)$	= Kronecker impulse $\delta(n) = \begin{cases} 1 & \text{if } n = 0 \\ 0 & \text{otherwise} \end{cases}$

1.6.2 Acronyms

A-CDMA	:	Asynchronous CDMA
AMPS	:	Advanced
AWGN	:	Additive White Gaussian Noise
BER	:	Bit Error Rate
BPSK	:	Binary Phase Shift Keying
CCI	:	Co-Channel Interference
CDMA	:	Code-Division Multiple-Access
CMA	:	Constant Modulus Algorithm
CRB	:	Cramér-Rao Bound
DF	:	Direction Finding
DOA	:	Direction-of-Arrival
ESPRIT	:	Estimation of Signal Parameters via Rotational Invariance Techniques
EVD	:	EigenValue Decomposition
FDD	:	Frequency Division Duplex
FDMA	:	Frequency Division Multiple Access
FIR	:	Finite Impulse Response
FSD	:	Fast Subspace Decomposition
GSM	:	Global System for Mobile Communications
ICI	:	Inter-Chip Interference
ILSP	:	Iterative Least-Squares with Projection Algorithm
ISI	:	Inter-Symbol Interference
LMS	:	Least Mean Squares
MAC	:	Multiple Access Channel
MAI	:	Multiple Access Interference
ML	:	Maximum Likelihood
MMSE	:	Minimum Mean Squared Error
MSE	:	Mean Squared Error

MUI	:	Multi User Interference
MUSIC	:	MUltiple SIgnal Classification
PC	:	Principal Component
PCS	:	Personal Communications Services
RMSE	:	Root Mean Square Error
SAS	:	Smart Antenna Systems
S-CDMA	:	Synchronous CDMA
SCORE	:	Self COherence REstoral
SDMA	:	Space-Division-Multiple-Access
SNR	:	Signal-To-Noise Ratio
SINR	:	Signal-To-Interference-Noise Ratio
SIR	:	Signal-To-Interference Ratio
SS	:	Spatial Signature
SVD	:	Singular Value Decomposition
TDD	:	Time Division Duplex
TDMA	:	Time Division Multiple Access
ZF	:	Zero Forcing

Chapter 2

A Capacity Measure for Space-Division Multiple-Access Channels

In digital communications [19, 36], the distance between the points in the signal constellation determines the probability that one point will be erroneously detected. If the points are closer, then they are more likely to be mistaken with another point. Thus, the *minimum distance* (d_{min}) between the points in the signal constellation is an alternative measure to compare the different signal constellations. Of course, the more points the constellation has, the more power the communication system requires to have the same noise immunity with a constellation which has fewer points. In this dissertation, we examine the performance of SDMA channels from a fundamental point of view, *i.e.* by using the minimum distance of the constellation. We evaluate SDMA performance in different scenarios — different number of antennas, co-channel signals, and relative user positions.

2.1 Introduction

We consider the uplink on which users transmit to the base station. We assume a system which is a multiple access system with additive white Gaussian noise (AWGN) channels and multiple receivers at the base station. The multiple re-

receivers observe the spatial diversity among users and consist of a uniform linear array with M sensors with spacing Δ . We also invoke the usual assumptions — narrowband signals, planar wavefront propagation, and slowly varying antenna responses.

With P ($P > 1$) co-channel users in the absence of noise, the vector of array outputs at time k may be expressed as

$$\mathbf{x}(k) = [x_1(k) \ \cdots \ x_m(k)]^T \quad (2.1)$$

Similarly, let $\mathbf{s}(k) = [s_1(k) \ \cdots \ s_P(k)]^T$ be the vector of symbols from alphabet \mathcal{S} at time k generated by the P signals. Then

$$\mathbf{x}(k) = \sum_{i=1}^P \mathbf{a}_i s_i(k) = \underbrace{[\mathbf{a}_1 \ \cdots \ \mathbf{a}_P]}_{\mathbf{A}} \underbrace{\begin{bmatrix} s_1(k) \\ \vdots \\ s_P(k) \end{bmatrix}}_{\mathbf{s}(k)} \quad (2.2)$$

where \mathbf{a}_i is called the antenna response of the i th signal (sometimes referred to as *spatial signature*), which is in general a complex vector.

For general applications, the spatial signature \mathbf{a}_i takes into account both the direct path and multipath components of the i th user and can be decomposed into

$$\mathbf{a}_i = \sum_{k_i=1}^{L_i} \alpha_{k_i} \mathbf{a}(\theta_{k_i}) \quad (2.3)$$

where L_i is the total number of paths associated with $s_i(k)$, and α_{k_i} represents the complex gain of the k_i^{th} multipath of the i th user. In the absence of multipath (direct path only), normalizing each element in \mathbf{a}_i with respect to its first element yields

$$\mathbf{a}_i = [1 \ e^{j2\pi \sin \theta_i \Delta / \lambda} \ \cdots \ e^{j(M-1)2\pi \sin \theta_i \Delta / \lambda}] \quad (2.4)$$

where θ_i is the Direction of Arrival (DOA) angle of the incoming signal from i th user. In this special case, the spatial signature is called the steering vector or array response vector.

2.2 Minimum Distance of SDMA Channels

The minimum distance parameter, d_{min} , plays an important role in quantifying the performance of SDMA systems. The probability of error in an AWGN channel decreases exponentially with the increase in d_{min} . An upper bound on d_{min} can be used to determine a lower bound on the probability of error achieved by the best reception method.

2.2.1 Two-User Case

To simplify the discussion and provide insight on how the minimum distance parameter determines SDMA performance, we first examine the two-user case

$$\mathbf{x}(k) = \mathbf{a}_1 s_1(k) + \mathbf{a}_2 s_2(k) = \mathbf{A}\mathbf{s}(k) \quad (2.5)$$

For the case in which the transmitted signals are BPSK signals in the alphabet $\{-1, 1\}$, the alphabet set which contains all combinations of inputs can be written as

$$\mathcal{S} = \begin{bmatrix} 1 & 1 & -1 & -1 \\ 1 & -1 & 1 & -1 \end{bmatrix}. \quad (2.6)$$

Then, the matrix of all possible antenna outputs is $\mathcal{X} = \mathbf{A}\mathcal{S}$. With this in mind, we derive the minimum distance relationship. The minimum distance between pairs of outputs is defined as

$$d_{min} = \min_{i \neq j} \|\mathcal{X}_i - \mathcal{X}_j\| \quad \forall i, j \quad (2.7)$$

where the norm is the L_2 (Euclidean) norm, and i, j denotes the column index of \mathcal{X} . \mathcal{X}_i is the output corresponding to the input \mathcal{S}_i . Thus, the squared minimum distance is

$$\begin{aligned} d_{min}^2 &= \min_{i \neq j} \|\mathbf{A}(\mathcal{S}_i - \mathcal{S}_j)\|^2 \\ &= \min_{i \neq j} (\mathcal{S}_i - \mathcal{S}_j)^H \mathbf{A}^H \mathbf{A} (\mathcal{S}_i - \mathcal{S}_j). \end{aligned} \quad (2.8)$$

$\mathbf{A}^H \mathbf{A}$ is real, symmetric, and can therefore be factored as

$$\mathbf{A}^H \mathbf{A} = \mathbf{U} \Lambda \mathbf{U}^H \quad (2.9)$$

where \mathbf{U} is the 2×2 orthonormal matrix whose columns are the eigenvectors of $\mathbf{A}^H \mathbf{A}$, and $\Lambda = \text{diag}[\lambda_1, \lambda_2]$, where λ_1 and λ_2 are the real, nonnegative eigenvalues of $\mathbf{A}^H \mathbf{A}$. Then the minimum distance can be written as

$$d_{min} = \min_{i,j} \|\Lambda^{1/2} (\mathbf{U}^H \mathcal{S}_i - \mathbf{U}^H \mathcal{S}_j)\| \quad (2.10)$$

As seen from (2.8), d_{min} is a function of \mathbf{a}_1 and/or \mathbf{a}_2 . Once the minimum distance is found, the probability of error of SDMA signals P_e is expressed as

$$P = \frac{1}{2} \text{erfc} \left(\frac{d_{min}}{2\sqrt{N_o}} \right) \quad (2.11)$$

where $\text{erfc}(x)$ is the complementary error function defined as $\frac{2}{\sqrt{\pi}} \int_x^\infty e^{-t^2} dt$; and N_o is the power spectral density of the additive noise in the system.

2.2.2 Effect of User Positions

As shown in Figure 2.1, the angle between two spatial signatures is a key factor to determine the minimum distance. In this section, we investigate the effect of relative user position. Intuitively, one would expect that the minimum distance varies depending on the relative locations of different users.

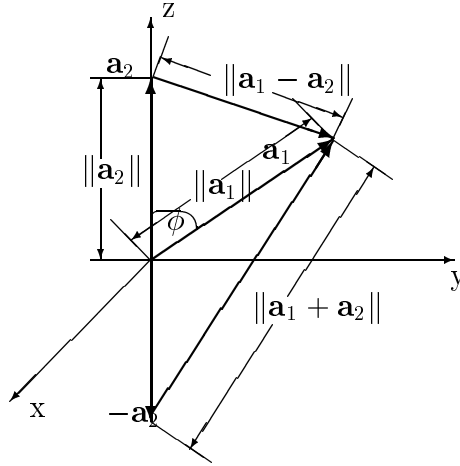


Figure 2.1: Illustration of possible minimum distance measures in a two-user system

Theorem 1 *In a two-user SDMA system with BPSK signals and $\|\mathbf{a}_1\| = \|\mathbf{a}_2\|$, the minimum distance is maximum when the angle between the users' array response vectors is more than 60 degrees.*

Proof:

We shall prove this theorem by using the minimum distance formulation in (2.7).

$d_{min} = \|\mathbf{a}_1\| = \|\mathbf{a}_2\| = c$ is maximum when

$$\begin{aligned} \|\mathbf{a}_1 - \mathbf{a}_2\| &\geq c \\ (\mathbf{a}_1^H - \mathbf{a}_2^H)(\mathbf{a}_1 - \mathbf{a}_2) &\geq c^2 \\ \|\mathbf{a}_1\|^2 - \mathbf{a}_2^H \mathbf{a}_1 - \mathbf{a}_1^H \mathbf{a}_2 + \|\mathbf{a}_2\|^2 &\geq c^2 \end{aligned}$$

Using $c = \|\mathbf{a}_1\| = \|\mathbf{a}_2\|$ and $\mathbf{a}_2^H \mathbf{a}_1 = \|\mathbf{a}_1\| \|\mathbf{a}_2\| \cos(\phi)$, we obtain

$$\begin{aligned} c^2 - 2c^2 \cos(\phi) + c^2 &\geq c^2 \\ c^2 - 2c^2 \cos(\phi) &\geq 0 \\ \cos(\phi) &\geq \frac{1}{2} \end{aligned}$$

$$\phi \geq 60^\circ.$$

□

The result of this theorem can be observed from Figure 2.1.

2.2.3 Effect of the Number of Receivers

If we employ more receivers, then the minimum distance of a multi-user SDMA system will be closer to that of single user system. Depending on the angle between the spatial signatures, the minimum distance of the multi-user system will be the same as the single user system. When the number of receivers increases, the required difference between the users' DOA (direct path only) to satisfy the maximum minimum distance decreases. By denoting $\psi = 2\pi \sin \theta \Delta / \lambda$, we rewrite the steering vector in (2.4) with M receivers more concisely as

$$\mathbf{a}(\psi) = [1, e^{j\psi}, \dots, e^{j(M-1)\psi}]^T.$$

For any $\psi_i \neq \psi_j$, $\cos^2 \phi = \cos^2 \angle(\mathbf{a}(\psi_i), \mathbf{a}(\psi_j))$ can be expressed as

$$\frac{|\mathbf{a}^H(\psi_i)\mathbf{a}(\psi_j)|^2}{|\mathbf{a}(\psi_i)|^2 \cdot |\mathbf{a}(\psi_j)|^2} = \frac{1}{M^2} \left| \frac{1 - e^{jM(\psi_j - \psi_i)}}{1 - e^{j(\psi_j - \psi_i)}} \right|^2. \quad (2.12)$$

Definition 1 *The efficiency of an SDMA system for the k^{th} user, e_k , is defined as the ratio between the minimum distance of the constellation of the k^{th} user and minimum distance of SDMA channels.*

2.3 P-User SDMA System

We consider the case where there are more than two users accommodated by an SDMA system. With the minimum distance formulation obtained in the

previous section for a two-user system, it is now relatively easier to derive a similar formulation for a P -user SDMA system. In this case, the alphabet set \mathcal{S} in (2.6) contains 2^P distinct columns.

2.4 Numerical Results

In this section, we give numerical examples to demonstrate the usefulness of the minimum distance measure to evaluate the SDMA approach. Figure 2.2 shows the real part of an SDMA constellation for $P = 2$ signals drawn from the BPSK alphabet $\{-1,1\}$ with SNR=7 dB.

In the first example, we investigated the effect of the relative users' location through a computer simulation for two users direct path only case. For this simulation, we used an 8-element antenna array, fixed the first user's location, and changed the other user's location relative to the first user transmitting the same power. In Figure 2.3, we see that beyond a certain angle difference, the minimum distance reaches a threshold value which is determined by the lowest user power.

In the next example, spatial signatures for two users were obtained from real RF field experiments using the smart antenna testbeds described in the Appendix. Using (2.10), we evaluated d_{min} vs. number of antennas and the minimum probability of error vs SNR. We see in Figure 2.4 that by increasing the number of antennas, the minimum distance of the constellation of SDMA channels increases. Hence, we observe that an increase in the distance between SDMA channels reduces the probability of error detection.

Figure 2.5 shows the results of a comparison experiment. The curve

with the solid line shows the probability of error which was predicted by the formulation in (2.11). The curve with the dashed lines shows the probability error found through simulation. In this comparison experiment, we used a five-element uniform linear array with half wavelength separation. Two sources impinged on the array with DOAs 90° and θ where θ varied from 0° to 180° . These two sources had 7 dB SNR. In this example, we observe that the minimum distance may be a good criteria to predict the performance of the SDMA approach.

The last example shown in Figure 2.6 shows the change in minimum distance in a three-user system with varying DOAs. This example suggests the required DOA separation of 60° among users in order to reach single user performance.

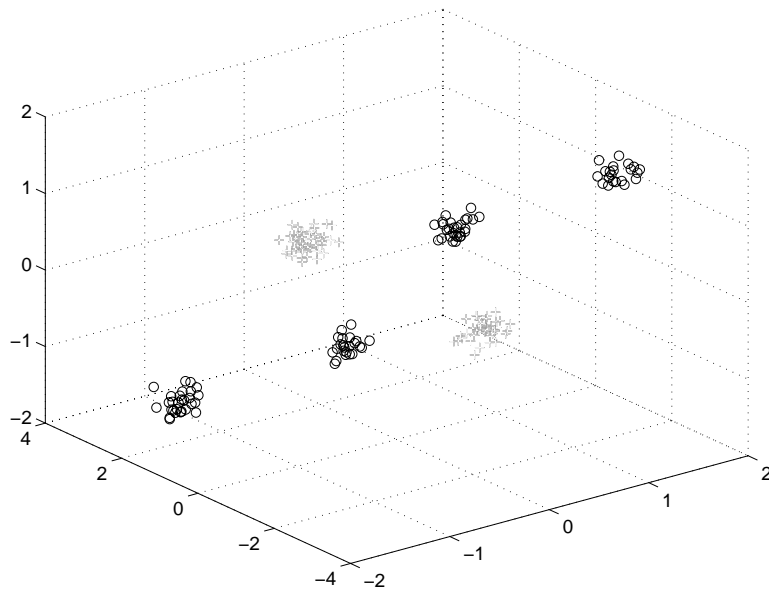


Figure 2.2: An SDMA constellation for $P = 2$ BPSK signals with $M = 3$ antennas. Only the real part of the constellation is plotted.

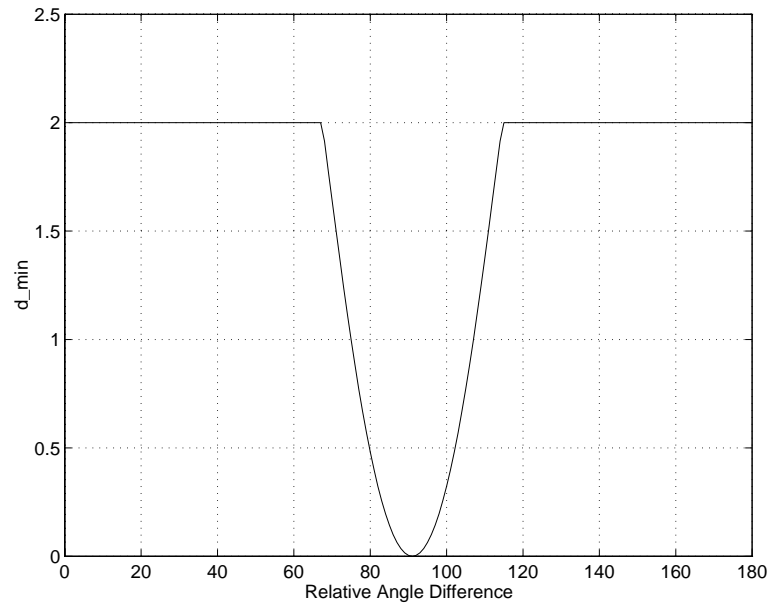


Figure 2.3: Minimum distance vs. relative angle difference

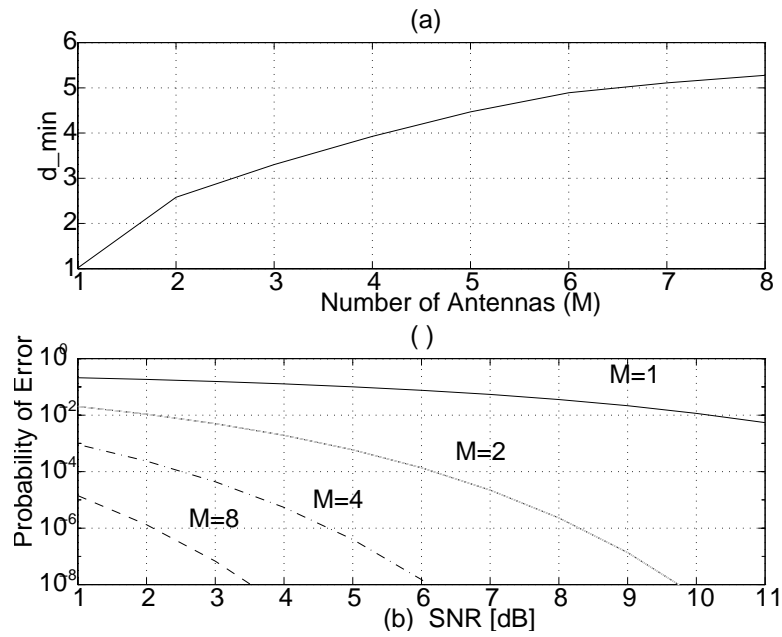


Figure 2.4: (a) Minimum distance vs. number of antennas, and (b) minimum probability of error vs. SNR.

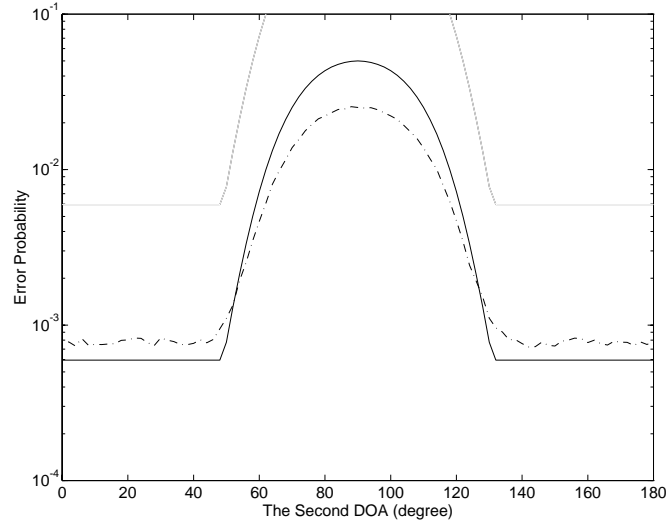


Figure 2.5: Error probability vs. the second user DOA.

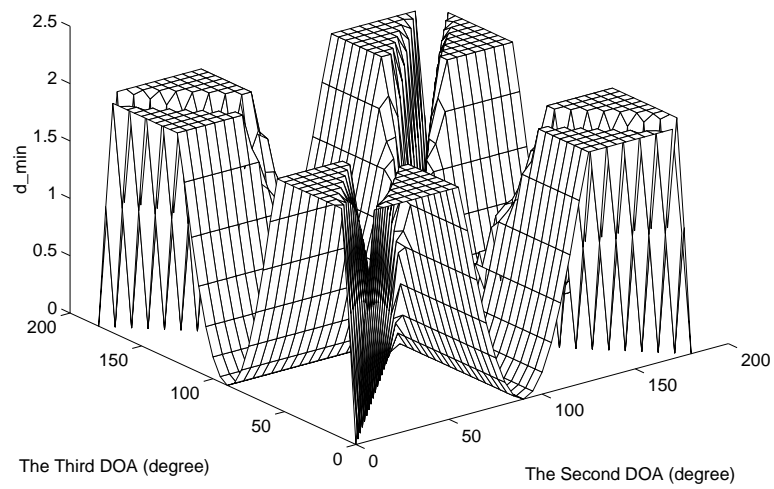


Figure 2.6: Minimum distance vs. the second user's DOA vs. the third user's DOA.

2.5 Summary

In this chapter, the minimum distance of the constellation of SDMA channels under different scenarios is investigated when the signals are restricted to a finite alphabet. The minimum distance formulation was derived by considering the simple two-user case. The minimum distance of SDMA channels were evaluated for different numbers of antennas, co-channel signals and relative user positions.

Here, the minimum distance criterion was primarily used to quantify the uplink performance enhancement promised by SDMA. For downlink SDMA signals; however, it is important to design broadcast or transmit weight vectors to achieve the maximum capacity of smart antenna systems. In the next chapter, the problem of designing optimum downlink weight vectors will be considered.

Chapter 3

Fast Estimation of Weight Vectors to Optimize Multi-Transmitter Broadcast Channel Capacity

Capacity of broadcast channels by employing multiple transmitters and exploiting the spatial diversity among the users is improved. We derive fast algorithms to compute *orthogonal*, *near-optimal*, and *optimal* weight vectors for broadcasting message signals to two and three users. The key innovation is that we decouple the weight vectors in the measure of channel capacity to simplify the optimization problem. Based on the decoupled formulation, we find the optimal solution by searching for the maxima of a smooth multidimensional function and derive closed-form expressions for the orthogonal and near-optimal solutions.

3.1 Introduction

In a multi-transmitter broadcast system, the weight vector for each message signal can provide an additional degree of freedom for signal enhancement and interference suppression by taking advantage of the spatial diversity among the users. Since Cover's novel work in single-transmitter broadcast channels [16], researchers have been exploring the use of both multi-transmitter and

multi-receiver systems [17, 18, 37]. In a multi-transmitter broadcast channel, an antenna array transmits to two or more receiving users. To optimize the performance of the communications system, we must find the weight vector for each message signal that maximizes the overall channel capacity. In this dissertation, we assume independent decoding since it is more feasible to implement in practical systems than joint decoding.

The design of the weight vectors that maximize the overall channel capacity of the broadcast channels, however, is still an open problem. The primary reason is that under certain power constraints, the channel capacity R is a highly nonlinear function of the M -dimensional weight vectors $\{\mathbf{w}_i\}$, where M is the number of transmitters [7]. Hence, finding a closed-form algebraic solution that maximizes R over $\{\mathbf{w}_i\}$ does not seem to be tractable.

In this chapter, we decouple the weight vectors in R to reduce the optimization problem to a search for the maxima of a smooth multidimensional function, which has $P(P - 1)$ dimensions for P users. Based on this decoupling, we derive two algorithms for computing orthogonal and optimal weight vectors for the two-user and three-user cases: orthogonal and optimal. We also present a near-optimum algorithm for the two-user case. The optimal algorithm requires an iterative search, whereas the orthogonal and near-optimal algorithms rely on closed-form solutions. The orthogonal and near-optimal algorithms require many fewer computations than the optimal algorithm, and can be implemented on a programmable digital signal processor. Section 3.2 states the problem. The decoupling of weight vectors and the algorithms for two-user case are given in Section 3.3 and in Section 3.4, respectively. Three-user case is investigated in Section 3.5. Section 3.6 compares the performance

of the algorithms.

3.2 Problem Statement

In [8], we consider maximizing the channel capacity in a two-user broadcast system with multiple transmitters. We let $\{s_i(t)\}$ be the set of message signals. The base station weighs each message signal with a *weight* vector and then transmits the superimposed signal of d users from an array of M elements ($d \leq M$):

$$\mathbf{y}(t) = \sum_{i=1}^d \beta_i \mathbf{w}_i s_i(t).$$

The signals $\{s_i(t)\}$ are assumed to be i.i.d. with Gaussian distribution; $\{\mathbf{w}_i\}$ is the set of normalized weight vectors, i.e., $\|\mathbf{w}_i\| = 1 \forall i = 1, \dots, d$; and $\{\beta_i\}$ is the set of the transmitting magnitudes which are subject to power constraints. For simplicity, we assume

$$\beta_1^2 + \dots + \beta_d^2 = 1.$$

If independent decoding were employed at the user receivers, then the achievable channel capacity R_i for each user i can be expressed as $\log(1 + \text{SINR})$, where SINR is the signal-to-interference noise ratio:

$$R_i = \frac{1}{2} \log \left(1 + \frac{\alpha_i^2 \beta_i^2 \mathbf{w}_i^H \mathbf{a}_i \mathbf{a}_i^H \mathbf{w}_i}{1 + \sum_{j=1, j \neq i}^d \alpha_j^2 \beta_j^2 \mathbf{w}_j^H \mathbf{a}_i \mathbf{a}_i^H \mathbf{w}_j} \right) \quad (3.1)$$

Here, $\mathbf{a}_i = (a_{i,1} \ a_{i,2} \ \dots \ a_{i,M})^T$ is a unit vector representing the direction of the spatial signature vector of the i^{th} user, and α_i is the magnitude of the spatial signature vector of the i^{th} user. Thus, the spatial signature vector, a.k.a. the

steering vector¹, of the i^{th} user represents the propagation pattern of the i^{th} user, and is equal to $\alpha_i \mathbf{a}_i$. The noise power has been normalized to unity.

The goal is to select the weight vectors $[\mathbf{w}_1 \cdots \mathbf{w}_d]$ that maximize the total channel capacity

$$R = \sum_{i=1}^P R_i. \quad (3.2)$$

Maximizing the total channel capacity is different than maximizing the signal-to-interference-noise (SINR) ratio for each user, as is seen in (3.1). Maximizing the SINR, however, is a first-order approximation to the total channel capacity. The first term in the Taylor series for $\log(1 + \text{SINR})$ about $\text{SINR} = 0$ is equal to SINR. To a first-order approximation, (3.2) is equal to $\text{SINR}_1 + \cdots + \text{SINR}_d$, which is the total SINR.

3.3 Decoupling Weight Vectors

Theorem 2 *The optimal weight vectors $\{\mathbf{w}_i\}$ that maximize the channel capacity are in signal subspace \mathbf{A} and can be written as linear combinations of spatial signature vectors $\{\mathbf{a}_i\}$.*

Proof:

$$\mathbf{w}_i = \lambda_{ai} \mathbf{A} + \lambda_{bi} \mathbf{B} \quad (3.3)$$

where $\mathbf{A} = [\mathbf{a}_1 \cdots \mathbf{a}_d]$ is the spatial signature matrix; $\mathbf{B} = [\mathbf{b}_{d+1} \cdots \mathbf{b}_M]$ which denotes the orthogonal subspace of \mathbf{A} , i.e., $\mathbf{A} \perp \mathbf{B}$; $\lambda_{ai} = [\lambda_{ai,1} \cdots \lambda_{ai,s}]$ and $\lambda_{bi} = [\lambda_{bi,s+1} \cdots \lambda_{bi,M}]$. Clearly, we have to show that $\|\lambda_{bi}\|^2 = 0$. As seen

¹This is only true for one direction of propagation.

from the capacity formulation in (3.2), $\{\lambda_{bi}\}$ will be in the power constraint

$$\|\mathbf{w}_i\| = \|\lambda_{ai}\|^2 + \|\lambda_{bi}\|^2 = 1. \quad (3.4)$$

We want $\|\lambda_{bi}\|^2 = 0$ so as not to waste any energy in the orthogonal subspace.

□

A similar theorem is also applicable to the case in which the average SINR is maximized [9].

3.4 Two-User Case

For a given pair of transmission magnitudes (β_1, β_2) and a given pair of spatial signatures $(\mathbf{a}_1, \mathbf{a}_2)$, our goal is to find the weight vectors \mathbf{w}_1 and \mathbf{w}_2 that optimize the total channel capacity $R = R_1 + R_2$. Denote

$$\begin{aligned} \kappa_{11} &= \mathbf{w}_1^H \mathbf{a}_1 \mathbf{a}_1^H \mathbf{w}_1 & \kappa_{12} &= \mathbf{w}_2^H \mathbf{a}_1 \mathbf{a}_1^H \mathbf{w}_2 \\ \kappa_{21} &= \mathbf{w}_1^H \mathbf{a}_2 \mathbf{a}_2^H \mathbf{w}_1 & \kappa_{22} &= \mathbf{w}_2^H \mathbf{a}_2 \mathbf{a}_2^H \mathbf{w}_2 \end{aligned} \quad (3.5)$$

where $\kappa_{ij} = \cos^2 \angle(\mathbf{w}_i, \mathbf{a}_j)$ is a measure of the angle between the i th weight vector and the j th spatial signature vector. Thus, each κ_{ij} term is confined to $[0, 1]$.

From (3.1) and (3.2), R is optimal that for certain κ_{11} and κ_{22} if the relationship between $\kappa_{21} = \mathbf{w}_1^H \mathbf{a}_2 \mathbf{a}_2^H \mathbf{w}_1 = \cos^2 \angle(\mathbf{w}_1, \mathbf{a}_2)$ and $\kappa_{12} = \mathbf{w}_2^H \mathbf{a}_1 \mathbf{a}_1^H \mathbf{w}_2 = \cos^2 \angle(\mathbf{w}_2, \mathbf{a}_1)$ is determined. We find the maximum values of κ_{11} and κ_{22} in terms of κ_{21} and κ_{12} or we find the minimum values of κ_{21} and κ_{12} in terms of κ_{11} and κ_{22} , respectively. By substituting (3.4) into the first two equations in (3.5) and normalizing \mathbf{w}_i so that $\mathbf{w}_1^H \mathbf{w}_1 = 1$,

$$\lambda_{11}^2 + \lambda_{12}^2 + 2\lambda_{11}\lambda_{12}\sqrt{\zeta} = 1 \quad (3.6)$$

$$\begin{aligned}\lambda_{11}^2 + \lambda_{12}^2 \zeta + 2\lambda_{11}\lambda_{12}\sqrt{\zeta} &= \kappa_{11} \\ \lambda_{11}^2 \zeta + \lambda_{12}^2 \zeta + 2\lambda_{11}\lambda_{12}\sqrt{\zeta} &= \kappa_{21}\end{aligned}$$

where

$$\zeta = \mathbf{a}_1^H \mathbf{a}_2 \mathbf{a}_2^H \mathbf{a}_1 = \cos^2 \angle(\mathbf{a}_1, \mathbf{a}_2). \quad (3.7)$$

so $0 \leq \zeta \leq 1$. Although $\{\lambda_{ij}\} = r_{\lambda_{ij}} e^{j\theta_{\lambda_{ij}}}$ and $\mathbf{a}_1^H \mathbf{a}_2 = \sqrt{\zeta} e^{j\theta_\zeta}$ are usually complex numbers, we can always adjust their phases so that they cancel each other out without affecting the values of κ_{ij} and the norm of the weight vectors and the spatial signature vectors. Therefore, we solve (3.6) for absolute values of λ_{11} , λ_{12} , and κ_{11} using Lagrange multipliers, and find the relationship between κ_{11} and κ_{21} to be [7]

$$\kappa_{11} = \left(\sqrt{\zeta \kappa_{21}} + \sqrt{(1-\zeta)(1-\kappa_{21})} \right)^2. \quad (3.8)$$

If we follow the same procedure for \mathbf{w}_2 , we will see that the similar function is true for \mathbf{w}_2 . The channel capacity can be rewritten in terms of κ_{12} and κ_{21} .

The optimization problem can be written as

$$\begin{aligned}\max_{\kappa_{12}, \kappa_{21}} \frac{1}{2} \log &\left(1 + \frac{\gamma_{11} \left(\sqrt{\zeta \kappa_{21}} + \sqrt{(1-\zeta)(1-\kappa_{21})} \right)^2}{1 + \gamma_{12} \kappa_{12}} \right) + \\ \frac{1}{2} \log &\left(1 + \frac{\gamma_{22} \left(\sqrt{\zeta \kappa_{12}} + \sqrt{(1-\zeta)(1-\kappa_{12})} \right)^2}{1 + \gamma_{21} \kappa_{21}} \right).\end{aligned} \quad (3.9)$$

subject to the constraints

$$\begin{aligned}0 &\leq \kappa_{12} \leq \zeta \leq 1 \\ 0 &\leq \kappa_{21} \leq \zeta \leq 1\end{aligned} \quad (3.10)$$

where

$$\begin{aligned}\zeta &= \mathbf{a}_1^H \mathbf{a}_2 \mathbf{a}_2^H \mathbf{a}_1 = \cos^2 \angle(\mathbf{a}_1, \mathbf{a}_2) \\ \gamma_{ij} &= \alpha_i^2 \beta_j^2 \text{ for } i, j = 1, 2.\end{aligned} \quad (3.11)$$

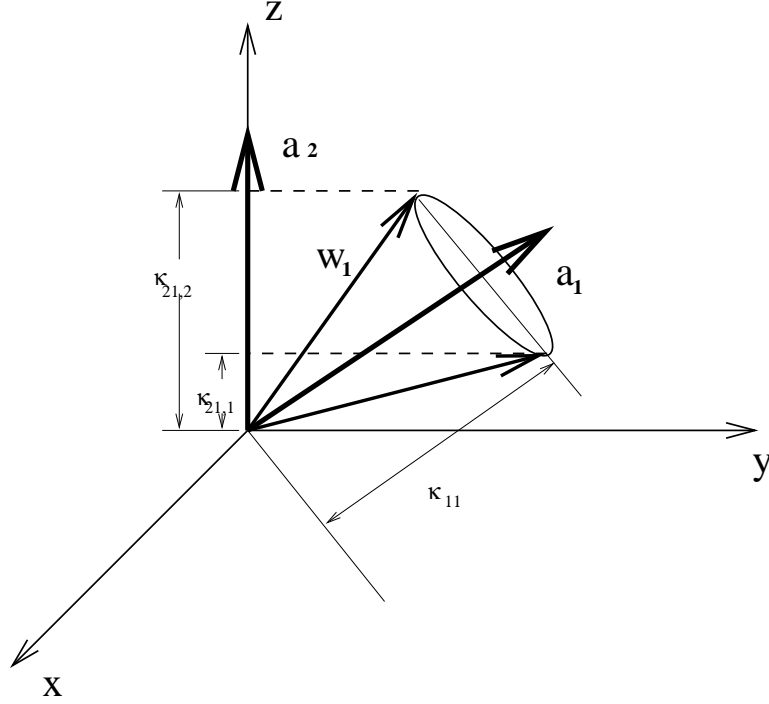


Figure 3.1: Illustration of search for an optimal weight vector.

3.4.1 Orthogonal Weight Vector Algorithm

Due to the additional degrees of freedom introduced by multiple transmitters, one can manipulate the complex weight vectors to enhance the desired signal while suppressing the interference. There exists \mathbf{w}_i such that $\mathbf{w}_i^H \mathbf{a}_i = \delta_{ij}$ which can completely eliminate the interference from one user to the other. When $\mathbf{w}_i^H \mathbf{a}_j = \delta(i-j)$, the channels are orthogonal and each message can be transmitted without interference. As shown in Figure 3.1, \mathbf{w}_1 should be in the direction of $\mathbf{P}_{\mathbf{a}_2}^\perp \mathbf{a}_1$, where $\mathbf{P}_{\mathbf{a}_2}^\perp$ denotes the projection operator onto the orthogonal space of \mathbf{a}_2 . Orthogonal weight vectors correspond to the following parameter values:

$$\begin{aligned} \kappa_{11} &= 1 - \zeta & \kappa_{12} &= 0 \\ \kappa_{21} &= 0 & \kappa_{22} &= 1 - \zeta \end{aligned} \quad (3.12)$$

1. Choose values for κ_{12} and κ_{21} .
2. For the given $(\kappa_{12}, \kappa_{21})$ pair, find the legitimate \mathbf{w}_1 which maximizes $\cos^2 \angle(\mathbf{w}_1, \mathbf{a}_1)$ and \mathbf{w}_2 which maximizes $\cos^2 \angle(\mathbf{w}_2, \mathbf{a}_2)$. Evaluate R using (3.9).
3. Repeat steps 1 and 2 for a finite number of times and identify the optimal pair $(\kappa_{12,opt}, \kappa_{21,opt})$ which maximize R in (3.9).
4. The weight vectors that correspond to $\kappa_{12,opt}$ and $\kappa_{21,opt}$ in step 2 are the solutions.

Figure 3.2: Optimum weight vector design with an iterative search algorithm for two-user case

However, this selection is generally not optimal in terms of channel capacity, since the desired signal power at the receiver may be reduced as well.

3.4.2 Optimal Weight Vector Algorithm

To find the optimal weight vectors, we maximize the non-linear objective function in (3.9) with respect to variables κ_{11} and κ_{22} subject to (3.10). The objective function is continuous and twice differentiable, the constraints are continuous and twice differentiable, and the solution space is convex. As a consequence, the optimization problem has a global maximum. Although a closed-form solution for the global maximum may not exist, numerical methods can be used to search for the global maximum. For example, the global optimum solution will always be found by the iterative Sequential Quadratic Programming method [38]. An alternative iterative search algorithm is proposed in Figure 3.2. Step 3 involves only a two-dimensional search, which is tractable but computational expensive. Next, we derive a near-optimum closed-form solution that is simple to compute.

3.4.3 Near-Optimal Weight Vector Algorithm

After substituting $\kappa_{21} = \cos^2(\theta_2)$, $\kappa_{12} = \cos^2(\theta_1)$, and $\zeta = \cos^2(\phi)$ into (3.9) and performing logarithmic manipulations, the channel capacity can be rewritten as

$$\frac{1}{2} \log(\mathbf{J}(\theta_1, \theta_2)) = \frac{1}{2} \log \left\{ \left(1 + \frac{\gamma_{11} \cos(\theta_2 - \phi)^2}{1 + \gamma_{12} \cos(\theta_1)^2} \right) \left(1 + \frac{\gamma_{22} \cos(\theta_1 - \phi)^2}{1 + \gamma_{21} \cos(\theta_2)^2} \right) \right\}. \quad (3.13)$$

The maximum total capacity of a two-user broadcasting system depends on two variables, θ_1 and θ_2 . These variables denote the angles between the weight vectors and the spatial signature vectors, as seen in (3.5). Since the logarithm is a monotonic, increasing, one-to-one function over the positive numbers, maximizing the total channel capacity in (3.13) is equivalent to maximizing $\mathbf{J}(\theta_1, \theta_2)$. A good initial guess at the optimum value is $\theta_1 = \phi$ and $\theta_2 = \phi$, which are the left endpoints of κ_{12} and κ_{21} , respectively, because they bring the cosine terms in the numerators in (3.13) to 1. We refine this approximation using perturbation (sensitivity) analysis to find the local optimal value [8]. The near optimum angle between the i th weight vector and the j th spatial signature vector is

$$\theta_i = \phi + 2 \cos^2(\phi) \Delta\theta_i \quad (3.14)$$

where

$$\Delta\theta_i = \frac{\gamma_{ji} \gamma_{jj} \cos(\phi) \sin(\phi) (1 + \gamma_{ii} + \gamma_{ij} \cos^2(\phi))}{\gamma_{ii} (1 + \gamma_{ji} \cos^2(\phi)) (1 + \gamma_{jj} + \gamma_{ji} \cos^2(\phi))} \quad (3.15)$$

such that $i, j = 1, 2$ and $i \neq j$. Since the perturbation analysis returns an approximation of the local optimum angles, the boundary conditions must be explicitly checked to ensure that the local optimum value is a local maximum. For each angle, two boundary conditions on k_{ij} (i.e., $\theta_i = \phi$ and $\theta_i = \pi$) and

1. Compute $\zeta = \cos^2(\phi)$ in (3.7) using the given $(\mathbf{a}_1, \mathbf{a}_2)$ spatial signature pair.
2. For $i = 1, 2$ and $j = 1, 2$, compute γ_{ij} in (3.11) using the given (α_i, β_j) values.
3. Compute near-optimum θ_1 and θ_2 angles in (3.14) and (3.15).
4. Check boundary conditions and near-optimum angle values by substituting all nine possible angle pairs for $\mathbf{J}(\theta_1, \theta_2)$ in (3.13) and keep the angle pair (θ'_1, θ'_2) that gives the largest value of $\mathbf{J}(\theta_1, \theta_2)$.
5. The weight vectors corresponding to (θ'_1, θ'_2) are the solutions.

Figure 3.3: Fast near-optimum weight vector method for the two-user case

one local optimum value (i.e., θ_i in (3.14)) exist. With two angles, a total of nine angle pairs (three times three) must be substituted into $\mathbf{J}(\theta_1, \theta_2)$ and the pair that produces the largest $\mathbf{J}(\theta_1, \theta_2)$ value is the local maximum. Using the closed-form solutions in (3.14), the near-optimum weight vectors can be found by the following algorithm in Figure 3.3. Also, Table 3.1 shows the implementation complexities of orthogonal and near-optimum solutions.

Operations	Orthogonal	Near-Optimal
Multiplications	2M	2M+12
Divisions	0	2

Table 3.1: Comparison of implementation complexity of orthogonal and near-optimal algorithm for two-user case.

3.5 Three-User Case

For the three-user case, I maximize the total channel capacity $R = R_1 + R_2 + R_3$.

As in the two-user case, denote

$$\kappa_{ji} = \cos^2 \angle(\mathbf{w}_i, \mathbf{a}_j). \quad (3.16)$$

Now, the focus of the problem is to find the relationship between κ_{ii} and $\{\kappa_{ji}, j \neq i\}$. Applying Theorem 1, we derive the following relation between κ_{11} and $(\kappa_{21}, \kappa_{31})$:

$$\begin{aligned} \kappa_{11} = & \left(\sqrt{\zeta_{12}\kappa_{21}} - \sqrt{\zeta_{13}\zeta_{23}\kappa_{21}} + \sqrt{\zeta_{13}\kappa_{31}} - \right. \\ & \left. \sqrt{\zeta_{12}\zeta_{23}\kappa_{31}} + \sqrt{(1 - \zeta_{12} - \zeta_{13} + 2\zeta_{12}\zeta_{13}\zeta_{23} - \zeta_{23})} \times \right. \\ & \left. \sqrt{(1 - \zeta_{23} - \kappa_{21} + 2\zeta_{23}\kappa_{21}\kappa_{31} - \kappa_{31})} \right)^2 / (1 - \zeta_{23})^2 \end{aligned} \quad (3.17)$$

where $\zeta_{ij} = \cos^2 \angle(\mathbf{a}_i, \mathbf{a}_j)$. Similar derivations can be carried out to find the relations between κ_{22} and $(\kappa_{12}, \kappa_{32})$ and between κ_{33} and $(\kappa_{13}, \kappa_{23})$. Using the relations, channel capacity can be expressed in terms of $(\kappa_{21}, \kappa_{31}, \kappa_{12}, \kappa_{32}, \kappa_{13}, \kappa_{23})$. For each κ_{ii} , the solution amounts to solving a set of linear equations and substituting the result into $\mathbf{w}^H \mathbf{w} = 1$. The parameter values for orthogonal weight vectors are $\kappa_{ij} = 0, i \neq j$ and $\kappa_{11} = (1 - \zeta_{12} - \zeta_{13} + 2\zeta_{12}\zeta_{13}\zeta_{23} - \zeta_{23}) / (1 - \zeta_{23})$, and $(\kappa_{22}, \kappa_{33})$ can be found similar to κ_{11} . However, as in the two-user case, this selection is generally not optimal in channel capacity. To find optimal weight vectors for the three-user case, we have to maximize the channel capacity with respect to variables $(\kappa_{21}, \kappa_{31}, \kappa_{12}, \kappa_{32}, \kappa_{13}, \kappa_{23})$. An iterative algorithm similar to the one in Section 3.4.2 can be used to search for the maximum.

3.6 Numerical Examples

Figure 3.4 compares the performance of our numerical search and the near-optimum closed-form algorithms with single antenna, orthogonal, and naive time-sharing schemes. The system uses a linear uniform array with 8 antenna elements to transmit to two users. The angle between spatial signature vectors and the gains of spatial signature vectors, respectively, are $\phi = 54^\circ$, $\alpha_1 = 1.22$, and $\alpha_2 = 1.333$. Figure 3.5 compares the maximum total capacity for the orthogonal weight vectors and the optimal weight vectors with respect to the angle between the spatial signatures. The difference between the two techniques becomes very significant when the angle between the spatial signature vectors is small.

3.7 Summary

The capacity of broadcast channels were improved by employing multiple transmitters and exploiting the spatial diversity among the users. Fast algorithms were developed to compute *orthogonal*, *near-optimal*, and *optimal* weight vectors for broadcasting message signals to two and three users. The key innovation is that the weight vectors are decoupled in the measure of channel capacity to simplify the optimization problem to a search for the maxima of a smooth multidimensional function and derive closed-form expressions for the orthogonal and near-optimal algorithms.

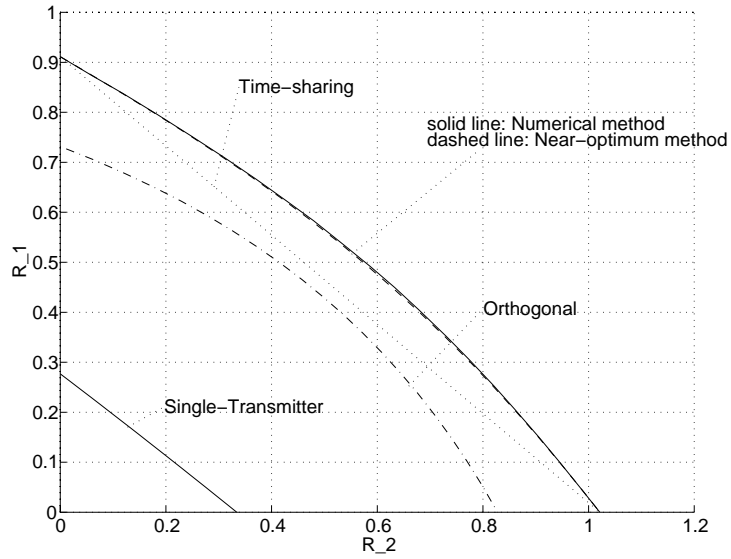


Figure 3.4: Channel capacity using different weight vectors. Near-optimum solution is within 1% of optimum capacity.

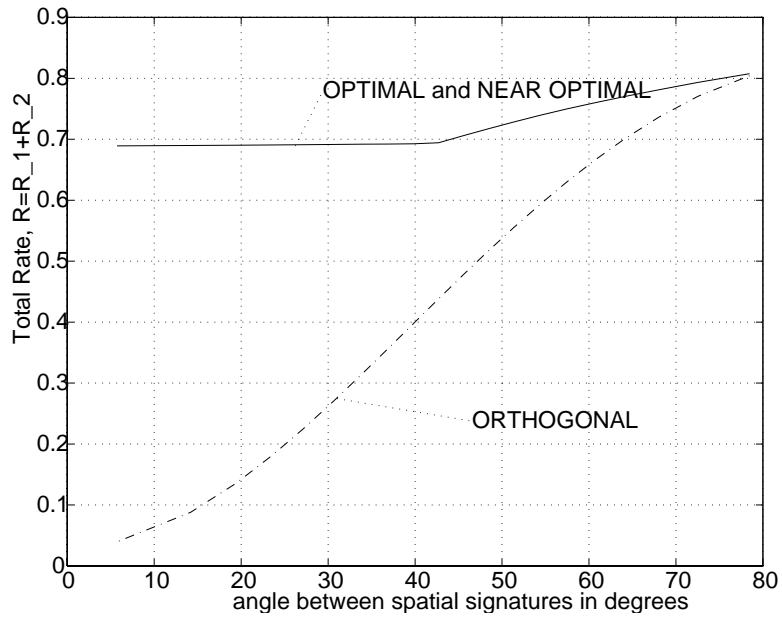


Figure 3.5: Maximum channel capacities vs. ϕ .

Chapter 4

Uplink Channel Estimation: CDMA Systems with Periodic Spreading Sequences

While the utilization of smart antenna systems has been very attractive in FDMA and TDMA, it can also be used in code division multiple access (CDMA) schemes such as the IS-95 standard. Direct sequence code division multiple access techniques underlie the IS-95 standard and the emerging third-generation wireless standards. CDMA offers efficient use of available bandwidth, resistance to interference, and adaptability to variable traffic patterns in mobile wireless systems. In CDMA systems, several independent users simultaneously use the same transmission medium, but are distinguishable at the receiver by different user-specific signature waveforms.

4.1 Introduction

If all mobile radio signals arriving at the base station are synchronized to within a fraction of a chip-time interval, then it is possible to reduce the effect of mutual interference dramatically [39]. For such synchronous CDMA (S-CDMA) systems, the use of orthogonal codewords can greatly enhance performance [34]. However, for large cells with large multipath delays, it may be difficult to synchronize mobile transmitters so that their signals arrive at the cell site

within a fraction of a chip time. The synchronization of the users in the reverse link becomes even more difficult as the data rate increases. Thus, the channels from mobile users to the base station are better characterized as asynchronous CDMA (A-CDMA).

A-CDMA systems are generally assumed to be more sensitive to co-channel interference than S-CDMA systems, since the transmission time of A-CDMA users is not coordinated. An A-CDMA receiver requires the suppression of multipath induced interchip-interference (ICI), which causes intersymbol interference (ISI), and highly structured multiple user interference (MUI). Moreover, the propagation delays should be incorporated in such receivers. A conventional receiver that is matched to the spreading code treats both ISI and MUI as noise. Hence, it is severely interference limited.

Conventional approaches in A-CDMA for estimating the channels rely on training sequences sent periodically [11]. Consequently, using training sequences causes a significant reduction of channel efficiency [26]. Alternatively, subspace-based algorithms [27, 28, 29, 30] have been successfully developed for different CDMA schemes which eliminates the use of training sequences. However, these methods are only applicable when the system is underloaded or when a few users are active. For instance, the methods proposed in [27, 28] will fail if the spreading gain (L_c) is less than four times of the number users (P), *i.e.* $L_c \leq 4P$. Although other subspace-based methods in [29, 30] have been proposed to estimate the associated time delay of each user, the method in [29] is only applicable to A-CDMA communication systems operating over an AWGN channel. The extension of this method in [30] can estimate the time delays of a few users, *i.e.* $P \leq L_c/(2L)$. Thus, new methods need to be

developed to *fully* exploit the rich structure inherent in CDMA systems.

By using smart antennas, we provide a method to handle overloaded systems, in which the number of users exceeds the spreading factor. However, the computation cost is relatively high due to complicated matrix manipulation which motivates further research efforts in implementation and simplification.

The rest of the chapter is organized as follows. Section 4.2 and Section 4.3 describe the signal model. Section 4.4 introduces the algorithm and discusses its implementation. Section 4.5 extends our algorithm to handle overloaded systems. Section 4.6 derives the MSE of the signature waveform estimates. Section 4.7 discusses the results of extensive computer simulations of the capacity of an A-CDMA system using the proposed approach. Section 4.8 describes RF field experiments conducted to validate the simulation results using the *Smart Antenna Testbed* at The University of Texas at Austin. Section 4.9 gives a summary.

4.2 Model and Data Formulation

To simplify the derivation, we temporarily ignore the noise and leave the accommodation of noisy data for later discussion. We describe an A-CDMA baseband signal with a single receiver from P users as

$$x(t) = \sum_{i=1}^P \sum_{n=-\infty}^{\infty} s_i(n)g_i(t - nT_s) \quad (4.1)$$

where subscript i denotes the user index; P is the number of users; $\{s_i(n)\}$ is the set of information symbols from a finite set of alphabets, *e.g.*, $\{\pm 1\}$ for BPSK; T_s is the symbol duration. Assume that $\{c_i(1), c_i(2), \dots, c_i(L_c); c_i(k) = \pm 1\}$ is the preassigned spreading code of the i^{th} user; and L_c is the code length.

The signature waveform of the i^{th} user with support $t \in [0, L_g^{(i)}T_s]$ is defined as

$$g_i(t) = \sum_{k=1}^{L_g^{(i)}L_c} c_i(k - k_i)h_i(t - kT) \quad (4.2)$$

where T is the chip duration; k_i is the chip delay index; and $\{h_i(t)\}$ is the set of channels which represents the multipath fading environment between the users and the receiver. It is generally plausible to model $\{h_i(t)\}$ as a finite impulse response (FIR) filter which has a finite support $t \in [0, LT]$ [19]. In addition, we may assume that the channel order $L \ll L_c$ since the maximum delay spread of the channel is usually insignificant relative to the symbol period T_s [40]. Thus, depending upon the relative time delay and the channel length, the signature waveforms may last at most three symbol periods. For the sake of simplicity, we assume $L_g^{(i)} = 2$ for each user throughout the paper.

4.3 Discrete-Time Representation

By sampling (4.1) at the chip rate so that $T_s = L_cT_c$ and $t = lT_c$, and we obtain

$$x(l) = \sum_{i=1}^P \sum_{n=-\infty}^{\infty} s_i(n)g_i(l - nL_c) \quad (4.3)$$

We may represent the data vector which is composed of samples with a symbol period in a matrix form \mathbf{X} as

$$\begin{bmatrix} x((N - n)L_c + 1) & x((N - n + 1)L_c + 1) & \cdots & x((2N - 1 - n)L_c + 1) \\ x((N - n)L_c + 2) & x((N - n + 1)L_c + 2) & \cdots & x((2N - 1 - n)L_c + 2) \\ \vdots & \vdots & \cdots & \vdots \\ x((N - n + 1)L_c) & x((N - n + 2)L_c) & \cdots & x((2N - n)L_c) \end{bmatrix}. \quad (4.4)$$

Using the assumption that $L_g^{(i)} = 2 \forall i$, the discrete counterpart of the signature waveform in (4.2) is given by

$$g_i(l) = \sum_{k=1}^{2L_c} c_i(k - k_i)h_i(l - k) = \sum_{k=1}^L h_i(k)c_i(l - k + k_i), \quad l = 1, \dots, 2L_c \quad (4.5)$$

where k_i is the chip delay index which is known to the receiver. Although we assume that the set of $\{k_i\}$ is known during the derivation phase of our algorithm, we introduce a blind initialization scheme to estimate $\{k_i\}$ in [32].

The convolution in (4.5) can be represented as

$$\mathbf{g}_i = \begin{bmatrix} \mathbf{g}_i(1) \\ \mathbf{g}_i(2) \end{bmatrix} = \underbrace{\begin{bmatrix} 0 & \cdots & c_i(1) & c_i(2) & \cdots & c_i(L_c) & 0 & 0 & \cdots & 0 \\ 0 & \cdots & 0 & c_i(1) & c_i(2) & \cdots & c_i(L_c) & 0 & \cdots & 0 \\ \vdots & \vdots & \ddots & \ddots & \ddots & \ddots & \ddots & \ddots & \ddots & \vdots \\ 0 & \cdots & 0 & 0 & c_i(1) & c_i(2) & \cdots & c_i(L_c) & \cdots & 0 \end{bmatrix}^T}_{\mathbf{c}_i, 2L_c \text{ blocks}} \mathbf{h}_i \quad (4.6)$$

where \mathbf{c}_i is the *kernel* matrix with dimension $2L_c \times L$. If we partition

$$\mathbf{c}_i = \begin{bmatrix} \mathbf{c}_i(1) \\ \mathbf{c}_i(2) \end{bmatrix}, \quad \mathbf{c}_i(j) \text{ is } L_c \times L, \quad j = 1, 2, \quad (4.7)$$

then

$$\mathbf{g}_i(j) = \mathbf{c}_i(j) \mathbf{h}_i, \quad j = 1, 2. \quad (4.8)$$

The set $\{\mathbf{g}_i\}$ is uniquely determined by the unknown channel vectors $\{\mathbf{h}_i\}$. For consistency, we assume that $\{\mathbf{h}_i\}$ are of unit norm, *i.e.* $\|\mathbf{h}_i\| = 1$. Thus, (4.8) becomes $\mathbf{g}_i(j) = \alpha_i \mathbf{c}_i(j) \mathbf{h}_i$ where α_i is the complex gain of the signal from the i^{th} user.

Stacking KL_c successive samples of the received signal in vector form, we obtain

$$\mathbf{X} = \begin{bmatrix} \mathbf{X}(N) \\ \mathbf{X}(N-1) \\ \vdots \\ \mathbf{X}(N-K+1) \end{bmatrix} = \underbrace{\begin{bmatrix} \mathbf{G}_1 & \mathbf{G}_2 & \cdots & \mathbf{G}_P \end{bmatrix}}_{\mathbf{G}} \underbrace{\begin{bmatrix} \mathbf{S}_1(r) \\ \mathbf{S}_2(r) \\ \vdots \\ \mathbf{S}_{P(r)} \end{bmatrix}}_{\mathbf{S}}$$

$$\mathbf{X} = \sum_{i=1}^P \mathbf{X}_i = \sum_{i=1}^P \mathbf{G}_i \mathbf{S}_i(r) \quad (4.9)$$

where K is defined as the *smoothing factor* and $r = K + 1$. Then, we describe the algebraic relation between the input and output matrices \mathbf{X}_i for the i^{th} user as

$$\underbrace{\begin{bmatrix} \mathbf{g}_i(2) & \mathbf{g}_i(1) & \mathbf{0} & \cdots & \mathbf{0} \\ \mathbf{0} & \mathbf{g}_i(2) & \mathbf{g}_i(1) & \cdots & \mathbf{0} \\ \vdots & \vdots & \ddots & \ddots & \vdots \\ \mathbf{0} & \cdots & \mathbf{0} & \mathbf{g}_i(2) & \mathbf{g}_i(1) \end{bmatrix}}_{\mathbf{G}_i, K+1 \text{ blocks}} \underbrace{\begin{bmatrix} s_i(1) & s_i(2) & \cdots & s_i(N-r+1) \\ s_i(2) & s_i(3) & \cdots & s_i(N-r+2) \\ \vdots & \vdots & \cdots & \vdots \\ s_i(r) & s_i(r+1) & \cdots & s_i(N) \end{bmatrix}}_{\mathbf{S}_i(r), r=K+1}. \quad (4.10)$$

The *signature waveform* matrix \mathbf{G}_i associated with user i has rich structure which we can exploit to improve system performance. Denoting

$$\mathbf{G}_i = \underbrace{\begin{bmatrix} \mathbf{c}_i(2) & \mathbf{c}_i(1) & \mathbf{0} & \cdots & \mathbf{0} \\ \mathbf{0} & \mathbf{c}_i(2) & \mathbf{c}_i(1) & \cdots & \mathbf{0} \\ \vdots & \vdots & \ddots & \ddots & \vdots \\ \mathbf{0} & \cdots & \mathbf{0} & \mathbf{c}_i(2) & \mathbf{c}_i(1) \end{bmatrix}}_{\mathbf{C}_i, (K+1) \times L} \underbrace{\begin{bmatrix} \mathbf{h}_i & \mathbf{0} & \cdots & \mathbf{0} \\ \mathbf{0} & \mathbf{h}_i & \vdots & \vdots \\ \vdots & \vdots & \ddots & \vdots \\ \mathbf{0} & \cdots & \mathbf{0} & \mathbf{h}_i \end{bmatrix}}_{\mathbf{H}_i, K+1 \text{ blocks}} \quad (4.11)$$

\mathbf{C}_i is the *Toeplitz kernel* matrix. When $K = 1$, the signature waveform matrix \mathbf{G} has a dimension of $L_c \times 2P$. It cannot be of full column rank if the spreading factor is less than twice as the number of users, *i.e.* $L_c < 2P$. Before we derive our method, the primary differences between our method and other existing *blind* subspace channel estimation methods [27, 28, 31] are how to construct the data matrix and how much of the data structure the method exploits. In our model, we arrange the data vectors so that the data matrix has a Hankel block structure. We use the Hankel structure to smooth output data vectors and to restore the rank of \mathbf{G} up to $P \approx L_c$ so that we accommodate more users than

existing techniques. Moreover, when $P > L_c$, it is always possible to restore the rank of \mathbf{G} by employing multiple receivers, which we will elaborate on in Section 4.5.

4.4 Multi-User Channel Estimation

The previous section derives a restrictive structure for \mathbf{G} in which $\mathbf{G}_i = \mathbf{C}_i \mathbf{H}_i$. Therefore, the estimation of the signature vectors is equivalent to the determination of the channel vectors. In the presence of additive white noise, the data matrix becomes

$$\mathbf{X} + \mathbf{N} = \mathbf{G}\mathbf{S} + \mathbf{N}.$$

In a manner similar to standard blind methods [41, 42], we perform subspace decomposition of $X + N$ using singular value decomposition (SVD) [43]

$$\mathbf{X} + \mathbf{N} = \begin{pmatrix} \mathbf{U}_s & \mathbf{U}_o \end{pmatrix} \begin{pmatrix} \boldsymbol{\Sigma}_s & \mathbf{0} \\ \mathbf{0} & \boldsymbol{\Sigma}_o \end{pmatrix} \begin{pmatrix} \mathbf{V}_s^H \\ \mathbf{V}_o^H \end{pmatrix} = \mathbf{U}_s \boldsymbol{\Sigma}_s \mathbf{V}_s^H + \mathbf{U}_o \boldsymbol{\Sigma}_o \mathbf{V}_o^H \quad (4.12)$$

The vectors in \mathbf{U}_s , associated with the L_s *signal* eigenvalues, span the *signal subspace* defined by the columns of \mathbf{G} . The vectors in \mathbf{U}_o , associated with the L_o *noise* eigenvalues, span the *noise subspace*

$$\mathbf{U}_o = [\mathbf{U}_1 \ \mathbf{U}_2 \ \cdots \ \mathbf{U}_{KL_c - P(K+1)}]. \quad (4.13)$$

The dimensions of \mathbf{U}_s and \mathbf{U}_o are $KL_c \times P(K+1)$ and $KL_c \times KL_c - P(K+1)$. Due to the orthogonality between the noise subspace and the signal subspace, the columns of \mathbf{G} are orthogonal to any vector in the noise subspace. Therefore, we have

$$\mathbf{U}_o \perp \mathbf{G} \Rightarrow \mathbf{U}_o^H \mathbf{G}_i = \mathbf{0}, \quad i = 1, \dots, P, \quad (4.14)$$

where $(\cdot)^H$ denotes the transpose conjugation operation. Here, we assume that (i) the set $\{\mathbf{g}_i\}$ in \mathbf{G} are linearly independent and (ii) \mathbf{S} has more than $P(K+1)$ columns and is of full row rank. Both are reasonable conditions considering the randomness of the symbol sequences and multipath channels [31].

4.4.1 Algorithm

We develop an algorithm to estimate $\{\mathbf{G}_i\}$ from \mathbf{X} without the knowledge of \mathbf{S} . The structure of $\{\mathbf{G}_i\}$ can be used to link the orthogonal subspace with the channel vector estimation. Substituting $\mathbf{G}_i = \mathbf{C}_i \mathbf{H}_i$ into (4.14) yields

$$\mathbf{U}_o^H \mathbf{C}_i \mathbf{H}_i = \mathbf{0}, \quad i = 1, \dots, P. \quad (4.15)$$

This indicates that the channels can be determined from the orthogonal subspace of the data matrix \mathbf{X} . Thus, we can identify $\{\mathbf{H}_i\}$ constructed from the estimated channel vectors as

$$\hat{\mathbf{h}}_i = \arg \min_{\|\mathbf{h}_i\|=1} \mathbf{h}_i^H \mathbf{c}_i^H \left(\sum_{l=1}^{KL_c - P(K+1)} \tilde{\mathbf{U}}_l \tilde{\mathbf{U}}_l^H \right) \mathbf{c}_i \mathbf{h}_i \quad (4.16)$$

where

$$\tilde{\mathbf{U}}_l = \begin{bmatrix} \mathbf{u}_1^{(l)} & \mathbf{u}_2^{(l)} & \dots & \mathbf{u}_K^{(l)} & \mathbf{0} \\ \mathbf{0} & \mathbf{u}_1^{(l)} & \mathbf{u}_2^{(l)} & \dots & \mathbf{u}_K^{(l)} \end{bmatrix}, \quad \mathbf{U}_l = \begin{bmatrix} \mathbf{u}_1^{(l)} \\ \vdots \\ \mathbf{u}_K^{(l)} \end{bmatrix}, \quad \mathbf{u}_k^{(l)} \text{ is } L_c \times 1, \quad k = 1, \dots, K. \quad (4.17)$$

If $KL_c - P(K+1) \geq L/2$, then (4.15) is generally an overdetermined set of linear equations and has a nontrivial solution. Equations (4.15) and (4.16) efficiently compute the channel vector up to a phase ambiguity directly from the data matrix.

1. Construct the data matrix \mathbf{X} in (4.9).
2. Apply SVD to \mathbf{X} , or equivalently, eigenvalue decomposition (EVD) to $\mathbf{X}\mathbf{X}^H$ to obtain the orthogonal subspace \mathbf{U}_o .
3. For each user, estimate the channel vector \mathbf{h}_i using (4.16).
4. Reconstruct the signature vectors $\{\mathbf{g}_i\}$ and $\{\mathbf{G}_i\}$ from (4.10) and (4.5), respectively.

Figure 4.1: Blind multi-user channel estimation algorithm

An outline of the algorithm is given in Figure 4.1. This algorithm exploits the fact that each signature vector is a *linear* function of a unique spreading code. Thus it is possible to determine \mathbf{h}_i using linear operations on the noise-free data vectors. The major computational cost in the proposed algorithm comes from the subspace decomposition of the data matrix. The recent development of fast subspace decomposition techniques provides computationally efficient and easily applicable methods for data decomposition [44].

Since the implementation of some multiuser detectors, *i.e.* MMSE multiuser detector, requires the knowledge of the signal power with gain $\sigma_s^2|\alpha_i|^2$ and the noise power σ_n^2 , we now consider a method for estimating the received power of the signals and the noise. We assume that both noise and symbols in \mathbf{S} are zero-mean *i.i.d.* with variance σ_n^2 and σ_s^2 , respectively. Note that

$$\tilde{\mathbf{R}}_{\mathbf{X}} = \frac{1}{N} (\mathbf{X} + \mathbf{N})(\mathbf{X} + \mathbf{N})^H = \mathbf{G}\tilde{\Sigma}_s^2\mathbf{G}^H + \sigma_n^2\mathbf{I}, \quad (4.18)$$

where $\tilde{\mathbf{R}}_{\mathbf{X}}$ is the sample data covariance matrix. The noise power can be determined by the least significant eigenvalue of $\tilde{\mathbf{R}}_{\mathbf{X}}$. Using the channel estimates,

the signal power and gains can be estimated by

$$\begin{pmatrix} \hat{\sigma}_s^2 |\hat{\alpha}_1|^2 & & 0 \\ & \ddots & \\ 0 & & \hat{\sigma}_s^2 |\hat{\alpha}_P|^2 \end{pmatrix} = [\hat{\mathbf{g}}_1, \dots, \hat{\mathbf{g}}_P]^\dagger \tilde{\mathbf{R}}_{\mathbf{X}} [\hat{\mathbf{g}}_1, \dots, \hat{\mathbf{g}}_P]^{\dagger H} - \hat{\sigma}_n^2 \mathbf{I}.$$

where \dagger denotes the left pseudo-inverse.

4.4.2 Identifiability

As stated earlier, the number of users P must satisfy $KL_c \geq P(K+1) + L/2$ or $P \leq (KL_c + L/2)/(K+1)$ in order to determine $\{\mathbf{h}_i\}$. However, this is only a necessary condition for a unique channel vector estimate. From (4.16), it is clear that the determination of the signature vector for the noise-free case is simply a matter of finding a vector $\hat{\mathbf{g}}_i$ within the span of the kernel matrix and the signal subspace

$$\{\hat{\mathbf{G}}_i : \hat{\mathbf{G}}_i \perp \mathbf{U}_o, \hat{\mathbf{G}}_i \in \text{span}(\mathbf{C}_i)\}$$

where $\text{span}(\cdot)$ denotes the column range span. The true signature vector \mathbf{g}_i (\mathbf{G}_i) obviously satisfies the above condition. The sufficient and necessary condition is given by Theorem 3.

Theorem 3 \mathbf{g}_i can be uniquely determined from (4.16) if and only if the dimension of $\{\text{span}(\mathbf{c}_i) \cap \text{span}([\mathbf{g}_1, \dots, \mathbf{g}_P])\}$ is equal to 1.

Proof:

The proof is immediate. Suppose \mathbf{g}_i and $b_k \mathbf{g}_i^k$, $k = 1, \dots, n$ are a basis for $\{\text{span}(\mathbf{c}_i) \cap \text{span}([\mathbf{g}_1, \dots, \mathbf{g}_P])\}$, in other words they are vectors both in $\text{span}(\mathbf{c}_i)$ and in $\text{span}([\mathbf{g}_1, \dots, \mathbf{g}_P])$. Then, $\dim(\{\text{span}(\mathbf{c}_i) \cap \text{span}([\mathbf{g}_1, \dots, \mathbf{g}_P])\}) = n + 1$.

The dimension of the null space of $\mathbf{U}_o^H \mathbf{c}_i$ will be $n + 1$. In order to uniquely determine \mathbf{g}_i , the condition of $b_k = 0$, $k = 1, \dots, n$ must be satisfied. \square

An interesting observation of Theorem 3 is that even if the channel vector cannot be uniquely determined, e.g. when \mathbf{c}_i is *ill-conditioned*, then the signature vector still has a unique solution provided that the *if and only if* condition is satisfied. Although \mathbf{c}_i cannot be rank deficient, it may have a large *eigenvalue spread* [11]. When \mathbf{c}_i has a large *eigenvalue spread*, the MSE of the channel vector estimates becomes larger than that of the signature waveform estimates in the noisy case. An illustrative example for this claim is given in Section 4.7.

4.4.3 Blind Initial Synchronization

In the algorithm derivation in Section 4.4.1, we assumed that the users' delays were known to the receiver or were estimated. The procedure for establishing initial synchronization is critical to the algorithm performance. Therefore, the proposed algorithm must resort to estimating the chip time delay index for each user defined in Section 4.2. The problem of initial synchronization may still be viewed as searching for the best possible \mathbf{g}_i . I denote

$$\mathbf{Q}_{ik} = \mathbf{c}_{ik}^H \left(\sum_{l=1}^{KL_c - P(K+1)} \tilde{\mathbf{U}}_l \tilde{\mathbf{U}}_l^H \right) \mathbf{c}_{ik} \quad (4.19)$$

where \mathbf{c}_{ik} is the *kernel* matrix as in (4.6) by letting $k_i = k$; $k = 0, \dots, L_c - 1$.

The channel vector and delay of the i th user can be estimated by optimizing

$$J(\hat{\mathbf{h}}_i, \hat{k}_i) = \bar{\mathbf{h}}_i^H \begin{bmatrix} \mathbf{Q}_{i1} & \mathbf{0} & \cdots & \mathbf{0} \\ \mathbf{0} & \mathbf{Q}_{i2} & \cdots & \mathbf{0} \\ \vdots & \vdots & \ddots & \vdots \\ \mathbf{0} & \cdots & \mathbf{0} & \mathbf{Q}_{iL_c} \end{bmatrix} \bar{\mathbf{h}}_i, \quad (4.20)$$

where

$$\bar{\mathbf{h}}_i = \left[\underbrace{0 \ \cdots \ 0}_{Lk_i} \quad \mathbf{h}_i^H \quad \underbrace{0 \ \cdots \ 0}_{L(L_c - k_i - 1)} \right]^H. \quad (4.21)$$

To avoid the trivial all-zero solution, we use a power constraint $\|\mathbf{h}_i\| = 1$ ($\|\hat{\mathbf{h}}_i\| = 1$). After acquiring the chip delay index of each user, the channel vector estimation procedure can be switched to the original algorithm in Section 4.4.1. An alternative approach for estimating the channel vectors $\{\mathbf{h}_i\}$ with unknown delays is to overestimate the channel orders, *i.e.*, $L_c + L - 1$. In other words, we construct $\{\mathbf{c}_i\}$ the *kernel* matrixes with a dimension of $2L_c \times (L_c + L - 1)$ instead $2L_c \times L$. The drawback of this approach is that the number of unknowns increases from $L/2$ to $(L_c + L - 1)/2$. Therefore, when $K = 1$, the number of users P whose channel vectors can be estimated may not exceed $L_c/4$ due to the inadequacy of the dimension of the orthogonal subspace \mathbf{U}_o . However, as K increases, this approach converges to the original method.

In practice, after the initial estimation of the delays, it is necessary to update the delay estimates in a time-varying wireless communication environment. One method of tracking delay for each user is constructing $\{\mathbf{Q}_{ik}\}$ as in (4.19) using a longer channel order L_e ($> L$) and minimizing $J(\hat{\mathbf{h}}_i, \hat{k}_i)$ in (4.20). Let us first consider the noise-free case. If we use a longer channel order L_e , form $\{\mathbf{Q}_{ik}\}$ in (4.19), and minimize $J(\hat{\mathbf{h}}_i, \hat{k}_i)$ in (4.20), then $J(\hat{\mathbf{h}}_i, \hat{k}_i)$ has $L_e - L + 1$ zeros. We claim that any of the following $L_e - L + 1$ channel vectors

$$\{\underbrace{[0 \ \dots \ 0]}_l \mathbf{h}_i^T \underbrace{[0 \ \dots \ 0]}_{L_e-L-l}\}^T, l = 0, \dots, L_e - L \quad (4.22)$$

is a solution to $J(\hat{\mathbf{h}}_i, \hat{k}_i)$, $L_e > L$. Therefore, the chip delay index estimate may be updated as

$$\hat{k}_i = \hat{k}_i + l, \quad l = 0, \dots, L_e - L$$

depending upon which vector we choose from (4.22). In the presence of additive noise, we can detect $L_e - L + 1$ zeros by checking how many smaller values of $J(\hat{\mathbf{h}}_i, \hat{k}_i)$ are below a predetermined threshold. This subject is also related to the channel order selection which is discussed in the next section.

4.4.4 Channel order selection

In the settings of the previous section, we assumed that (i) the channel orders for all users are equal, (ii) the channel order L is known, and (iii) the orders of the signature waveforms for all users $L_g^{(i)}$ are equal ($L_g^{(i)} = 2$). While the first assumption can be relaxed further, the last two conditions are only made for convenience of presentation. These assumptions do not imply that the channels and signature waveforms should actually be of the same length. The orders of signature waveforms may vary from 1 to 3 depending upon the users' delays and the channel orders. The modification of the algorithm corresponding to this variation is straightforward. If the channel order for each user is known *a priori*, then the computational cost of the algorithm can be considerably reduced. In other words, additional zeros in \mathbf{h}_i will not affect the signature vector estimates. Based on this property, L should be determined by the *maximum* channel order among all users. In practice, one may select the maximum channel spread value [19] for a particular application.

4.5 Capacity Increase via Smart Antennas

An A-CDMA system with code length L_c cannot accommodate more than L_c users. Also in a multipath fading environment, the system performance becomes more sensitive to the capacity increase because the signature correlations become significant. The employment of the multiuser detector and sometimes multiple receivers may be imperative. The increase of system capacity by using multiple receivers (antenna array) has been discussed by many researchers [15, 45, 46].

Since the maximum number of signature waveforms is limited to $P \leq L_c K / (K + 1) \approx L_c$ in the proposed approach, we need to adjust the algorithm so that it can manage an overloaded system ($P \geq L_c$). The breakdown of the proposed algorithm in an overloaded system is due to the inadequacy of (4.16), since the dimension of the orthogonal subspace \mathbf{U}_o reduces and may eventually become zero as the number of users increase. To implement the subspace algorithm, additional orthogonal vectors are required to guarantee more equations than unknowns. This can be achieved by spatially oversampling by means of multiple receivers.

Assume M receivers at the base station and denote the superscript as the receiver index. We may stack the data vectors (matrices), the signature vectors, and the channel vectors from all receivers as follows:

$$\mathbf{X} = \begin{bmatrix} \mathbf{X}^1 \\ \vdots \\ \mathbf{X}^M \end{bmatrix} = \sum_{i=1}^P \underbrace{\begin{bmatrix} \mathbf{G}_i^1 \\ \vdots \\ \mathbf{G}_i^M \end{bmatrix}}_{\mathbf{G}_i} \mathbf{S}_i(r). \quad (4.23)$$

$\mathbf{X} = \mathbf{G}\mathbf{S}$ still holds, and so does the subspace space relation between \mathbf{X} and \mathbf{G} . However, the number of orthogonal vectors in \mathbf{U}_o has been substantially

increased to $MKL_c - P(K + 1)$. The number of vectors in \mathbf{U}_s remains fixed. The set $\{\mathbf{G}_i\}$ is given by the solution of the following linear equations through a new kernel matrix

$$\mathbf{U}_o^H \underbrace{\begin{bmatrix} \mathbf{C}_i & \mathbf{0} \\ \mathbf{0} & \mathbf{C}_i \end{bmatrix}}_{M \text{ blocks}} \mathbf{H}_i = \mathbf{0}; \quad i = 1, \dots, P. \quad (4.24)$$

The signature vector \mathbf{g}_i is determined by the ML -channel vector \mathbf{h}_i whose estimate can be formulated as

$$\hat{\mathbf{h}}_i = \arg \min_{\|\mathbf{h}_i\|=1} \mathbf{h}_i^H \begin{bmatrix} \mathbf{c}_i & \mathbf{0} \\ \mathbf{0} & \mathbf{c}_i \end{bmatrix}^H \left(\sum_{l=1}^{L_o} \tilde{\mathbf{U}}_l \tilde{\mathbf{U}}_l^H \right) \begin{bmatrix} \mathbf{c}_i & \mathbf{0} \\ \mathbf{0} & \mathbf{c}_i \end{bmatrix} \mathbf{h}_i \quad (4.25)$$

Because of the additional diversity provided by the multiple receivers, the number of equations vs. the number of unknowns is now $MKL_c - P(K + 1)$ vs. $ML/2$, which means that in theory, $P \approx ML_c$ channels can be estimated and A-CDMA systems can accommodate more users.

4.6 Algorithm Performance

The first-order performance of the proposed algorithm is analyzed in this section. The analysis is based on a single receiver A-CDMA system model and we resort to the first order perturbation theory introduced in [47] to derive the bias and MSE expression of the signature waveform estimates. We have also imported the following Lemma from [47].

Lemma 1 *Let*

$$\mathbf{X} = \begin{pmatrix} \mathbf{U}_s & \mathbf{U}_o \end{pmatrix} \begin{pmatrix} \Sigma_s & \mathbf{0} \\ \mathbf{0} & \mathbf{0} \end{pmatrix} \begin{pmatrix} \mathbf{V}_s^H \\ \mathbf{V}_o^H \end{pmatrix} \quad (4.26)$$

be the SVD of \mathbf{X} , and \mathbf{N} be an additive perturbation to \mathbf{X} . The first order approximation of the perturbation to \mathbf{U}_o is given by

$$\Delta\mathbf{U}_o = -\mathbf{U}_s\boldsymbol{\Sigma}_s^{-1}\mathbf{V}_s^H\mathbf{N}^H\mathbf{U}_o = -\mathbf{X}^\dagger\mathbf{N}^H\mathbf{U}_o \quad (4.27)$$

where \dagger denotes the pseudo-inverse. This Lemma states a general first-order expression to study the perturbation of subspaces. In [37], this expression was applied to obtain perturbation of the direction-of-arrival estimates which are single quantities in a different framework. However, we applied this expression to our problem where the estimates are vector quantities. For simplicity of derivation, we consider the data matrix $\mathbf{X} = [\mathbf{X}(N) \ \mathbf{X}(N-1)]^T$ by setting the *smoothing factor* $K = 2$. Thus, the noise corrupted data matrix can be written as

$$\mathbf{X} + \mathbf{N} = \mathbf{G}\mathbf{S} + \mathbf{N}.$$

By Lemma 1, the perturbation of the orthogonal subspace \mathbf{U}_o can be expressed as

$$\Delta\mathbf{U}_o = -\mathbf{X}^\dagger\mathbf{N}^H\mathbf{U}_o. \quad (4.28)$$

Denote $\mathbf{T}_i = \mathbf{c}_i^H\mathbf{U}_o$, it immediately follows that

$$\Delta\mathbf{T}_i = \mathbf{c}_i^H\Delta\mathbf{U}_o = -\mathbf{c}_i^H\mathbf{X}^\dagger\mathbf{N}^H\mathbf{U}_o. \quad (4.29)$$

Since in the noise free case, the \mathbf{h}_i estimate is obtained from the unitary null vector of \mathbf{T}_i , we can apply Lemma 1 again and obtain the perturbation term of the channel estimate,

$$\Delta\mathbf{h}_i = -\mathbf{T}_i^\dagger\Delta\mathbf{T}_i^H\mathbf{h}_i. \quad (4.30)$$

Substituting (4.29) into the above equation yields

$$\Delta \mathbf{h}_i = \mathbf{T}_i^\dagger \mathbf{U}_o^H \mathbf{N} \mathbf{X}^{\dagger H} \underbrace{\mathbf{c}_i \mathbf{h}_i}_{\mathbf{g}_i}. \quad (4.31)$$

Consequently, the perturbation of the waveform estimate is given by

$$\Delta \mathbf{g}_i = \mathbf{c}_i \Delta \mathbf{h}_i = \mathbf{c}_i \mathbf{T}_i^\dagger \mathbf{U}_o^H \mathbf{N} \mathbf{X}^{\dagger H} \mathbf{g}_i \quad (4.32)$$

Since the noise elements in \mathbf{N} are assumed to be *i.i.d.* and of zero mean, and the $\Delta \mathbf{g}_i$ is linear with respect to \mathbf{N} , it is clear that the bias of the estimated signature waveform is zero: $E(\Delta \mathbf{g}_i) = \mathbf{0}$.

To obtain the MSE of the signature waveform estimate, denote $\Delta \mathbf{g}_i(k)$ the k^{th} element of $\Delta \mathbf{g}_i$ and \mathbf{e}_j a column vector with the j^{th} element 1 and all the rest 0, we have $\Delta \mathbf{g}_i(k) = \mathbf{e}_k^H \Delta \mathbf{g}_i$. Therefore,

$$E(\Delta \mathbf{g}_i^H(k) \Delta \mathbf{g}_i(k)) = E\left(\|\mathbf{e}_k^H \mathbf{c}_i \mathbf{T}_i^\dagger \mathbf{U}_o^H \mathbf{N} \mathbf{X}^{\dagger H} \mathbf{g}_i\|^2\right) \quad (4.33)$$

$$= \sigma_n^2 \|\mathbf{e}_k^H \mathbf{c}_i \mathbf{T}_i^\dagger\|^2 \quad (4.34)$$

where the second equation is due to (38) in [47] and the fact that $\mathbf{U}_o^H \mathbf{U}_o = \mathbf{I}$. In the same paper, it is shown that $\|\mathbf{g}_i^H \mathbf{X}^\dagger\|^2 = \frac{1}{N \sigma_s^2 |\alpha_i|^2}$. Thus,

$$E(\Delta \mathbf{g}_i^H \Delta \mathbf{g}_i) = \frac{\sigma_n^2}{N \sigma_s^2 |\alpha_i|^2} \sum_k \|\mathbf{e}_k^H \mathbf{c}_i \mathbf{T}_i^\dagger\|^2. \quad (4.35)$$

Since $\sum_k \|\mathbf{e}_k^H \mathbf{c}_i \mathbf{T}_i^\dagger\|^2 = \|\mathbf{c}_i \mathbf{T}_i^\dagger\|^2$, we obtain the final expression of the MSE for the signature waveform estimates.

4.7 Computer Simulations

Simulation examples are presented in this section for several representative cases to illustrate the effectiveness of the proposed algorithm. In all of the

following examples, the channel response of each user was generated based on (1.3), where the pulse function was raised-cosine with a roll-off factor of 0.5. For each user, the user delay, the multipath delay, and the number of multipath components were uniformly distributed within $[1, L_c]$, $[0, 3T]$, and $[1, 10]$, respectively.

4.7.1 Single Antenna

The performance improvement due to the incorporation of signature vector estimates in detection is showed in Figures 4.3 and 4.4. We simulated a single receiver A-CDMA system with $L_c = 16$, $P = 11$, $K = 4$, and SNR= 10 dB. The code for each user were randomly generated rather than optimizing over deterministic sequences. We applied 100 data vectors to the proposed method for channel estimation. L was pre-selected to be 4 unless specified otherwise. After $\{\mathbf{h}_i\}$ were determined, the signature vectors $\{\mathbf{g}_i\}$ were reconstructed. We then constructed a zero-forcing equalizer to recover the original signal for each user¹. Figure 4.3 illustrates the channel responses used in the simulations and processing results for one of the users. The energy distribution of the channel suggests that most delays were within a small fraction of T , and thus the actual channel length was close to $2T$. Comparing the signal constellations using zero-forcing equalizer and RAKE receiver [19], we can see that the proposed method clearly accomplished satisfactory channel estimation. Figure 4.4 shows the same results for another user. In this case, stronger and longer delay multipath components existed, which led to a longer effective channel. Again,

¹Here, we just used the zero-forcing equalizer to demonstrate the quality of our channel estimates. For other detection techniques, the reader is referred to [21, 35, 33, 48, 49].

the proposed algorithm successfully determined the signature waveform and recovered the message signal. Another interesting observation of our algorithm is shown in Figure 4.5 when we increase the *smoothing factor* K to 10. This leads to an increase of the number of users that we can handle, $P = 14$. In this example, we used 250 symbols to estimate the signature waveforms while SNR is set to 10 dB. Moreover, we observed effects of the *smoothing factor* (K) in Figure 4.7 via a simulation conducted with 500 trials and 10 users. The performance improvement due to smoothing the data matrix is evident especially when K is relatively small. This can be best explained with the identifiability condition that is $P \leq (KL_c + L/2)/(K + 1)$. Furthermore, we performed another simulation with 500 trials, $P = 8$, and varying channel length L . As shown in Figure 4.6, the average RMSE and BER seem to degrade gradually while L increases. This indicates that the new algorithm is indeed robust to the channel order selection up to a reasonable extent.

The next example is primarily given to demonstrate how well the theoretical expressions predict the performance of the signature vector estimates under different SNRs. 500 trials were conducted with SNR varying from 0 to 30 dB. The sample root MSE of the signature vector estimates was then calculated and compared to that predicted by the corresponding theoretical expressions. The result of the simulations for one user is plotted in Figure 4.8. The symbols \circ represent the sample RMSE of the signature vector estimates, the solid line represents the error predicted by (4.35). Note the excellent agreement between predicted and simulated values, even for the leftmost case where the SNR is very low. A comparison study is summarized in Table 4.1 which shows average RMSEs of the channel vector estimates and the signature waveform estimates

with small and large *eigenvalue spread*. For this simulation, 500 trials were carried out with SNR=10 dB, $P = 10$, $K = 3$, and $L_c = 16$. This example indicates that utilization of spreading code with poor autocorrelation properties does not appear to affect significantly the performance of the proposed algorithm for the signature waveform estimation while it appears to increase RMSE of the channel vector estimates.

To demonstrate how close the channel estimates to the actual channels are, we simulated two different receivers. In Figure 4.9, the average BER for A-CDMA systems applying zero-forcing (ZF) and MMSE equalizers using the channel estimates and the actual channels is depicted versus the average SNR. In Figure 4.10, another comparison study was mainly given to show the performance of our method (*blind*) with adaptive MMSE receiver proposed in [25]. While we assumed perfect knowledge of the desired user's signature waveform and the associated timing for the adaptive MMSE receiver, we did not make available any of this information to the proposed method. Clearly, our method outperforms the receiver with the prior knowledge of the signature waveform and the associated timing for the desired user. We also assumed the adaptive MMSE receiver's weights already converged to the optimum values and the results may be more optimistic than those from the adaptive algorithms. Also, the near-far resistance of our algorithm was investigated through computer simulations. We simulated the worst case scenario where all users were close to the base station except only one user. The near-far ratio is defined as $20 \log_{10}(\alpha_l/\alpha_1)$ for $l \neq 1$. The RMSE of the signature waveform estimates and BER for A-CDMA systems applying zero-forcing (ZF) using the channel estimates and the time delay estimates were plotted as a function of near-far ratio

and with SNR= 5 dB in Figure 4.11. The proposed method is indeed near-far resistant. In these simulation examples, 500 trials were conducted with $P = 9$, $K = 2$, $L_c = 16$, and $N = 200$.

4.7.2 Multiple Antennas

As an example of the application of our approach to an overloaded multi-receiver system, consider the simulation results presented in Figure 4.13. Two receiver antennas were employed in a 22-user system. The channel response values are given in Tables 4.3 and 4.4. The rest of the setup remained the same as in Figures 4.3 and 4.4. Comparing these four plots, we can see that the performance of channel vector estimation and equalization is relatively insensitive to an increase in the number of users. The average BER vs. average SNR curves for an overloaded multi-receiver system applying ZF and MMSE equalizers based on both channel estimates and actual channels have been obtained by conducting a simulation with $P = 18$, $K = 2$, $L_c = 16$, $M = 2$ and $N = 200$. The results of the simulation are depicted in Figure 4.12. Although the performance of our algorithm for the multi-receiver system seems slightly worse than that for the single receiver system, the average BER for the multi-receiver system is better than that for the single receiver system for the same SNR values. In fact, as shown in Table 4.2 which compares the STD of the signal constellations after equalization, the overloaded 11-user/one-receiver system actually outperforms the original 22-user/two-receiver system, at least in this case. To some extent, this validates the performance enhancement promised by the multi-receiver, multi-user detection methods.

4.8 Experimental Results

All the RF field experiments were conducted in a suburban setting at the J.J. Pickle Research Campus of The University of Texas at Austin, using the 900 MHz smart antenna testbed described in the Appendix. Thus, the operating frequency is near the cellular band at approximately 900 MHz. We created the short-delay multipath environments by positioning a remote transceiver unit at the different locations. To compensate for lack of mobile transceivers, we collect single-user CDMA signals from different locations and then sum these signals with arbitrary time delays to artificially create a multiuser asynchronous-CDMA (A-CDMA) environment. We set $L_c = 16$ and $P = 25$, and we also used BPSK modulation scheme and employed three-element antenna array. The proposed algorithm used 150 snapshots of data for signature waveform estimation. The estimated waveforms were then used for equalization and equalized signal phase patterns were plotted in Figures 4.14 and 4.15, which experimentally validate the proposed approach.

4.9 Summary

A subspace based approach for blind multi-user channel estimation in A-CDMA systems has been presented. The algorithm exploits the fact that the signature waveform (vector) is the intersection of the signal subspace and the kernel subspace, thus allows it to be uniquely determined without any knowledge of the input signals. The extension of the new approach to an overloaded system was also presented. Extensive computer simulations have been performed to demonstrate the capacity of an A-CDMA system using the proposed approach. RF field experiments have also been conducted to validate the simulation results

Eigenvalue spread	Average RMSE _h	Average RMSE _g
<3	0.0904	0.0859
>3	0.1368	0.1005

Table 4.1: Comparison of RMSEs of channel and signature waveform estimates.

	Average STD	Max. STD	Min. STD
11-user, 1-receiver	0.0154	0.0380	0.0049
22-user, 2-receiver	0.0137	0.0232	0.0063

Table 4.2: Comparison of a 11-user/1-receiver and a 22-user/2-receiver Systems.

using the *Smart Antenna Testbed* at the University of Texas at Austin.

One of the practical features of existing and emerging CDMA standards is the use of aperiodic spreading codes. Aperiodic spreading codes distribute the signal spectrum over the allotted bandwidth uniformly, have inherent interference averaging capabilities. Since aperiodic spreading codes prevent the use of blind channel estimation method developed here, an iterative method to estimate multipath parameters in CDMA systems with aperiodic spreading sequences will be developed in the next chapter.

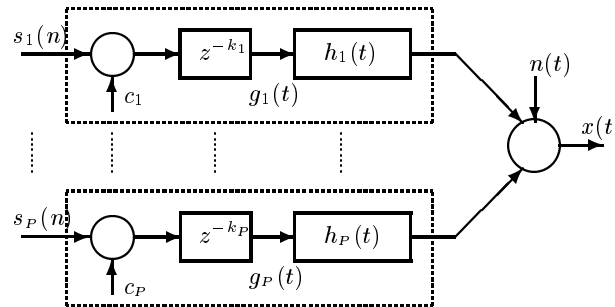


Figure 4.2: An asynchronous-CDMA system

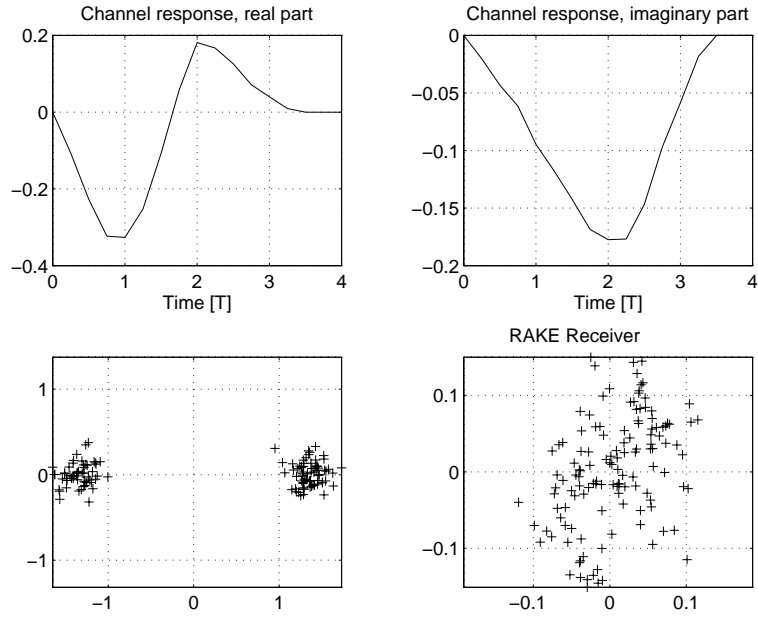


Figure 4.3: Channel responses and signal constellations for user #1 for BPSK signals. RAKE receiver breaks down. Our method with MMSE equalization exhibits robustness.

i	$h_i(0)$	$h_i(1)$	$h_i(2)$	$h_i(3)$
1	-0.2498 - 0.1614j	-0.7574 - 0.4894j	0.0198 - 0.0041j	0.0198 - 0.0041j
2	0.1710 - 0.2240j	0.5183 - 0.6790j	0.0539 - 0.0399j	0.0539 - 0.0399j

Table 4.3: FIR Channel responses of user #11 for $M = 2$ case.

i	$h_i(0)$	$h_i(1)$	$h_i(2)$	$h_i(3)$
1	0.1290 + 0.1242j	0.4378 + 0.4141j	0.1084 + 0.0573j	0.0617 + 0.0196j
2	-0.1856 + 0.0045j	-0.6404 + 0.0522j	-0.0774 + 0.1502j	0.0004 + 0.1115j

Table 4.4: FIR Channel responses of user #22 for $M = 2$ case.

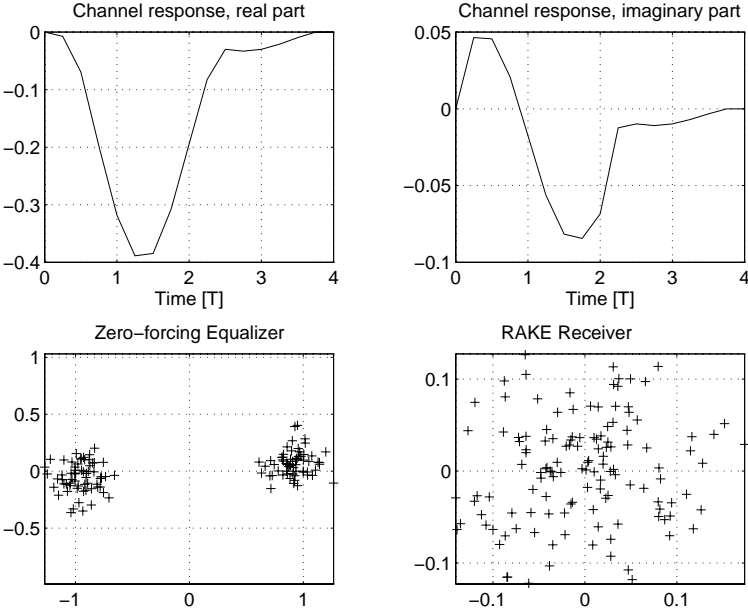


Figure 4.4: Channel responses and signal constellations for user #11 for BPSK signals. RAKE receiver breaks down. Our method exhibits robustness with ZF equation.

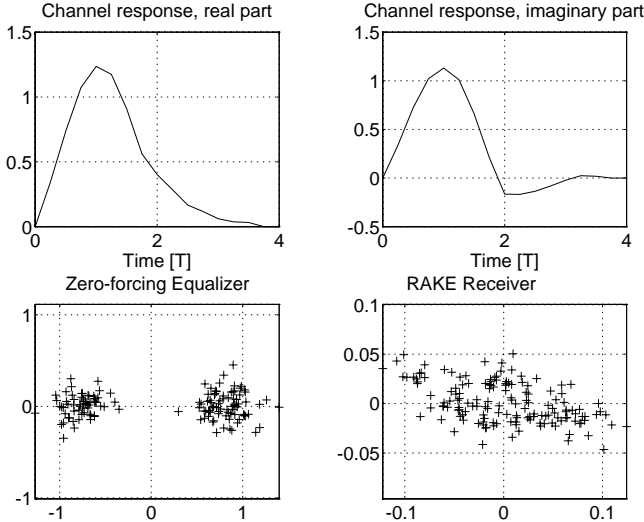


Figure 4.5: Channel responses and signal constellations for user #9 for $P = 14$ users transmitting BPSK signals. RAKE receiver breaks down. Our method with ZF equalization shows robustness.

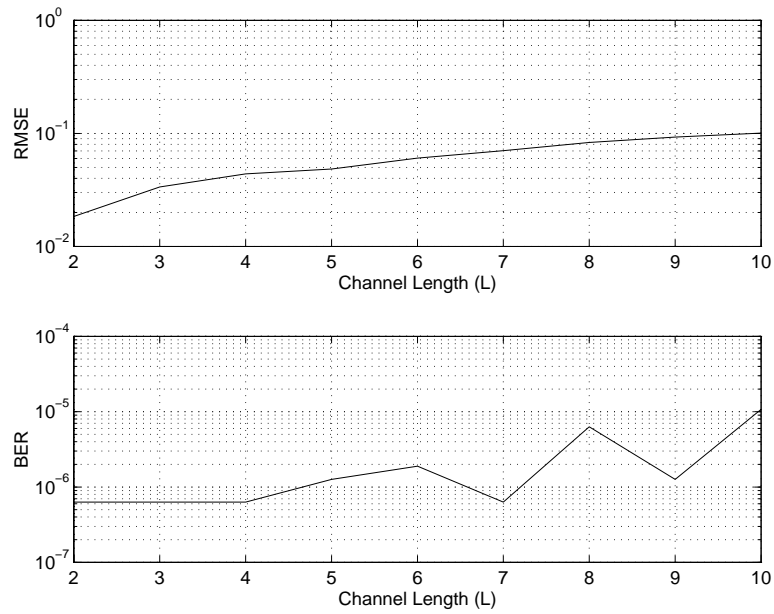


Figure 4.6: BER and RMSE of channel estimates vs. channel length.

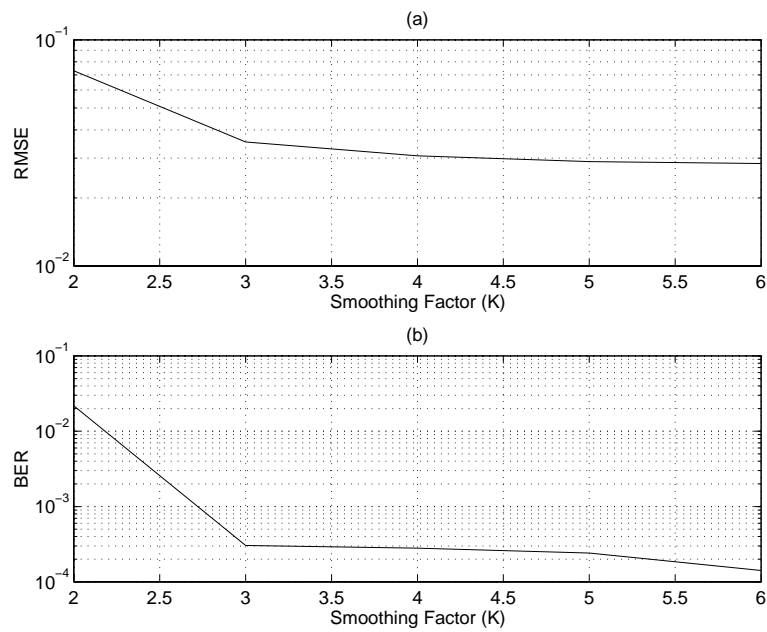


Figure 4.7: BER and RMSE of channel estimates vs. smoothing factor.

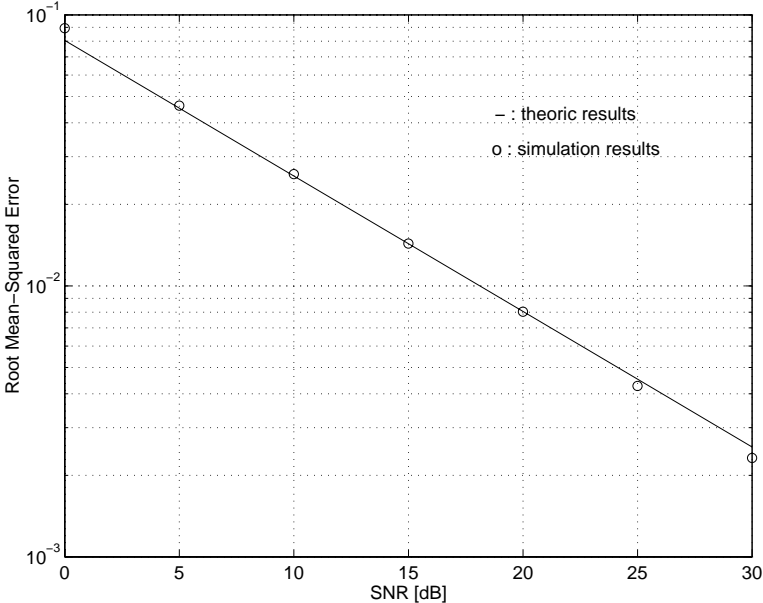


Figure 4.8: RMSE of received constellations vs. SNR for user #1.

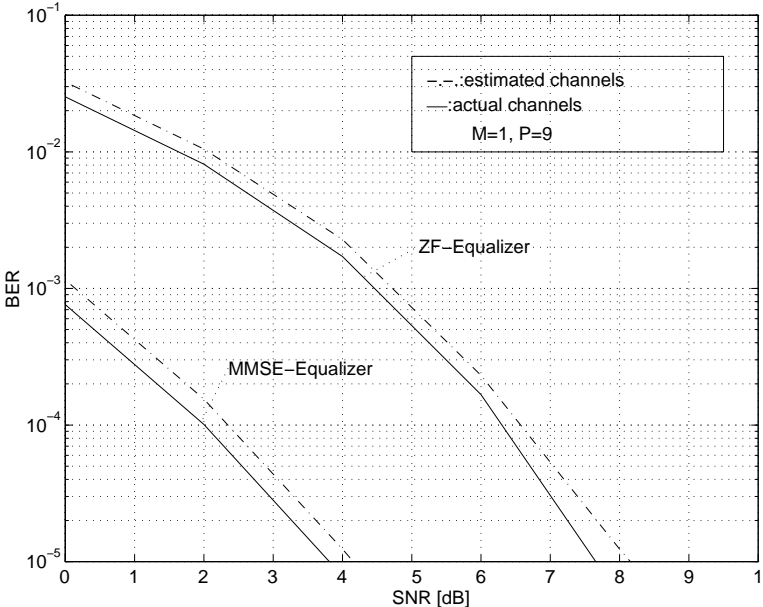


Figure 4.9: Average BER for A-CDMA systems employing different receivers with the estimated channels and the actual channels.

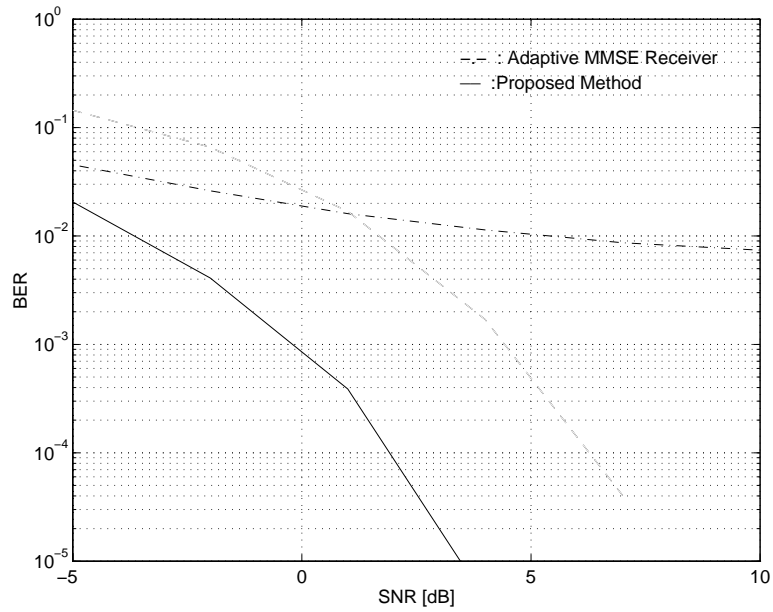


Figure 4.10: Comparison of the receiver using proposed method and adaptive MMSE receiver.

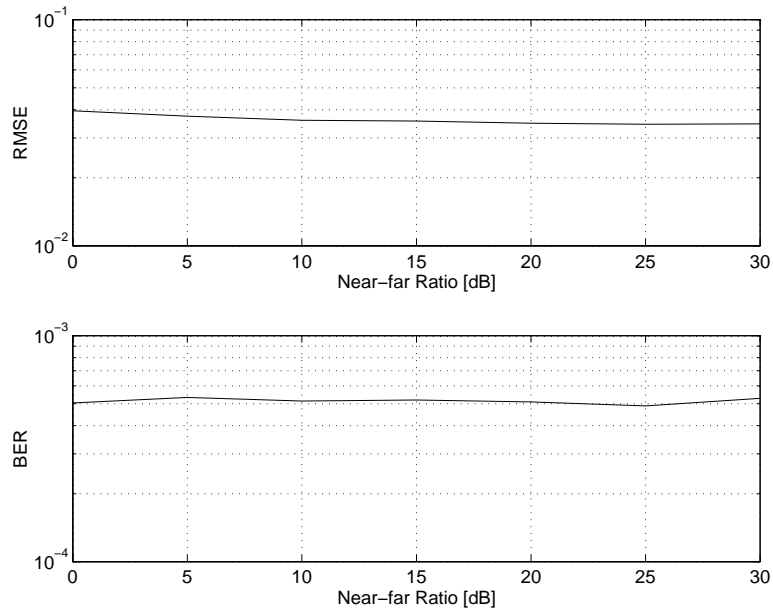


Figure 4.11: RMSE and BER of the receiver using the proposed method vs. near-far ratio.

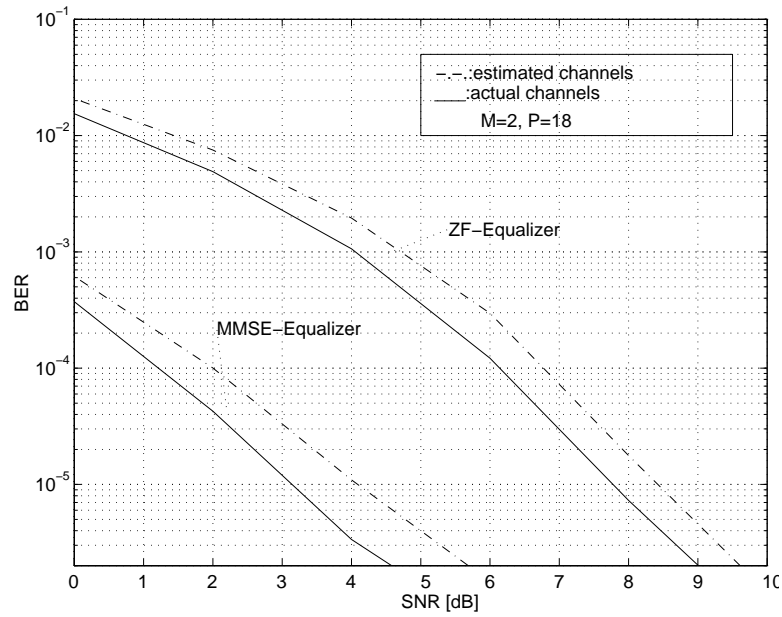


Figure 4.12: Average BER for overloaded A-CDMA systems employing different receivers with the estimated channels and the actual channels.

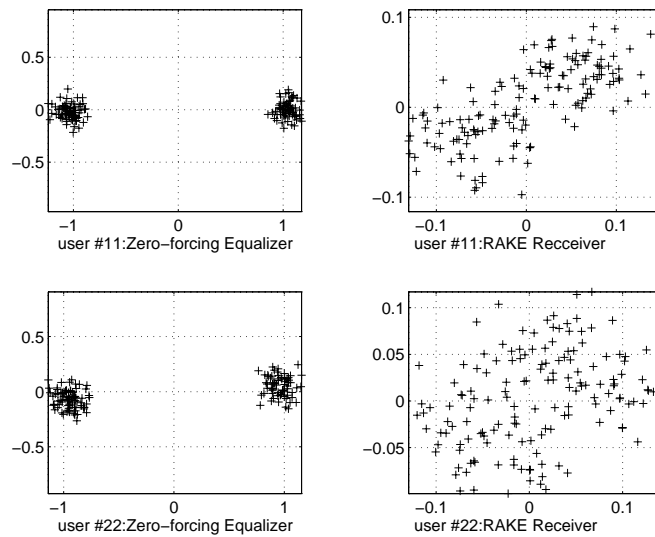


Figure 4.13: Two antennas and 22 users transmitting BPSK signals. RAKE receiver breaks down. Our method with ZF equalization exhibits robustness.

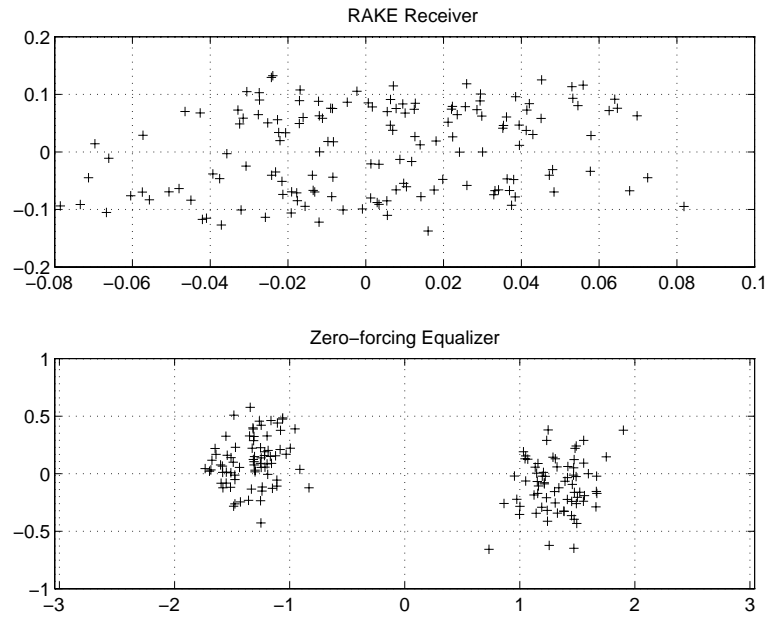


Figure 4.14: Signal constellations for user #2 with a four-element antenna array.

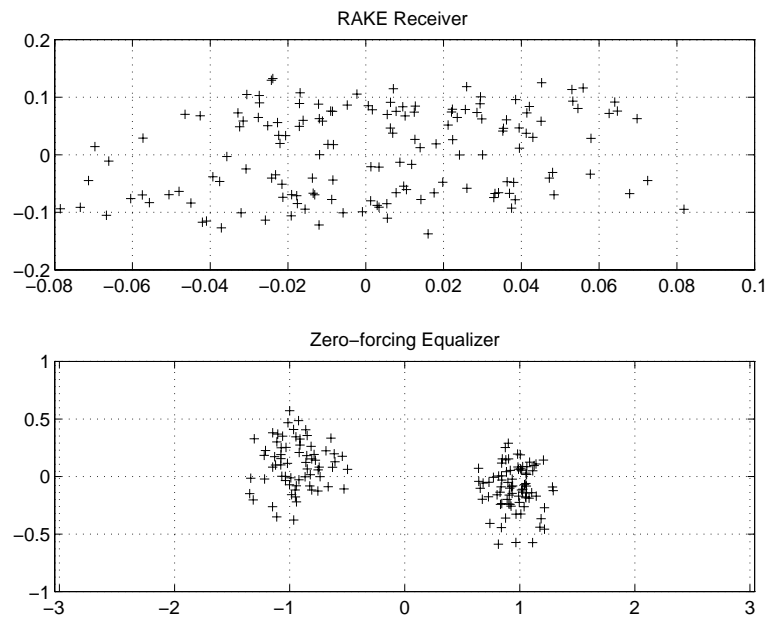


Figure 4.15: Signal constellations for user #25 with a four-element antenna array.

Chapter 5

Uplink Channel Estimation: CDMA Systems with Aperiodic Spreading Sequences

Wideband CDMA signals often suffer from interference due to frequency-selective fading and signals of other users. To reduce interference, a receiver could employ multiuser channel estimation. Blind multiuser channel estimation is complicated in CDMA systems, such as IS-95 and emerging third-generation systems, that use aperiodic spreading sequences. For Wideband CDMA systems, 1-D and 2-D RAKE receivers could perform blind multiuser channel estimation, but they would not be able to exploit the code structure in Wideband CDMA signals fully. In this chapter, we develop a robust blind multiuser channel estimation method for single and multiple antenna CDMA systems with aperiodic spreading sequences. The method jointly estimates the multipath channel parameters and transmitted symbols by using iterative least squares projection to alternate between two steps. The first step computes channel parameters given an estimate of the transmitted symbols, and the second step calculates the transmitted symbols given an estimate of the channel parameters. For the method, we provide a fast implementation and an extension to multirate systems. We also derive a Cramér-Rao Bound for CDMA systems with aperiodic spreading sequences. Simulation results show an average of 10 dB gain for

channel parameter estimation, and an average of 7 dB SINR improvement at 15 dB SNR, over RAKE receivers.

5.1 Introduction

Narrowband Code-Division Multiple-Access (CDMA) systems have been successfully deployed worldwide with millions of subscribers. With the convergence of wireless services and the Internet, new Wideband CDMA (W-CDMA) technology for next-generation mobile systems must provide high-rate data services in the field. Wideband wireless channels are subject to frequency-selective fading and multiuser interference; therefore, multiuser channel estimation is crucial for W-CDMA communications.

In synchronous W-CDMA systems, all mobile radio signals arriving at the base station are synchronized to within a fraction of a chip time interval. For the synchronous case, the effect of mutual interference may be reduced dramatically by using orthogonal codewords [34]. Synchronization at the base station, however, is especially difficult in large cells with large multipath delays, and becomes more difficult as the data rate increases.

W-CDMA channels from the mobile users to the base station are usually characterized as asynchronous, and hence, codewords are not guaranteed to be orthogonal at the base station. For asynchronous W-CDMA systems with periodic spreading sequences, it would be possible to perform blind FIR channel estimation using subspace-based methods and avoid the need for training sequences [21, 27, 32, 31]. Although the periodicity of the spreading codes simplifies the use of multiuser detection techniques [25, 33], one of the practical features of existing and emerging CDMA standards is the use of aperiodic

spreading codes.

Aperiodic spreading codes distribute the signal spectrum over the allotted bandwidth uniformly, have inherent interference averaging capabilities, and are beneficial to the soft capacity in W-CDMA systems [34]. RAKE receivers are commonly used to estimate channel parameters and alleviate multipath fading, but cannot fully exploit the rich structure of W-CDMA signals. Aperiodic spreading codes prevent the use of many signal reception and blind channel estimation methods [32, 35] that can fully exploit the structure of W-CDMA signals.

In this chapter, we present an iterative method to estimate multipath parameters in W-CDMA systems with aperiodic spreading sequences. This method also applies to W-CDMA systems with periodic spreading sequences. The proposed estimation method relies on the finite alphabet structure of the information symbols and the known pseudo-noise spreading codes. The finite alphabet structure has been previously exploited in TDMA systems [50, 51, 52]. These TDMA methods are not directly applicable to CDMA systems because of the large number of users. For a large number of CDMA users, we can perform finite alphabet restoration by exploiting knowledge of the pseudo-noise spreading codes and estimating channel parameters. The channel parameters can be used in a receiver to extract each symbol from the received data.

The proposed estimation method alternates between two steps using iterative least squares projection. The first step estimates the FIR channel parameters at the chip level. The second step forms a joint block equalizer to extract all of the user symbols. In simulation, the proposed method typically converges in 4 or 5 iterations. To reduce computation, we could reduce the

number of symbols used for each iteration. After identifying the channels, we can jointly detect all of the symbols by using all of the packet data.

Section 5.2 models the received data. Section 5.3 introduces the two estimation steps of the proposed estimation method. Section 5.4 describes the proposed estimation method and a fast implementation for it. Section 5.5 extends the proposed estimation method to the multirate case in which users may have different spreading gains and consequently different transmission rates. Section 5.6 derives a Cramér-Rao Bound for CDMA systems with aperiodic spreading sequences, to which we compare the performance of the proposed estimation method. Section 5.7 compares the proposed method against 1-D and 2-D RAKE receivers. Section 5.8 concludes the paper.

5.2 Data Model

The direct sequence wideband CDMA signal transmitted by a mobile user is given by

$$r(t) = c(t) s(t) e^{j2\pi f_c t} \quad (5.1)$$

where f_c is the carrier frequency of the transmitted signal, $s(t)$ is the binary message signal and $c(t)$ is a binary spreading sequence [34]. At the base station in an asynchronous W-CDMA system, an array of M antennas receives P signals through wideband frequency-selective wireless channels. The receiver front end down-converts the in-phase and quadrature components of the received signals to baseband. The wideband multipath channel between the i th user and the antenna array can be characterized by a *composite vector* FIR

channel [53, 54]

$$\mathbf{h}_i(t) = \begin{bmatrix} h_{1,i}(t) \\ \vdots \\ h_{M,i}(t) \end{bmatrix} = \sum_{l=1}^{L_i} \mathbf{a}_i(\theta_l) p(t - \tau_i(l)) \quad (5.2)$$

where $p(t)$ is the pulse shaping function; $\tau_i(l)$ and $\mathbf{a}_i(\theta_l)$ are the delay and array response vector of the l th multipath signal for the i th user, respectively; and L_i is the total number of paths for the i th user. We assume that the channels do not vary for the duration of one data frame. The proposed method does not require knowledge of $\tau_i(l)$, θ_l , or L_i .

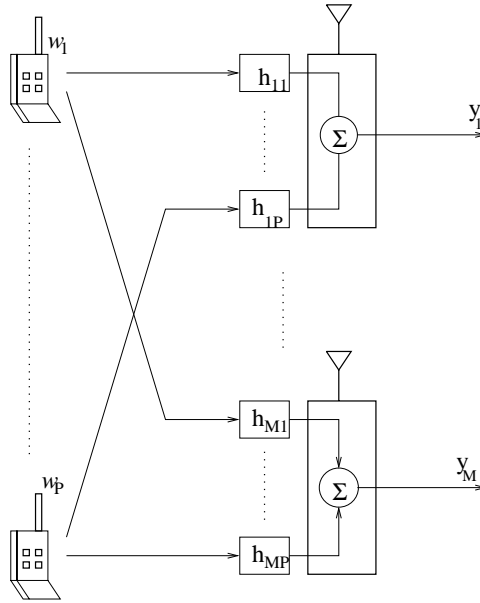


Figure 5.1: Channel model for a P -user CDMA System with an M -element antenna array.

Figure 5.1 illustrates the channel model for a multiuser multi-receiver system. The baseband signals at the antenna outputs can be written in vector notation as

$$\mathbf{y}(t) = \sum_{i=1}^P \sum_{n=1}^N w_i(n) \mathbf{h}_i(t - nT_c) + \mathbf{v}(t) \quad (5.3)$$

where T_c is the chip period; $\mathbf{h}_i(t)$ is defined in (5.2); N is the number of symbols in one frame of data;

$$w_i(k) = s_i(n) c_i(k - nL_c - k_i) \quad (5.4)$$

such that L_c is the number of chips per symbol and $n = \left\lfloor \frac{k - k_i}{L_c} \right\rfloor$ where the chip delay index k_i ($0 \leq k_i < L_c$) is assumed to be known; and $\mathbf{v}(t)$ is a wide sense stationary, zero-mean noise vector random process having the autocorrelation matrix

$$\mathbf{R}_{\mathbf{v}\mathbf{v}}(t, \tau) = E \{ \mathbf{v}(t) \mathbf{v}^H(t + \tau) \} = \sigma_{\mathbf{v}}^2 \mathbf{I}_M \delta(t - \tau)$$

such that \mathbf{I}_M is an $M \times M$ identity matrix. When we perform channel estimation, we assume that the spreading codes are known and do not need to be identified. In the proposed method, the channels are initially estimated by using the transmitted aperiodic spreading sequences as training sequences.

5.3 A Blind Iterative Channel Estimation Approach

In blind estimation, FIR channel parameters are estimated without the use of training sequences. Many blind subspace-based methods have been developed for multiuser FIR channel estimation in CDMA systems with *periodic* spreading sequences [27, 32, 31, 21]. Periodicity of spreading sequences also simplifies multiuser detection [25, 33]. Many practical CDMA systems, such as IS-95 and cdma2000, use *aperiodic* spreading sequences to achieve a uniform signal spectrum and identify cell sites uniquely.

Blind multiuser methods for aperiodic CDMA systems include 2-D RAKE receivers [26, 55] and post-despreading processing [53]. RAKE receivers combine the spread signal constructively and determine channel parameters by us-

ing matched filters. The blind 2-D RAKE receiver methods in [55, 26], however, assume knowledge of all multipath delays and attenuations. A post-despreading method [53] estimates the channel parameters from the post-despreading data based on a discrete-time model of the CDMA system. The post-despreading method offers considerable increase in performance over the traditional 2-D RAKE receivers, but falls short of the performance obtained for W-CDMA systems with periodic spreading sequences.

This section derives a new iterative two-step channel estimation algorithm for W-CDMA systems with aperiodic spreading sequences. The two steps are complementary. The first step, described in Section 5.3.1, estimates the channel parameters given the transmitted symbols. The second step, described in Section 5.3.2, estimates the transmitted symbols given the channel parameters. Based on the two steps, we construct the proposed iterative multiuser channel estimation method in Section 5.4.

5.3.1 Step 1: Estimation of Channel Parameters Given Transmitted Symbols

The data matrix for the received baseband signal sampled at the chip rate for N_t symbols is

$$\mathbf{Y} = \mathbf{H}\mathbf{W} + \mathbf{V} = \begin{bmatrix} \mathbf{h}_1 & \mathbf{h}_2 & \cdots & \mathbf{h}_P \end{bmatrix} \begin{bmatrix} \mathbf{w}_1(N_t) \\ \mathbf{w}_2(N_t) \\ \vdots \\ \mathbf{w}_P(N_t) \end{bmatrix} \quad (5.5)$$

where $N_t \ll N$; \mathbf{h}_i is an $M \times L$ matrix such that $\mathbf{h}_i = [\mathbf{h}_i(L-1) \ \mathbf{h}_i(L-2) \ \cdots \ \mathbf{h}_i(0)]$ where L is the channel length and $\mathbf{h}_i(n) = [h_i^1(l) \ h_i^2(l) \ \cdots \ h_i^M(l)]^T$, $l =$

$0, \dots, L - 1$; and

$$\mathbf{w}_i = \begin{bmatrix} w_i(1) & w_i(2) & \cdots & w_i(N_t L_c - L + 1) \\ w_i(2) & w_i(3) & \cdots & w_i(N_t L_c - L + 2) \\ \vdots & \vdots & \cdots & \vdots \\ w_i(L) & w_i(L + 1) & \cdots & w_i(N_t L_c) \end{bmatrix} \quad (5.6)$$

such that $w_i(n)$ is computed by using (5.4), which depends on the transmitted symbols and aperiodic spreading sequences. We assume that channel length L is known, or that we can select it depending on the cell size and application. We also assume that the pseudo-noise spreading sequence is known, and that the transmitted symbols are known or estimated. We decompose \mathbf{W} into

$$\mathbf{W} = \mathcal{S} \mathcal{C} \quad (5.7)$$

where \mathcal{C} contains the spreading codes and \mathcal{S} contains the transmitted symbols such that

$$\mathcal{S} = \left[\left(\begin{array}{cccc} s_1(1) & 0 & \cdots & 0 \\ 0 & s_2(1) & \ddots & \vdots \\ \vdots & \ddots & \ddots & \vdots \\ 0 & \cdots & 0 & s_P(1) \end{array} \right) \cdots \left(\begin{array}{cccc} s_1(N_t) & 0 & \cdots & 0 \\ 0 & s_2(N_t) & \ddots & \vdots \\ \vdots & \ddots & \ddots & \vdots \\ 0 & \cdots & 0 & s_P(N_t) \end{array} \right) \right] \otimes \mathbf{I}_L \quad (5.8)$$

where \otimes denotes convolution. By minimizing the maximum likelihood criterion,

$$\min_{\mathbf{H}} \|\mathbf{Y} - \mathbf{H} \mathcal{S} \mathcal{C}\|_F^2 \quad (5.9)$$

where $\|\cdot\|_F$ is the Frobenius norm [43], we obtain

$$\hat{\mathbf{H}} = \mathbf{Y} \mathbf{W}^\dagger = \mathbf{Y} \mathcal{C}^H \mathcal{S}^H (\mathcal{S} \mathcal{C} \mathcal{C}^H \mathcal{S}^H)^{-1} \quad (5.10)$$

where the operator $(\cdot)^\dagger$ denotes the pseudo-inverse. \mathbf{H} and $\hat{\mathbf{H}}$ are $M \times LP$ matrices. \mathbf{W} is an $LP \times (N_t L_c - L)$ matrix. \mathbf{Y} is an $M \times (N_t L_c - L)$ matrix.

5.3.2 Step 2: Estimation of Transmitted Symbols Given Channel Parameters

We stack the spatial data samples at each antenna element $1, 2, \dots, M$ to form the data matrix

$$\mathcal{Y} = \begin{bmatrix} \mathbf{y}^1 & \mathbf{y}^2 & \dots & \mathbf{y}^M \end{bmatrix}^T = \underbrace{\begin{bmatrix} \mathcal{G}_1 & \mathcal{G}_2 & \dots & \mathcal{G}_P \end{bmatrix}}_{\mathcal{G}} \underbrace{\begin{bmatrix} \mathbf{s}_1^T \\ \mathbf{s}_2^T \\ \vdots \\ \mathbf{s}_P^T \end{bmatrix}}_{\mathbf{s}} \quad (5.11)$$

where $\mathbf{s}_i = [s_i(1) \dots s_i(N_t)]$ and \mathcal{G}_i represents the block channel impulse response, including the spreading codes and wideband channel coefficients, as

$$\mathcal{G}_i = \underbrace{\begin{bmatrix} \mathcal{C}_i & \mathbf{0} \\ \dots & \dots \\ \mathbf{0} & \mathcal{C}_i \end{bmatrix}}_{M \text{ blocks}} \underbrace{\begin{bmatrix} (\mathbf{h}_i^1)^H \otimes \mathbf{I}_{N_t} \\ \vdots \\ (\mathbf{h}_i^M)^H \otimes \mathbf{I}_{N_t} \end{bmatrix}}_{\mathcal{H}_u} \quad (5.12)$$

where $\mathbf{h}_i^m = [h_i^m(L-1) \dots h_i^m(0)]$ for sensor m . The kernel matrix \mathcal{C}_i is defined using shifted blocks of the pseudo-noise spreading sequences

$$\mathcal{C}_i = \begin{bmatrix} \mathcal{C}_i(1) & & & & \mathbf{0} \\ & \mathcal{C}_i(2) & & & \\ & & \dots & & \\ & & & \dots & \\ \mathbf{0} & & & & \mathcal{C}_i(N_t) \end{bmatrix} \quad (5.13)$$

Each block covers one symbol period and has a Toeplitz structure due to the convolution effect of the FIR channel. Upper and lower blocks may be also

partial because of the asynchronous operation of the uplink. Thus, a complete block of $\mathbf{C}_i(n)$ for $n = 1, \dots, N_t$ may be written as

$$\mathbf{C}_i(n) = \underbrace{\left[\begin{array}{ccc} 0 & \cdots & 0 \\ \cdots & \ddots & \cdots \\ c_i(nL_c + 1) & \ddots & 0 \\ \vdots & \ddots & c_i(nL_c + 1) \\ c_i(nL_c + L_c) & \ddots & \vdots \\ 0 & \ddots & c_i(nL_c + L_c) \\ \vdots & \cdots & 0 \\ 0 & \cdots & 0 \end{array} \right]}_{L \text{ columns}} \left. \vphantom{\left[\begin{array}{ccc} 0 & \cdots & 0 \\ \cdots & \ddots & \cdots \\ c_i(nL_c + 1) & \ddots & 0 \\ \vdots & \ddots & c_i(nL_c + 1) \\ c_i(nL_c + L_c) & \ddots & \vdots \\ 0 & \ddots & c_i(nL_c + L_c) \\ \vdots & \cdots & 0 \\ 0 & \cdots & 0 \end{array} \right]} \right\} 2L_c \text{ rows} \quad (5.14)$$

If we use the same spreading code, i.e. $\mathbf{C}_i(1) = \mathbf{C}_i(2) = \dots = \mathbf{C}_i(N_t)$, then we can use the blind channel estimation method proposed in [32] as an alternative.

If we use (5.11) to solve for \mathbf{s} , then

$$\mathbf{s} = \mathcal{G}^\dagger \mathcal{Y} \quad (5.15)$$

By using the solutions for \mathbf{H} in (5.10) and \mathbf{s} in (5.15), we can use both steps to exploit the finite alphabet structure of CDMA signals and knowledge of spreading codes, as we discuss in more detail in the next section.

5.4 Blind Estimation Method

The proposed blind channel method given in Figure 5.2 uses iterative least squares with projections, which was originally developed for TDMA systems [50]. The proposed estimation method updates \mathbf{s} iteratively under the constraint that the information symbols in \mathbf{s} are from finite alphabets, which in turn updates \mathbf{W} and \mathbf{H} . Given an initial estimate of the transmitted symbols, the proposed method uses (5.10) to estimate \mathbf{H} . Using this estimate of \mathbf{H} , we

estimate \mathcal{G} to find \mathbf{s} and project \mathbf{s} to the closest alphabet values. We continue until either \mathbf{s} or \mathbf{H} converges. At each iteration, two least squares problems are solved.

The advantages of this method are the full exploitation of the CDMA code structure, simultaneous estimation of all channel parameters, an increase in system performance over RAKE receivers, and the ability to handle an overloaded system. The disadvantage is an increase in computational complexity over RAKE receivers. For the proposed method, Section 5.4.1 analyzes its computational complexity, and Section 5.4.2 develops a fast implementation.

5.4.1 Complexity Analysis

The complexity of the proposed channel estimation method in Figure 5.2 is dominated by the linear least squares equations in steps 2a and 2c. Without structure-exploiting methods, the complexity of step 2a is

$$\mathcal{O}\left(L_c N_t (MLP + (LP)^2) + (LP)^3\right)$$

multiplications and additions. Because \mathbf{W} is an $LP \times (N_t L_c - L)$ matrix, the pseudo-inverse of \mathbf{W} used to compute \mathbf{H} in (5.10) requires that

$$L(P + 1) \leq N_t L_c \tag{5.16}$$

Using (5.16), the complexity of step 2a becomes

$$\mathcal{O}\left(N_t L_c (LP)^2 + (LP)^3\right) \leq \mathcal{O}\left(2(N_t L_c)^3\right)$$

multiplications and additions, since $LP \leq L(P + 1)$. Similarly, the complexity of step 2c becomes

$$\mathcal{O}\left(MN_t L_c (N_t P)^2 + (N_t P)^3\right) \geq \mathcal{O}\left(MLP(N_t P)^2 + (N_t P)^3\right)$$

1. Randomly choose \mathcal{S}_0 and set the iteration count $l = 0$. The number of chips per symbol L_c and the data frame length in symbols N are determined by the application.

2. $l = l + 1$ and select the number of processed symbols N_t such that

$$\left\lceil \frac{L(P+1)}{L_c} \right\rceil \leq N_t < N$$

according to (5.16). The larger the value of N_t , the better the estimation performance and the greater the computational complexity (see Section 5.4.1). For an overloaded system, i.e. $P > L_c$, we would have $L \leq N_t < N$ and may have to increase N_t such that $L \leq \left\lceil \frac{N_t L_c}{P+1} \right\rceil$.

(a) $\hat{\mathbf{H}} = \begin{bmatrix} \mathbf{h}_{1,l} & \cdots & \mathbf{h}_{P,l} \end{bmatrix} = \mathbf{Y} \mathbf{W}_l^\dagger$ where

$$\mathbf{W}_l = \begin{bmatrix} \mathbf{w}_{1,l}(N_t L_c) \\ \vdots \\ \mathbf{w}_{P,l}(N_t L_c) \end{bmatrix} = \mathcal{S}_l \mathcal{C}$$

where $\mathbf{w}_{i,l}(n)$ is computed by using (5.4) with the estimated symbols and aperiodic spreading sequences.

(b) Construct \mathcal{G}_l with the estimated channel parameters and pseudo-noise sequences using (5.11), (5.12), and (5.13).

(c) Estimate \mathbf{s}_{l+1} by

$$\mathbf{s}_{l+1} = \mathcal{G}_l^\dagger \mathcal{Y}$$

(d) Project elements of \mathbf{s}_{l+1} to the closest discrete values.

3. Continue until $\mathbf{s}_{l+1} = \mathbf{s}_l$.

Figure 5.2: Proposed blind channel estimation method for wideband asynchronous CDMA base stations with M antennas and P users. The amount of computation increases with larger values of L , N_t , and P .

multiplications and additions. So, the method in Figure 5.2 requires on the order of cubic operations for L , L_c , N_t , and P , and linear operations for M . Furthermore, for steps 2a and 2c, the proposed method uses $2N_tL_cLP + 4(LP)^2 + 2MLP$ and $2MN_t^2L_cP + 4(N_tP)^2 + 2N_tP$ memory locations, respectively. The next section reduces the computational complexity by exploiting the structure of the linear least squares equations.

5.4.2 Fast Implementation

The blind estimation method in Figure 5.2 performs matrix-vector multiplications and solves systems of linear equations. This section provides a fast implementation of the method that is on the order of linear operations for L_c , M , and N_t , $n \log_2 n$ operations for L , and cubic operations for P . The fast implementation and the original method can be parallelized. The proposed method jointly estimates data for all users simultaneously instead of computing separate estimates for each single user. Hence, other user signals are not treated as noise. The solution of the data vector \mathbf{s} is a combination of each user's data, which can be rearranged as

$$\bar{\mathbf{s}} = \left[s_1(1) \quad s_2(1) \quad \dots \quad s_P(1) \quad \dots \quad s_1(N_t) \quad \dots \quad s_P(N_t) \right]^T \quad (5.17)$$

so that $\mathcal{G} \rightarrow \bar{\mathcal{G}}$ has a banded structure. Thus, the data estimation in (5.15) can be rewritten as

$$\bar{\mathbf{s}} = \bar{\mathcal{G}}^\dagger \mathcal{Y} = (\bar{\mathcal{G}}^H \bar{\mathcal{G}})^{-1} \bar{\mathcal{G}} \text{vec}(\mathbf{Y}) \quad (5.18)$$

where $\text{vec}(\cdot)$ is an operator which stacks the columns of a matrix into a vector. Since the data estimation in (5.18) is performed by a zero-forcing block linear equalizer, the resulting components are unbiased estimates of \mathbf{s} [56]. Estimation

of $\bar{\mathbf{s}}$ involves an inversion of the banded matrix $\bar{\mathcal{G}}^H \bar{\mathcal{G}}$. We exploit the banded structure of $\bar{\mathcal{G}}^H \bar{\mathcal{G}}$ to reduce the computational complexity of (5.18) by first rewriting it as

$$(\bar{\mathcal{G}}^H \bar{\mathcal{G}})\bar{\mathbf{s}} = \bar{\mathcal{G}}^H \text{vec}(\mathbf{Y}) \quad (5.19)$$

Since we order the equations in (5.19) so that the n th unknown symbol of the p th user, $s_p(n)$, appears in only a few neighboring equations. Regarding $\mathcal{R} = (\mathcal{R}_{i,j})$ as $P \times P$ block matrices with square diagonal blocks,

$$\mathcal{R}_N = \bar{\mathcal{G}}^H \bar{\mathcal{G}} = \begin{bmatrix} \mathcal{R}_{1,1} & \mathcal{R}_{1,2} & \mathbf{0} & \cdots & \mathbf{0} \\ \mathcal{R}_{2,1} & \mathcal{R}_{2,2} & \mathcal{R}_{2,3} & \ddots & \vdots \\ \mathbf{0} & \mathcal{R}_{3,2} & \mathcal{R}_{3,3} & \ddots & \vdots \\ \vdots & \ddots & \ddots & \ddots & \mathcal{R}_{N_t-1,N_t} \\ \mathbf{0} & \cdots & \cdots & \mathcal{R}_{N_t,N_t-1} & \mathcal{R}_{N_t,N_t} \end{bmatrix} \quad (5.20)$$

We can realize substantial simplification when solving banded systems because the factorization outputs are also banded. From Theorem 4.3.1 in [43], if $\mathcal{R} = \mathbf{L}\mathbf{U}$ is the LU factorization of \mathcal{R} , then \mathbf{L} and \mathbf{U} have the same banded structure. After LU factorization of

$$\mathcal{R}_N = \bar{\mathcal{G}}^H \bar{\mathcal{G}} = \begin{bmatrix} \mathbf{I} & \mathbf{0} & \cdots & \cdots & \mathbf{0} \\ \mathcal{L}_1 & \mathbf{I} & \ddots & \cdots & \vdots \\ \mathbf{0} & \ddots & \ddots & \vdots & \vdots \\ \vdots & \ddots & \ddots & \mathbf{I} & \mathbf{0} \\ \mathbf{0} & \cdots & \mathbf{0} & \mathcal{L}_{N_t-1} & \mathbf{I} \end{bmatrix} \begin{bmatrix} \mathcal{U}_1 & \mathcal{R}_{12} & \mathbf{0} & \cdots & \mathbf{0} \\ \mathbf{0} & \mathcal{U}_2 & \ddots & \cdots & \vdots \\ \vdots & \ddots & \ddots & \vdots & \mathbf{0} \\ \vdots & \ddots & \ddots & \mathcal{U}_{N_t-1} & \mathcal{R}_{N_t-1,N_t} \\ \mathbf{0} & \cdots & \cdots & \mathbf{0} & \mathcal{U}_{N_t} \end{bmatrix} \quad (5.21)$$

the computation of $\bar{\mathbf{s}}$ can be reduced to solving $\mathbf{A}^H \mathbf{z} = \bar{\mathcal{G}}^H \text{vec}(\mathbf{Y})$ and $\mathbf{A}^H \bar{\mathbf{s}} = \mathbf{z}$. 5.3.

In the fast implementation given in Figure 5.3, forward substitution cancels inter-symbol interference from the past symbols, and back substitution cancels inter-symbol interference from the future symbols. The complexity is

1. Randomly choose \mathcal{S}_0 and set the iteration count $l = 0$.
2. $l = l + 1$ and select the number of symbols $N_t < N$ as in step 2 of Figure 5.2
 - (a) $\hat{\mathbf{H}} = [\mathbf{h}_{1,l} \ \cdots \ \mathbf{h}_{P,l}] = \mathbf{Y}\mathbf{W}_l^H\mathbf{T}$ where \mathbf{W}_l is defined in step 2(a) in Figure 5.2 and $\mathbf{T} = (\mathbf{W}_l\mathbf{W}_l^H)^{-1}$ is computed using the fast inversion algorithm in [57]
 - (b) Construct $\bar{\mathcal{G}}$ according to step 2b in Figure 5.2 and form \mathcal{R}_{jj} , $\mathcal{R}_{j-1,j}$, and $\mathcal{R}_{j,j+1}$ for $j = 1, \dots, N_t$ according to (5.20).
 - (c) Estimate $\bar{\mathbf{s}}_{l+1}$ using the fast algorithm in [43]:
 - i. Use LU decomposition

$$\mathcal{U}_1 = \mathcal{R}_{11}$$
For $j = 2 : N_t$
 Solve $\mathcal{L}_{j-1}\mathcal{U}_{j-1} = \mathcal{R}_{j,j-1}$ for \mathcal{L}_{j-1}
 $\mathcal{U}_j = \mathcal{R}_{jj} - \mathcal{L}_{j-1}\mathcal{R}_{j-1,j}$
end
 - ii. Obtain the input symbols $\bar{\mathbf{s}}_{l+1}$

$$\mathbf{z}_1 = \mathcal{G}(1)\vec{\mathbf{Y}}(1)$$
For $j = 2 : N_t$
 $\mathbf{z}_j = \mathcal{G}(j)\text{vec}(\mathbf{Y}(j)) - \mathcal{L}_{j-1}\mathcal{G}(j)\text{vec}(\mathbf{Y}(j-1))$
end
 Solve $\mathcal{U}_{N_t}\mathbf{s}_{l+1}(N_t) = \mathbf{z}_{N_t}$ for $\mathbf{s}_{l+1}(N_t)$
For $j = N_t - 1 : -1 : 1$
 Solve $\mathcal{U}_j\mathbf{s}_{l+1}(j) = \mathbf{z}_j - \mathcal{R}_{j,j+1}\mathbf{s}_{l+1}(j+1)$ for $\mathbf{s}_{l+1}(j)$
end
 - (d) Project elements of $\bar{\mathbf{s}}_{l+1}$ to the closest discrete values
3. Continue until $\bar{\mathbf{s}}_{l+1} = \bar{\mathbf{s}}_l$

Figure 5.3: Fast implementation of the proposed estimation method in Figure 5.2. This implementation is valid as long as the \mathcal{U}_j matrices are nonsingular. These matrices should be non-singular because the spreading codes have low correlation.

$\mathcal{O}(8N_tP^3)$ arithmetic operations. Estimation of the channel impulse responses are performed efficiently by a fast algorithm since (5.10) involves solving a block Toeplitz system of equations. We adopt a fast algorithm to invert $\mathbf{W}\mathbf{W}^H$ [57] that uses the fast Fourier transform and requires $\mathcal{O}(LP \log_2 LP)$ computations. With common values of $L = 4$ and $P = 8$, the inversion can be easily implemented on a programmable digital signal processor. Because of the banded data structure, we can reduce the memory usage to vary linearly with N_t instead of N_t^2 .

5.5 Extension to Multirate Systems

An advantage of CDMA systems is adaptability to different data rates. Previous sections assumed that all users transmit at the same data rate, which is the case for IS-95 systems. Emerging third-generation systems, however, support different data rates. This section extends the proposed estimation method to multirate CDMA systems to handle different data rates.

We assume that Ω is the number of different rates supported by the system. The number of users using the same spreading gain of L_ζ is P_ζ . Thus, the total number of users in the system is $P = \sum_{\zeta=1}^{\Omega} P_\zeta$. We also assume that $\frac{L_c}{L_\zeta} = 2^t$ for integers t and ζ . We add the contributions from all users at the same rates to obtain

$$\mathbf{y}_\zeta(t) = \sum_{i=1}^{P_\zeta} \sum_{n=1}^{N_\zeta} w_i(n) \mathbf{h}_i(t - nT_c) \quad (5.22)$$

Adding the users at different rates and noise yields

$$\mathbf{y}(t) = \sum_{\zeta=1}^{\Omega} \mathbf{y}_\zeta(t) + \mathbf{v}(t) \quad (5.23)$$

Since we change the spreading gain while keeping the same chip rate, we allow some users to transmit at higher data rates than other users. However, the total number of users that a system can handle reduces. We adjust the method for fast implementation. To preserve the same banded structure in \mathcal{G} , we arrange the solution of the data vector \mathbf{s} as

$$\left[s_1(1) \quad \dots \quad s_1\left(\frac{L_c}{L_1}\right) \quad s_2(1) \quad \dots \quad s_1\left(\left(N-1\right)\frac{L_c}{L_1} + 1\right) \quad \dots \quad s_P\left(N\frac{L_c}{L_\Omega}\right) \right]^T \quad (5.24)$$

The rest of the fast implementation follows from Section 5.4.2.

5.6 Cramér-Rao Bound

Section 5.4 shows that the proposed method can blindly estimate the input symbols without the knowledge of the input statistics. This section derives a Cramér-Rao bound (CRB) for CDMA system with aperiodic spreading. In the derivation, we assume that the channel noise is white complex circular Gaussian with variance σ^2 , and the input sequence is unknown and deterministic. Based on [58, 59], this section derives the Fisher Information matrix for the channel parameters. The CRB of the variance of each parameter is given by the corresponding element on the diagonal of \mathbf{F}^{-1} . We will use the CRB formula that we derive to compare the performance of the proposed method vs. other methods. The CRB formula could also be used to compare methods for generating aperiodic spreading codes.

Except for σ^2 , the unknown parameters in this system are denoted by the $2MLP \times 1$ vector

$$\Phi = \begin{bmatrix} \Phi_{\mathbf{h}_R} \\ \Phi_{\mathbf{h}_I} \end{bmatrix} = \begin{bmatrix} \Re \{ \text{vec}(\mathbf{H}) \} \\ \Im \{ \text{vec}(\mathbf{H}) \} \end{bmatrix} \quad (5.25)$$

where \mathbf{H} are the impulse response matrix defined in (5.5). In order to find the Fisher Information matrix associated with Φ , we stack all the outputs in a vector form and reformulate (5.5) as

$$\mathcal{X} = \text{vec}(\mathbf{Y}) = \bar{\mathcal{G}}\bar{\mathbf{s}} + \mathbf{v} \quad (5.26)$$

$$= \underbrace{(\mathbf{I}_M \otimes (\mathcal{C}^T \mathcal{S}^T))}_{\mathcal{W}} \text{vec}(\mathbf{H}) + \mathbf{v} \quad (5.27)$$

The likelihood function of the data is given by

$$\mathcal{L}(\mathcal{X}) = \frac{1}{(\pi\sigma)^{M(N_t L_c - L + 1)}} e^{-\frac{1}{\sigma} [\mathcal{X} - \bar{\mathcal{G}}\bar{\mathbf{s}}]^H \cdot [\mathcal{X} - \bar{\mathcal{G}}\bar{\mathbf{s}}]}$$

Thus, the log-likelihood function is

$$\ln(\mathcal{L}) = \text{const} - \frac{1}{\sigma} [\mathcal{X} - \mathcal{G}\mathbf{s}]^H \cdot [\mathcal{X} - \mathcal{G}\mathbf{s}] \quad (5.28)$$

Using the results in [59], we calculate the partial derivatives of (5.28) with respect to Φ and $\bar{\mathbf{s}}$:

$$\frac{\partial \ln(\mathcal{L})}{\partial \Phi_{\bar{\mathbf{s}}}} = \frac{2}{\sigma} \{ \mathcal{G}^H \mathbf{v} \} \quad \frac{\partial \ln(\mathcal{L})}{\partial \Phi_{\mathbf{h}_R}} = \frac{2}{\sigma} \text{Re} \{ (\mathcal{W})^H \mathbf{v} \} \quad \frac{\partial \ln(\mathcal{L})}{\partial \Phi_{\mathbf{h}_I}} = \frac{2}{\sigma} \text{Im} \{ (\mathcal{W})^H \mathbf{v} \} \quad (5.29)$$

Using results in [58, 59], we obtain

$$\text{CRB}(\mathbf{h}) = \frac{\sigma^2}{2} (\mathbf{F}_{SS} - \mathbf{F}_{HS}^H \mathbf{F}_{HH}^{-1} \mathbf{F}_{HS})^{-1} \quad (5.30)$$

where

$$\mathbf{F}_{SS} = \begin{bmatrix} \Re \{ \mathcal{W}^H \mathcal{W} \} & -\Im \{ \mathcal{W}^H \mathcal{W} \} \\ \Im \{ \mathcal{W}^H \mathcal{W} \} & \Re \{ \mathcal{W}^H \mathcal{W} \} \end{bmatrix}$$

$$\mathbf{F}_{HS} = \begin{bmatrix} \Re \{ \mathcal{W}^H \mathcal{G} \} & -\Im \{ \mathcal{W}^H \mathcal{G} \} \\ \Im \{ \mathcal{W}^H \mathcal{G} \} & \Re \{ \mathcal{W}^H \mathcal{G} \} \end{bmatrix}$$

$$\mathbf{F}_{HH} = \begin{bmatrix} \Re \{ \mathcal{G}^H \mathcal{G} \} & -\Im \{ \mathcal{G}^H \mathcal{G} \} \\ \Im \{ \mathcal{G}^H \mathcal{G} \} & \Re \{ \mathcal{G}^H \mathcal{G} \} \end{bmatrix}$$

The CRB on the variance of each parameter is given by a corresponding element on the diagonal of \mathbf{F}^{-1} . We now have CRBs for the channel estimates. This CRB is a function of the input sequence and the spreading codes.

5.7 Computer Simulations

We compare the performance of conventional RAKE receivers and the proposed estimation method using simulation. For each user i , the number of multipath components L_i and the delay for the l th path $\tau_i(l)$ are uniformly distributed over $[1, 10]$ and $[0, 3T]$, respectively. We employ Binary Phase Shift Keying modulation for both symbols and spreading codes. All channel taps are assumed to fade independently and be time-invariant during transmission of a burst. Propagation delays for each user are uniformly distributed over $[0, L_c - L - 1]$. For the purposes of generating propagation delays for simulation, we assume that $L < L_c$, but the proposed blind estimation method does not impose this restriction. The 1-D and 2-D RAKE receivers use the principal components algorithm [53].

Figure reSignalConstellation:fig compares the received signal constellations of the proposed estimation method with the 1-D RAKE receiver for $P = 8$ users (upper two plots) and the 2-D RAKE receiver for $P = 13$ users and $M = 2$ antennas (lower two plots). We use $L_c = 16$ chips/symbol, $N = 40$ symbols, and $\text{SNR} = 15$ dB. We generate the spreading code for each user randomly and assume that the aperiodic CDMA signals are synchronous. We set N_t to 15 symbols for the proposed estimation method and 40 symbols for the RAKE receiver to show the performance of the proposed method for a reduced number of symbols. The proposed estimation method used $L = 3$. We

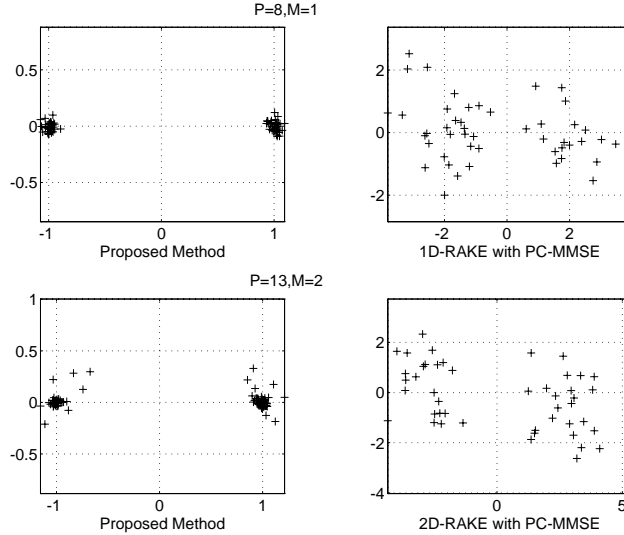


Figure 5.4: Signal constellations for 1-D RAKE, 2-D RAKE and the proposed estimation method for the 1-D ($M = 1$) and 2-D ($M = 2$) cases. The RAKE receivers use the Principal Components Minimum Mean Square Error (PC-MMSE) algorithm. The simulation uses $L_c = 16$, $\text{SNR} = 15$ dB, $N = 40$, and $L = 3$. N_t is set to 15 symbols for the proposed estimation method and 40 for the RAKE receivers.

ran all simulations 100 times and averaged the results. The simulation demonstrates that an increase in the number of users has a negligible effect on the performance of channel vector estimation and equalization. Table 5.1 gives the average number of iterations for the proposed estimation method to converge vs. the number of users in 1-D and 2-D.

Figure 5.5 compares the mean squared error (MSE) of the channel parameter estimates computed by the proposed method and the principal components algorithm RAKE receiver, for $P = 8$ users. In Figure 5.6, we vary the number of users and compare the MSE of the channel parameter estimates computed by the proposed estimation method and RAKE receivers in both 1-D and 2-D. The proposed estimation method offers better channel estimation.

# of Users	# of Antennas	
	$M = 1$	$M = 2$
4	3.06	2.86
6	3.83	3.19
8	4.44	3.45
10	-	3.89
12	-	4.23
14	-	4.56
16	-	5.11

Table 5.1: Average number of iterations for the proposed estimation method to converge vs. number of antennas M and users P . We used $L_c = 16$, $L = 3$, $N_t = 15$, and SNR = 15 dB, and ran the simulation 100 times for each setting of M and P .

The improvement, which increases with the number of users, is 10 dB for 6 users.

Figure 5.7 compares the root-mean squared error (RMSE) of the channel parameter estimates for the CRB computed in Section 5.6, the proposed estimation method for $P = 8$ users, and a single antenna system. We vary the SNR from 5 to 30 dB. The RMSE of the channel estimates decreases approximately as $1/\text{SNR}$ as that of the CRB.

Using results from Section 5.5, we to compare the two transmission schemes for mobile users. In the first scheme, the higher data rate stream is split into several parallel basic rate sub-streams for each frame. Each sub-stream is then spread by one of the spreading codes. The proposed method can be directly used at the basestation without any modifications. In the second scheme, each user is assigned a single spreading code with lower spreading gain while maintaining the chip rate on the channel. In the simulations, we use

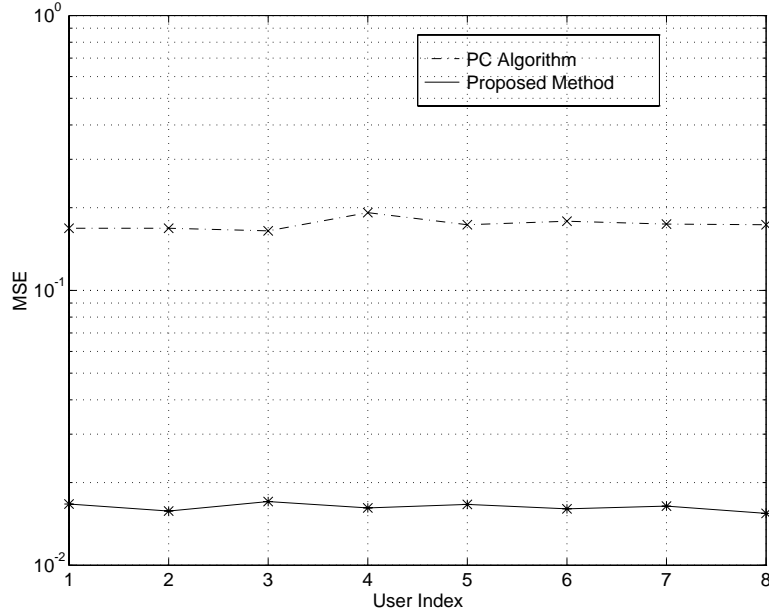


Figure 5.5: Comparison of the mean squared error (MSE) of the channel parameter estimates of the proposed estimation method and the 1-D RAKE receiver which uses the Principal Components (PC) algorithm. We use $P = 8$ users, $L_c = 16$, and $\text{SNR} = 15$ dB. The number of processed symbols N_t was 15 for the proposed estimation method and 40 for the PC algorithm. We used $L = 3$ in the proposed estimation method.

$L_c = 16$ and $P = 4$. Of the four users, two transmit at the same basic rate, one transmits at twice the basic rate, and the last transmits at four times the basic rate. Both schemes give nearly identical results, as shown in Figure 5.8.

5.8 Summary

For W-CDMA systems with aperiodic spreading sequences, we develop a blind multiuser method to estimate channel parameters and transmitted symbols for single and multiple antenna systems. The method uses iterative least squares projection to alternate between two new estimation steps that exploit the rich

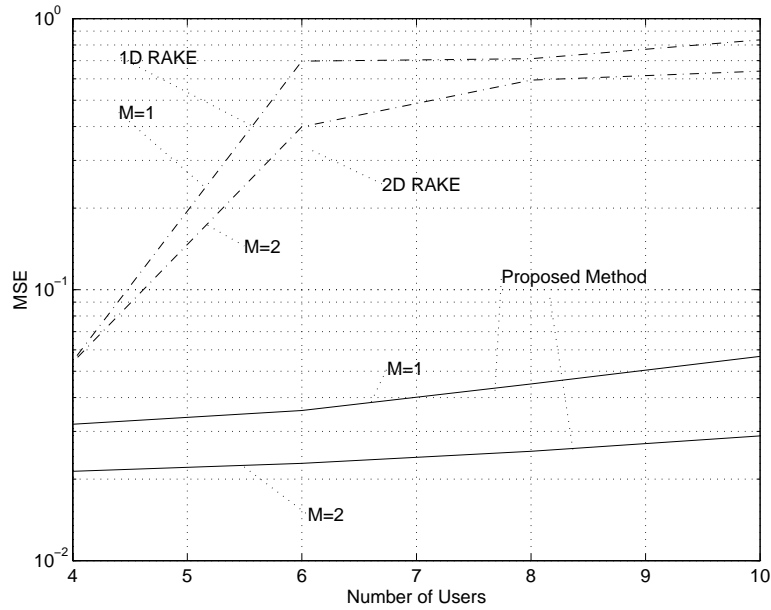


Figure 5.6: Mean-squared error of channel parameter estimates vs. number of users for different receivers: 1-D RAKE, 2-D RAKE, and the proposed estimation method in 1-D ($M = 1$) and 2-D ($M = 2$). Results were averaged over 200 runs using $L_c = 13$.

structure of W-CDMA signals. The method typically converges in 4 or 5 iterations in simulation. In simulation, the proposed estimation method shows an average of 10 dB gain in the mean-squared error of the channel parameter estimates over 1-D and 2-D RAKE receivers which use the principal component algorithm. The primary contributions of this chapter are (1) an iterative blind multiuser channel estimation method including a fast implementation, an extension to the multirate case, and its performance analysis, and (2) a Cramér-Rao Bound for W-CDMA systems with aperiodic spreading sequences.

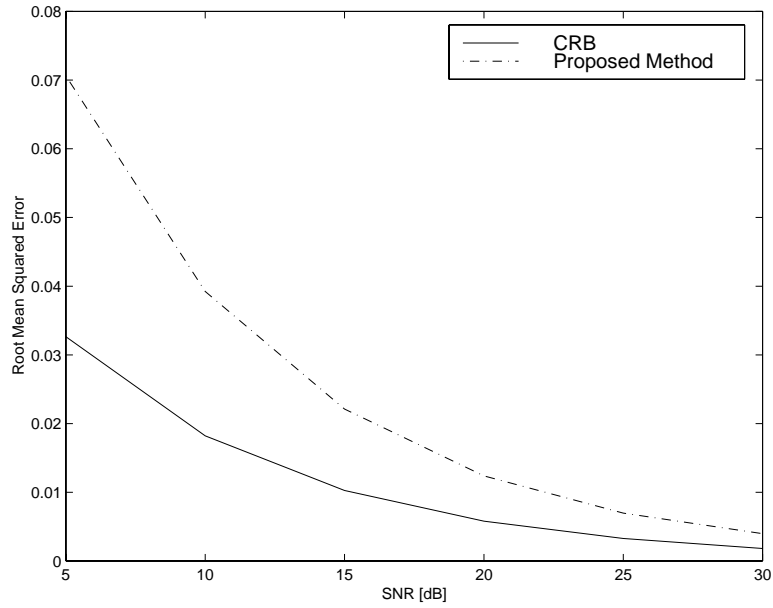


Figure 5.7: Root mean-square error of the channel estimates vs. the Cramér-Rao Bound with varying SNR for $P = 8$ users and $M = 1$ antenna. We used $L = 3$, $M = 1$, and $N_t = 15$ symbols.

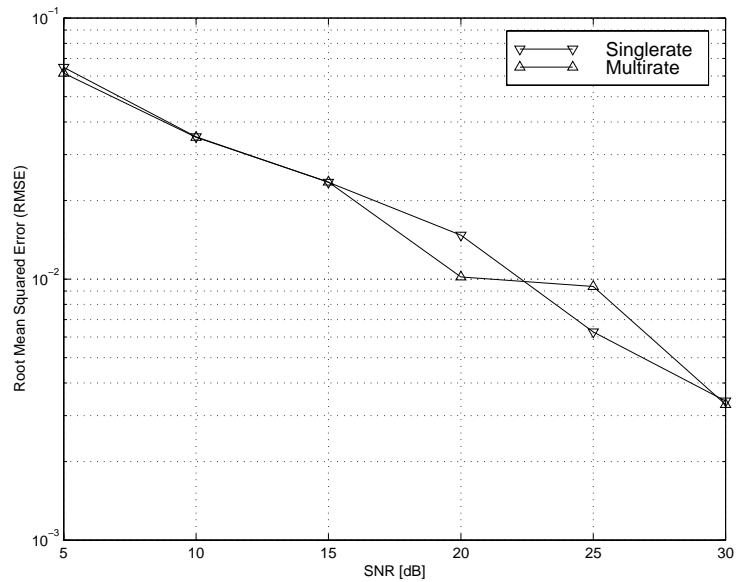


Figure 5.8: Root mean-square error of the channel estimates vs. the varying SNR for two transmission schemes.

Chapter 6

Conclusion

This dissertation focuses on improving the performance of wireless communication systems by combining antenna arrays and new signal processing methods at the basestation. I present fast methods for optimizing the downlink capacity and estimating uplink CDMA channels with smart antenna systems. I also derive a fundamental capacity measure for smart antenna systems.

6.1 Contributions

In Chapter 2, we introduce a novel approach to quantify the performance enhancement of the SDMA approach including increase in capacity and improvement in quality. We investigate the minimum distance of the constellation of SDMA channels under different scenarios when the signals are restricted to a finite alphabet. We first derive the minimum distance formulation by considering the simple two-user case. We also discuss the minimum distance of SDMA channels in different scenarios, *i.e.* different number of antennas, co-channel signals and relative user positions. Then, we demonstrate that the minimum distance provides an alternative criteria to evaluate the performance enhancement of the SDMA approach.

As seen in Chapter 3, optimal weighting vector design is a constrained

nonlinear optimization problem. However, we were able to improve capacity of broadcast channels by employing multiple transmitters and exploiting the spatial diversity among the users. We derived fast algorithms to compute *orthogonal*, *near-optimal*, and *optimal* weight vectors for broadcasting message signals to two and three users. The key innovation is that we decouple the weight vectors in the measure of channel capacity to simplify the optimization problem. The optimal solution reduces to a search for the maxima of a smooth multidimensional function. For the near-optimal and orthogonal solutions, we derive closed-form expressions that are amenable to fast implementation. Our solutions appear in [8].

In Chapter 4, we present a subspace based method for blind multi-user channel estimation in Asynchronous-CDMA systems. The method exploits the fact that the signature waveform (vector) is the intersection of the signal subspace and the user's code subspace, thereby allowing it to be uniquely determined without any knowledge of the input signals. We extend the new method to handle an overloaded system (in which the number of users exceeds the spreading gain).

For CDMA systems with aperiodic spreading sequences, we develop a blind multiuser method to estimate channel parameters and transmitted symbols for single and multiple antenna systems in Chapter 5. The method uses iterative least squares projection to alternate between two new estimation steps that exploit the rich structure of CDMA signals. The method typically converges in 4 or 5 iterations in simulation. In simulation, the proposed estimation method shows an average of 10 dB gain in the mean-squared error of the channel parameter estimates over 1-D and 2-D RAKE receivers which use the principal

components algorithm. The primary contributions of Chapter 5 are:

1. blind multiuser channel estimation method,
2. a fast implementation of the estimation method,
3. an extension of the estimation method to the multirate case,
4. a Cramér-Rao Bound for CDMA systems with aperiodic spreading sequences.

With the convergence of wireless services and the Internet, new wideband CDMA (W-CDMA) technology for next-generation mobile systems must provide high-rate data services in the field as well as voice communications to ordinary users. The blind channel estimation method with its fast implementation and adaptability to multirate data transmission will provide the same benefits of using aperiodic spreading sequences as methods for periodic spreading sequences.

6.2 Future Work

Third-generation (3G) systems introduces several new problems that need to be addressed including

- Downlink weight vector design for any number of users and any multiplexing method
- Downlink transmit weight FIR filter design for wideband channels
- Complexity associated with uplink channel estimation for W-CDMA systems with periodic spreading

- Downlink blind channel estimation for W-CDMA
- Asymptotic performance analysis for uplink channel estimation method for CDMA systems with aperiodic spreading
- Modify the proposed methods to work with the 3G standard proposals and assess the impact of the methods on these proposals.

Additional work is also needed in algorithm simplification, propagation studies and channel modeling, and digital signal processor implementations.

Appendix

Appendix A

Smart Antenna Testbeds

The experimental testbeds described here were developed at the Wireless Communications Laboratory location on the J. J. Pickle Research Campus of The University of Texas at Austin. Three smart antenna testbeds were completed, with the 1.5 GHz testbed (which consisted of a receive-only base station) completed in 1993, the 900 MHz testbed (transmit and receive to enable uplink and downlink beamforming) completed in 1994, and the 1.8 GHz test bed (capable of real-time uplink and downlink beamforming) completed in 1997.

The 900 MHz test bed, shown in Fig. A.1 and A.2, is comprised of the following subsystems: (1) one 8-element patch antenna array and four 1-element dipole antennas. The 8-element patch antenna array, arranged in a linear fashion with separation of about one half wavelength, is the base station. The dipole antennas are used by the four mobile units. (2) Twelve RF and IF up/down converters and switches operating in the RF band at around 900 MHz and IF band at around 144 MHz. (3) Two distribution boxes providing synthesized sources for RF and IF local oscillator signals. (4) Twelve A/D's and 24 D/A's. (5) Four digital multiplexing (MUX) and demultiplexing (DEMUX) boards. Each MUX/DEMUX board is connected to one of two high speed I/O boards installed in the s-bus slots of a Sparc 10 workstation. (6) Two

bi-directional high speed I/O boards installed in a Sparc 10 workstation.



Figure A.1: Overhead view of the 900 MHz Testbed

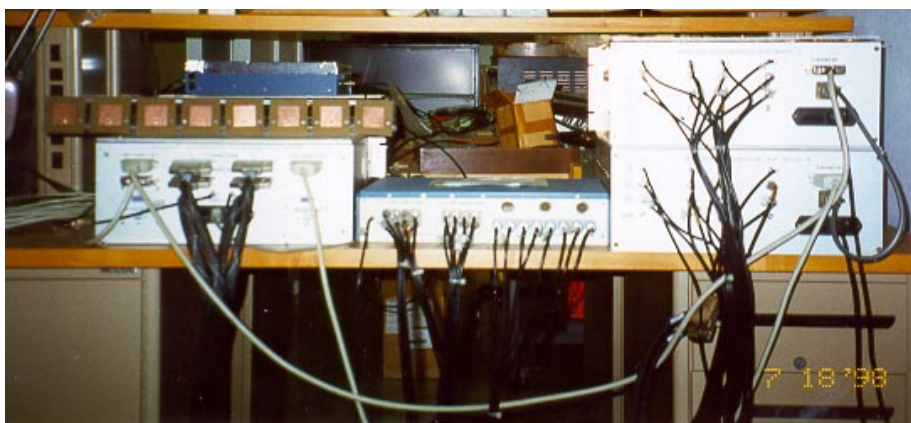


Figure A.2: Front view of the 900 MHz Testbed

The 1.8 GHz testbed was designed much like the 900 MHz testbed as described above. The key differences between the testbeds are that the 1.8 GHz testbed can perform real-time operations. The RF band is at 1.8 GHz instead of 900 MHz, and the IF band is at 70 MHz instead of 144 MHz. The 1.8 GHz smart antenna base site testbed consists of 8-channel transceivers, a DSP board with two Analog Devices SHARC DSPs, a backplane with frequency synthesizers,

RF and IF local oscillator distribution circuits, and timing generation circuits, a PC console, and telephone handsets. Fig. A.3 is a photograph showing the PC console and the two telephone handsets. Fig. A.4 is a photograph of a transmit/receive board, where the copper foil provides RF shielding to the analog circuits on the board. The transmit/receive channel operates in PCS band around 1.8 GHz. The smart antenna testbed uses an 8-element linear circular array on the top of 20m tower shown in Figs. A.6 and A.5. There are vocoders in the testbed for voice communications. The 8 kbps vocoders use Motorola DSP56166 fixed-point DSP chips plus support circuitry.

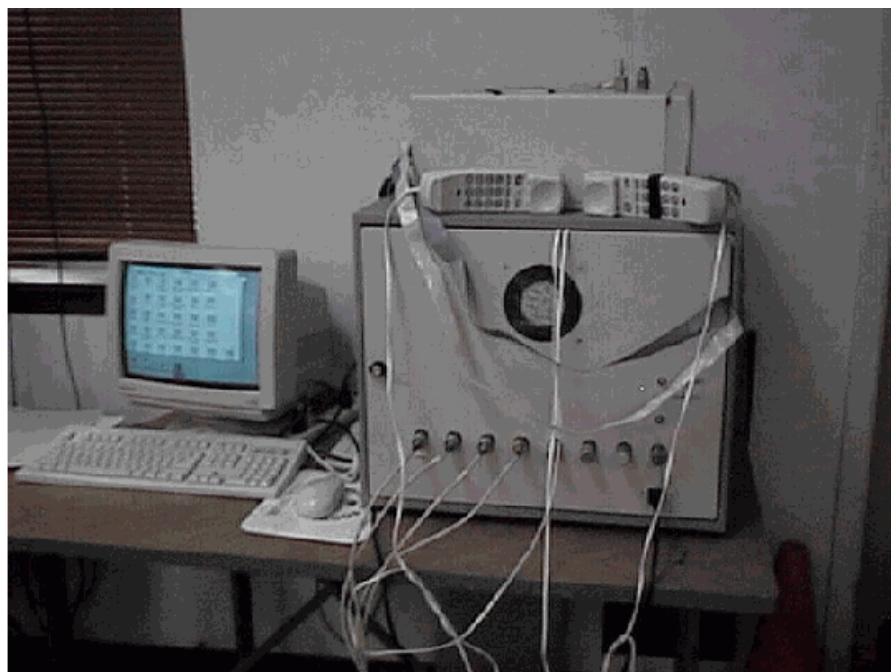


Figure A.3: Real-time smart antenna testbed base site.

In addition to the smart antenna testbed, we have also built several handsets. Each handset consists of an RF board with a single T/R channel, two Motorola DSP56166 chips for modem and vocoder functions. The handsets



Figure A.4: Base site transmit/receive board.

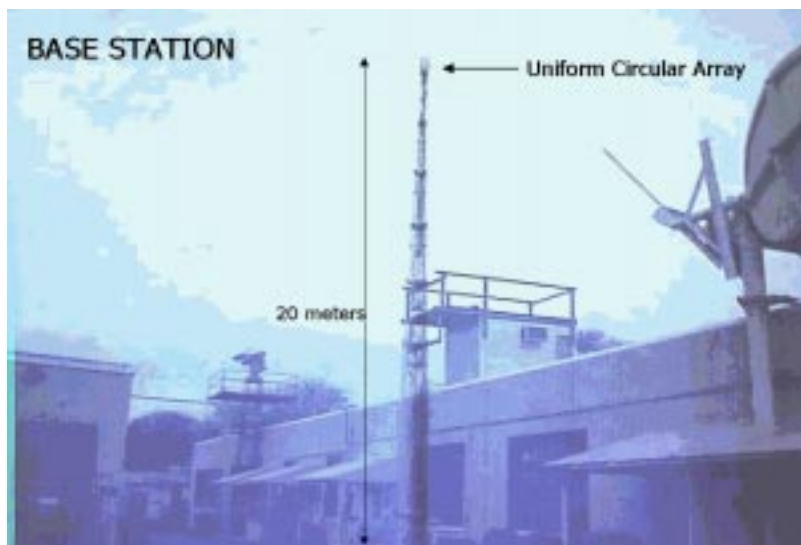


Figure A.5: Base site tower with antenna array.



Figure A.6: Circular antenna array



Figure A.7: A handset and emulator board

are programmed via an emulator connected to a PC computer. Fig. A.7 is a photograph of a handset and an emulator.

Bibliography

- [1] S. Andersson, M. Millnert, M. Viberg, and B. Wahlberg, “An adaptive array for mobile communication systems,” *IEEE Trans. on Vehicular Technology*, vol. 40, pp. 230–236, Jan. 1991.
- [2] S. C. Swales, M. A. Beach, D. J. Edwards, and J. P. McGreehan, “The performance enhancement of multibeam adaptive base-station antennas for cellular land mobile radio systems,” *IEEE Trans. on Vehicular Technology*, vol. 39, pp. 56–67, Feb. 1990.
- [3] G. Xu, H. Liu, W. Vogel, H. Lin, S. Jeng, and G. Torrence, “Experimental studies of space-division-multiple-access schemes for spectral efficient wireless communications,” in *Proc. IEEE Int. Conf. on Communications*, (New Orleans, LA), pp. 800–804, May 1994.
- [4] J. H. Winters, J. Salz, and R. D. Gitlin, “The capacity increase of wireless communication systems with antenna diversity,” in *Proc. IEEE Conf. on Information Science and Systems*, (Princeton, NJ), pp. 853–857, Mar. 1992.
- [5] M. Torlak, L. K. Hansen, and G. Xu, “A geometric approach to blind source separation for digital wireless applications,” *Signal Processing, Elsevier*, vol. 73, pp. 153–167, Feb. 1999.

- [6] M. Torlak, L. K. Hansen, and G. Xu, "A fast blind source separation for digital wireless applications," in *Proc. IEEE Int. Conf. on Acoustics, Speech, and Signal Processing*, vol. 6, (Seattle, WA), pp. 3305–3308, May 1998.
- [7] M. Torlak, G. Xu, B. L. Evans, and H. Liu, "Optimal weight vectors for broadcast channels," in *Proc. IEEE Asilomar Conf. on Signals, Systems & Computers*, vol. 1, (Pacific Grove, CA), pp. 65–69, Nov. 1996.
- [8] M. Torlak, G. Xu, B. Evans, and H. Liu, "Fast estimation of weight vectors to optimize multi-transmitter broadcast channel capacity," *IEEE Transactions on Signal Processing*, vol. 46, pp. 243–246, Jan. 1998.
- [9] W. Yang and G. Xu, "Channel capacity of space-division-multiple-access schemes," in *Proc. SPIE Conf. on Advanced Signal Proc. Algorithms, Arch., and Implementations*, (San Diego, CA), 1997.
- [10] W. Yang and G. Xu, "The optimal power assignment for smart antenna downlink weighting vector design," in *Proc. IEEE Vehicular Technology Conf.*, (Ottawa, Can), pp. 485–488, May 1998.
- [11] S. Haykin, *Adaptive Filter Theory*. Englewood Cliffs, NJ: Prentice-Hall, 2nd ed., 1991.
- [12] S. Widrow, B. and Stearns, *Adaptive Signal Processing*. Englewood Cliffs, NJ: Prentice-Hall, 1985.
- [13] A. Paulraj, B. Ottersten, R. Roy, A. Swindlehurst, G. Xu, and T. Kailath, "Subspace methods for direction finding and parameter estimation," in

Handbook of Statistics Volume 10 "Signal Processing and Its Applications"

(N. B. Ed. and C. Rao, eds.), Elsevier Science Publishers B.V., 1992.

- [14] G. Xu, H. Liu, L. Tong, and T. Kailath, "A least-squares approach to blind channel identification," *IEEE Trans. on Signal Processing*, vol. 43, pp. 2982–2993, Dec. 1995.
- [15] J. H. Winters, J. Salz, and R. D. Gitlin, "The impact of antenna diversity on the capacity of wireless communication systems," *IEEE Trans. on Communications*, vol. 42, pp. 1740–1751, Feb. 1994.
- [16] T. Cover and J. Thomas, *Elements of Information Theory*. New York, NY: John Wiley & Sons, Inc., 1991.
- [17] P. Balaban and J. Salz, "Optimum diversity combining and equalization in data transmission with application to cellular mobile radio - Part I: Theoretical considerations," *IEEE Trans. on Communications*, vol. 40, pp. 885–894, May 1992.
- [18] S. U. Pillai, *Array Signal Processing*. New York: Springer Verlag, 1989.
- [19] J. G. Proakis, *Digital Communications*. Polytechnic Institute of New York: McGraw-Hill Book Company, 2nd ed., 1989.
- [20] Y. Sato, "A method of self-recovering equalization for multilevel amplitude-modulation," *IEEE Trans. Commun.*, vol. 23, pp. 679–682, June 1975.
- [21] M. K. Tsatsanis and G. B. Giannakis, "Multirate filter banks for code-division-multiple-access systems," in *Proc. IEEE International Conf. on*

- Acoustics, Speech and Signal Processing*, (Detroit, MI), pp. 1484–1487, May 1995.
- [22] U. Mitra and H. V. Poor, “Adaptive receiver algorithm for near-far resistant CDMA,” *IEEE Trans. on Communications*, vol. 43, pp. 1713–1724, Apr. 1995.
- [23] M. Abdulrahman, D. D. Falconer, and A. U. H. Sheikh, “Equalization for interference cancellation in spread spectrum multiple access systems,” in *Proc. IEEE Vehicular Technology Conf.*, pp. 71–74, May 1992.
- [24] P. Rapajic and B. Vucetic, “A linear adaptive fractionally spaced single user receiver for asynchronous CDMA systems,” in *IEEE Int. Symp. on Information Theory*, p. 45, Jan. 1993.
- [25] M. L. Honig, U. Madhow, and S. Verdú, “Blind adaptive multiuser detection,” *IEEE Trans. on Information Theory*, vol. 41, pp. 944–962, July 1995.
- [26] A. F. Naguib and A. Paulraj, “A base-station antenna array receiver for cellular DS/CDMA with M-ary orthogonal modulation,” in *Proc. IEEE Asilomar Conf. on Signals, Systems and Computers*, (Pacific Grove, CA), pp. 858–862, Nov. 1994.
- [27] S. E. Bensley and B. Aazhang, “Subspace-based channel estimation for code division multiple access communication systems,” *IEEE Trans. on Communications*, vol. 44, pp. 1009–1020, Aug. 1996.

- [28] S. E. Bensley and B. Aazhang, "Subspace-based delay estimation for CDMA communication systems," in *Proc. IEEE International Symposium on Information Theory*, (Trodheim, Norway), p. 138, July 1994.
- [29] E. G. Ström, S. Parkvall, S. L. Miller, and B. E. Ottersten, "Sensitivity analysis of near-far resistant DS-SS receivers to propagation delay estimation errors," in *Proc. IEEE Vehicular Technology Conf.*, pp. 757–761, 1994.
- [30] E. G. Ström, S. Parkvall, S. L. Miller, and B. E. Ottersten, "Propagation delay estimation in asynchronous direct-sequence code-division multiple access systems," *IEEE Trans. on Communications*, vol. 44, pp. 84–93, Jan. 1996.
- [31] H. Liu and G. Xu, "A subspace method for signature waveform estimation in synchronous CDMA systems," *IEEE Trans. on Communications*, vol. 44, pp. 1346–1354, Oct. 1996.
- [32] M. Torlak and G. Xu, "Blind multi-user channel estimation in asynchronous CDMA systems," *IEEE Trans. on Signal Processing*, vol. 45, pp. 137–147, Jan. 1997.
- [33] R. Lupas and S. Verdú, "Linear multiuser detectors for synchronous CDMA channels," *IEEE Trans. on Information Theory*, vol. 1, pp. 123–136, Jan. 1989.
- [34] M. K. Simon, J. K. Omura, R. A. Scholtz, and B. K. Levitt, *Spread Spectrum Communications Handbook*. New York, NY: McGraw-Hill, revised ed., 1994.

- [35] M. K. Tsatsanis, "Inverse filtering criteria for CDMA systems," *IEEE Trans. on Signal Processing*, vol. 45, pp. 102–112, Jan. 1997.
- [36] E. A. Lee and D. G. Messerschmitt, *Digital Communications*. Kluwer-Academic Publishers, 2nd ed., 1994.
- [37] P. Balaban and J. Salz, "Optimum diversity combining and equalization in data transmission with application to cellular mobile radio - part II: Numerical results," *IEEE Trans. on Communications*, vol. 40, pp. 895–907, May 1992.
- [38] S. Wright, "Convergence of SQP-like methods for constrained optimization," *SIAM Journal on Control and Optimization*, vol. 27, pp. 13–26, Jan. 1989.
- [39] Z. Zvonar and D. Brady, "Linear multipath-decorrelating receivers for cdma frequency-selective fading channels," *IEEE Trans. on Communications*, pp. 650–653, June 1996.
- [40] W. C. Y. Lee, "Overview of cellular cdma," *IEEE Trans. on Vehicular Technology*, pp. 291–301, May 1991.
- [41] E. Moulines, P. Duhamel, J. Cardoso, and S. Mayrargue, "Subspace methods for the blind identification of multichannel FIR filters," *IEEE Trans. on Signal Processing*, vol. 43, pp. 516–525, Feb. 1995.
- [42] L. Tong, G. Xu, and T. Kailath, "Blind identification and equalization based on second-order statistics: A time domain approach," *IEEE Trans. on Information Theory*, vol. 40, pp. 29–31, Mar. 1994.

- [43] G. Golub and C. V. Loan, *Matrix Computations*. Baltimore, MD: Johns Hopkins University Press, 2nd ed., 1984.
- [44] G. Xu and T. Kailath, "Fast subspace decomposition," *IEEE Trans. on Signal Processing*, vol. 42, pp. 539–551, Mar. 1994.
- [45] B. Suard, G. Xu, H. Liu, and T. Kailath, "Channel capacity of spatial division multiple access schemes," in *Proc. 28th Asilomar Conference on Signals, Systems and Computers*, (Pacific Grove, CA), pp. 1159–1163, Nov. 1994.
- [46] A. F. Naguib and A. Paulraj, "Performance of wireless CDMA with M-ary orthogonal modulation and cell site arrays," *IEEE Journal on Selected Areas in Communications*, vol. 14, pp. 1770–1783, Dec. 1996.
- [47] F. Li, H. Liu, and R. J. Vaccaro, "Performance analysis for DOA estimation algorithms: Further unification, simplification, and observations," *IEEE Trans. Aerosp., Electron. Syst.*, vol. 29, pp. 1170–1184, Oct. 1993.
- [48] Z. Xie, R. T. Short, and C. K. Rushforth, "A family of suboptimum detectors for coherent multiuser communications," *IEEE Journal on Selected Areas in Communications*, pp. 683–690, May 1990.
- [49] A. Klein and P. W. Baier, "Linear unbiased data estimation in mobile radio systems applying CDMA," *IEEE Journal on Selected Areas in Communications*, pp. 1058–1066, Sep. 1993.
- [50] S. Talwar, M. Viberg, and A. Paulraj, "Blind estimation of multiple co-channel digital signals using an antenna array," *IEEE Signal Processing Letters*, vol. 1, pp. 29–31, Feb. 1994.

- [51] A. J. van der Veen, S. Talwar, and A. Paulraj, "A subspace approach to blind space-time signal processing for wireless communication systems," *IEEE Trans. on Signal Processing*, vol. 45, pp. 173–189, Jan. 1997.
- [52] M. Torlak, G. Xu, and H. Liu, "Self-recovery scheme in anti-jamming communications," in *Proc. IEEE International Conf. on Acoustics, Speech and Signal Processing*, (Atlanta,GA), pp. 2567–2570, May 1996.
- [53] H. Liu and M. D. Zoltowski, "Blind equalization in antenna array CDMA systems," *IEEE Trans. on Signal Processing*, vol. 45, pp. 161–172, Jan. 1997.
- [54] H. Liu and G. Xu, "Blind equalization for CDMA systems with aperiodic spreading sequence," in *Proc. IEEE International Conf. on Acoustics, Speech and Signal Processing*, (Atlanta,GA), pp. 2658–2661, May 1996.
- [55] B. H. Khalaj, A. Paulraj, and T. Kailath, "2D RAKE receivers for CDMA cellular systems," in *Proc. IEEE Global Communications Conf.*, (San Francisco, CA), pp. 400–404, May 1994.
- [56] A. Swindlehurst and J. Yang, "Using least squares to improve blind signal copy performance," *IEEE Signal Processing Letters*, vol. 1, pp. 80–82, May 1994.
- [57] G. Davis, "A fast algorithm for the inversion of block toeplitz matrices," *IEEE Trans. on Signal Processing*, vol. 43, no. 12, pp. 3022–3025, 1995.
- [58] P. Stoica and A. Nehorai, "MUSIC, Maximum Likelihood and Cramér-Rao bound," *IEEE Trans. on Acoustics, Speech, and Signal Processing*, vol. 37, pp. 720–741, May 1989.

- [59] W. M. Steedly and R. L. Moses, "The Cramér-Rao Bound for pole and amplitude coefficient estimates of damped exponential signals in noise," *IEEE Trans. on Signal Processing*, vol. 41, pp. 1305–1318, Mar. 1993.

Vita

Murat Torlak was born in Konya, Turkey, on August 12, 1971, as the son of Hatice Torlak and Halil İbrahim Torlak. He graduated from high school in 1987 from Sarayönü Lisesi, in Sarayönü, Konya, Turkey. He received the degree of Bachelor of Science in Electrical & Electronics Engineering from Hacettepe University in July, 1992, in Ankara, Turkey, and Master of Science in Electrical Engineering from The University of Texas at Austin, in December 1995. He received his PhD in the area of Telecommunications and Information Systems Engineering, Department of Electrical & Computer Engineering, The University of Texas at Austin, in August 1999.

Permanent address: 2601 N. Floyd Road, P.O. Box 830688 EC 33,
Richardson, TX 75083-0688

This dissertation was typeset with L^AT_EX[†] by the author.

[†]L^AT_EX is a document preparation system developed by Leslie Lamport as a special version of Donald Knuth's T_EX Program.